2013

Towards Elucidation of a Viral DNA Packaging Motor

Chad T. Schwartz
University of Kentucky, ctschw2@g.uky.edu

STUDENT AGREEMENT:

I represent that my thesis or dissertation and abstract are my original work. Proper attribution has been given to all outside sources. I understand that I am solely responsible for obtaining any needed copyright permissions. I have obtained and attached hereto needed written permission statements(s) from the owner(s) of each third-party copyrighted matter to be included in my work, allowing electronic distribution (if such use is not permitted by the fair use doctrine).

I hereby grant to The University of Kentucky and its agents the non-exclusive license to archive and make accessible my work in whole or in part in all forms of media, now or hereafter known. I agree that the document mentioned above may be made available immediately for worldwide access unless a preapproved embargo applies.

I retain all other ownership rights to the copyright of my work. I also retain the right to use in future works (such as articles or books) all or part of my work. I understand that I am free to register the copyright to my work.

REVIEW, APPROVAL AND ACCEPTANCE

The document mentioned above has been reviewed and accepted by the student's advisor, on behalf of the advisory committee, and by the Director of Graduate Studies (DGS), on behalf of the program; we verify that this is the final, approved version of the student's dissertation including all changes required by the advisory committee. The undersigned agree to abide by the statements above.

Chad T. Schwartz, Student

Dr. Peixuan Guo, Major Professor

Dr. Jim Pauly, Director of Graduate Studies

TOWARDS ELUCIDATION OF A VIRAL DNA PACKAGING MOTOR

DISSERTATION

A dissertation submitted in partial fulfillment of the requirements for the degree of Doctor of Philosophy in the College of Pharmacy at the University of Kentucky

By

Chad Schwartz

Lexington, KY

Director: Peixuan Guo, Professor of Pharmaceutical Sciences

Lexington, KY

2013

ABSTRACT OF DISSERTATION

TOWARDS ELUCIDATION OF A VIRAL DNA PACKAGING MOTOR

Previously, gp16, the ATPase protein of phi29 DNA packaging motor, was an enigma due to its tendency to form multiple oligomeric states. Recently we employed new methodologies to decipher both its stoichiometry and also the mechanism in which the protein functions to hydrolyze ATP and provide the driving force for DNA packaging. The oligomeric states were determined by biochemical and biophysical approaches. Contrary to many reported intriguing models of viral DNA packaging, it was found that phi29 DNA packaging motor permits the translocation of DNA unidirectionally and driven cooperatively by three rings of defined shape. The mechanism for the generation of force and the role of adenosine and phosphate in motor motion were demonstrated. It was concluded that phi29 genomic DNA is pushed to traverse the motor channel section by section with the aid of ATPase gp16, similar to the hexameric AAA+ family in the translocation of dsDNA. A new model of "Push through a One-way Valve" for the mechanism of viral DNA packaging motor was coined to describe the coordinated interaction among the hexameric packaging ATPase gp16 and the revolution mechanism of the dodecameric channel which serves as a control device to regulate the directional movement of dsDNA.

KEYWORDS: phi29 bacteriophage, viral DNA packaging, AAA+ family, gp16, viral maturation

Chad Schwartz

Student's Signature

May 2013

Date

TOWARDS ELUCIDATION OF A VIRAL DNA PACKAGING MOTOR

By

Chad Schwartz

Peixuan Guo, Ph. D.

Director of Dissertation

Jim Pauly, Ph. D.

Director of Graduate Studies

May 2013

Date

To both my parents and sisters for supporting me through this endeavor

ACKNOWLEDGEMENTS

I would first like to express my gratitude to my thesis advisor, Dr. Peixuan Guo, for his continued guidance and support which made this all possible. I am sincerely grateful that I was offered this opportunity to study at both the University of Cincinnati and the University of Kentucky to perform this intriguing research.

Many thanks also go to my committee members, Dr. Pat McNamara, Dr. Guo Min-Li, Dr. David Rodgers, and Dr. James Pauly, for their sincere instruction and help during the foreign transition back to the University of Kentucky. Without their diligence and attention to detail, completion of my qualifying exam and dissertation defense would not have been possible.

Furthermore, all members of Dr. Guo's laboratory have in the past and continue to be a valuable source of instruction not only on research matters and collaborations but on personal relationships and friendships alike. I would first like to acknowledge the members of the lab that have helped in training me to become a Ph.D. candidate. Dr. Tae Jin Lee, Dr. Gian Marco De Donatis, and Dr. Huaming Fang were absolutely critical to my development as a research scientist and I want to express my sincerest gratitude. I am also thankful for the remainder of the lab, past and present members, who have contributed to my success: Dr. Dan Shu, Dr. Hui Zhang, Dr. Farzin Haque, Dr. Mathieu Cinier, Dr. Randall Reif, Dr. Zhanxi Hao, Dr. Peng Jin, Dr. Anne Vonderheide, Dr. Faqing Yuan, Dr. Wenjuan Wang, Shuhui Wan, Jing Liu, Wei Li, Jia Geng, Daniel Binzel, Le Zhang, Fengmei Pi, Zhengyi Zhao, Hui Li, Danny Jasinski, Jeannie Haak, Shaoying Wang, and Nayeem Hossain. I would like to also thank the work study students.

I have been lucky to have great outside collaborators during my tenure as a Ph. D. student and I would like to acknowledge them here: Dr. Yuri Lyubchenko (University of Nebraska), Dr. Jarek Meller (University of Cincinnati), Dr. Tom Thompson (University of Cincinnati), Dr.

David Rodgers (University of Kentucky), Dr. Guo Min-Li (University of Kentucky), Dr. Wah Chiu (Baylor College of Medicine), Dr. Bruce Maley (University of Kentucky), and Dr. Joseph Wall (Brookhaven National Laboratory).

I would like to thank all other faculty and staff members throughout my graduate career, especially the graduate coordinators Julie Muenchen, Linda Moeller, and Barbara Carter, in College of Engineering and Applied Sciences at the University of Cincinnati , and Catina Rossol in the Department of Pharmaceutical Sciences at the University of Kentucky for their kind help in organizing class schedules, reserving rooms, and facilitating living arrangements.

Finally, I would like to express my love and appreciation to my family and girlfriend; my father Richard Schwartz, my mother Joan Schwartz, my two sisters Sherri Schwartz and Stacey Schwartz, and my girlfriend Lauren Burns. Their encouragement and support mean the world to me and they continue to make me a better person.

My work was supported by the National Institute of Health grants R01-GM59944 and EB012135 to Dr. Peixuan Guo.

TABLE OF CONTENTS

LIST OF FIGURES

Chapter 1: Introduction and Literature Review

Brief Summary

In the first chapter, an introduction to the phi29 DNA packaging motor will be provided in which the current knowledge and understanding of the phage will be outlined. This section will discuss the three major components of this packaging motor and how they interact with one another to perform the process of translocating dsDNA inside a procapsid shell during phage maturation. Next, early models of DNA packaging will be discussed in order to understand their limitations and how the new packaging model has been developed. Each one of the three major components of the motor will then be analyzed with further detail in regards to its responsibility in the packaging process. A new model will be proposed which takes into consideration the current understanding of all functioning units of the phage, and finally, current and potential applications of the phi29 motor in terms of nanotechnology and nanomedicine will be posed.

In the second chapter, the ATPase gp16 of the phi29 motor will be scrutinized in terms of its stoichiometry and function. There has long been a debate on whether or not this protein exists as a pentamer or hexamer on the base of phi29. A plethora of biochemical data will be provided in this chapter to validate the existence of a hexameric ATPase in solution and on the active packaging motor.

The third chapter focuses on the interaction of the ATPase gp16 with dsDNA and ATP. It was shown that the ATPase is a member of the AAA+ superfamily (ATPase Associated with diverse cellular Activities) of proteins and prefers binding to ATP which promotes a conformational change within the protein to increase it's affinity toward the dsDNA substrate. It was further proven that a power stroke occurs from the ATPase after hydrolysis of ATP to push itself away from the DNA, which relates directly to the translocation of the DNA inside the

prohead of the phage. A new model termed "push through a one-way valve" has been proposed to describe the packaging mechanism.

Next, the fourth chapter will explain the coordinated mechanism of the ATPase. It was recently discovered that the ATPase cooperatively binds and releases DNA between subunits to "hand off" the DNA substrate along the axis of the ATPase. It was also shown that the ATPase can bind and move directionally along tethered genomic DNA using single molecule total internal reflection fluoroscopy. Lastly, a revolving motor is described in which DNA translocation is regulated by making contact with the twelve subunits of the connector one-way valve portal protein.

Finally, in the fifth chapter, future directions to validate the findings herein will be examined. Also, the state of the field will be discussed. Lastly, analysis of how to translate DNA packaging to nanomedicine and nanotechnology will be provided.

Hypothesis

Bacteriophage phi29 packages its own genomic DNA inside a viral procapsid via a sequential action revolving "push through a one-way valve" mechanism.

Introduction

Phi29: A tiny, powerful molecular motor

DsDNA viruses package their genomic DNA into a procapsid using a force-generating nanomotor powered by ATP hydrolysis. Viral DNA packaging motors are mainly composed of a portal protein with which dsDNA passes during phage maturation and two DNA packaging

enzymes. The procapsid is a shell used merely to store the packaged DNA prior to infection. However, phi29 bacteriophage is unique in that it contains an RNA component (1). It is this component that leads researchers to believe that phi29 is one of the earliest viruses from the RNA world. The work presented here aims to elucidate the DNA packaging mechanism of this previously enigmatic virus.

The nanomotor of phi29 consists of an ATPase gp16, a hexameric packaging RNA ring (1), and a dodecameric connector with a central channel encircled by 12 copies of the protein gp10. All DNA packaging motors involve two DNA packaging components that are not fixed components in the purified procapsid. These components were classified in 1987 (2) into two categories according to their role in DNA packaging: the first category is the large subunit that is responsible for binding to the procapsid and contains an ATP binding consensus sequence; the second category is the smaller subunit which interacts with DNA (2).The channel serves as a path for dsDNA translocation. The ATPase gp16 converts energy from ATP hydrolysis into physical motion (2) and has recently been shown to be a member of the AAA+ family of proteins (3, 4). This motor is of particular interest in nanotechnology because it is simple and robust in structure and is functional when assembled from purified components *in vitro* (5).

Early Models of DNA Packaging

Many years have passed in a quest to understand the mechanism of viral DNA packaging and several different models have been proposed. These include, but are not limited to, the following: 1) DNA compression and relaxation (6-8), 2) force of osmotic pressure (9), 3) ratchet mechanism(10), 4) Brownian motion (11), 5) five-fold/six-fold mismatch connector rotating thread (12), 6) supercoiled DNA wrapping(13), 7) sequential action of motor components (14, 15), 8) electro-dipole within central channel(16), 9) connector contraction hypothesis (17), and

10) connector rotation model (16). However, none of these models have been conclusively supported by experimental data. There are cases where some models have been validated in one viral system but refuted in other systems. The 5-fold/6-fold mismatch connector rotation model, first proposed in 1978, was popular since it described the perpetual motion of the motor (12). This mechanical motor prototype has been prevalent based on the mismatch between the 5-fold symmetry of capsid at the vertex and 6-fold symmetry of the connector, which is a twelve-subunit dodecamer. Years later, however, another model was proposed in which the connector revolved during DNA packaging (16). In this model, the positively charged lysine residues inside the highly negatively-charged connector channel were thought to interact favorably with the negatively charged phosphate backbone of DNA in the process of driving the DNA into the procapsid. However, both the proposed connector rotation model (16) and the five-fold/six-fold mismatch connector rotating thread model (16) (18) have been invalidated by single molecule studies through fluorescent labeling of the connector (19) and by testing with connector cross-linking experiments (20, 21).

In 1998, it was proposed by Guo that the mechanism of viral DNA packaging motors is similar to that of the hexameric AAA+ ATPases that translocate along the strands of DNA (3). The superfamily of AAA+ proteins is a large group of enzymes that function in chromosome segregation, nucleic acid replication, DNA repair, genome recombination, viral DNA packaging, and translocation of cellular components (22, 23)}. Many of these motors display hexameric arrangements that facilitate DNA motion triggered by ATP (24-26). Based on the hexameric structure of pRNA (3, 27, 28), it was proposed that the mechanism of the phi29 viral DNA packaging motor is similar to that used by other hexameric DNA tracking motors of the AAA+ family (3). Recently, X-ray diffraction, AFM imaging, and single molecule studies have

confirmed that the motor consists of three-coaxial rings geared by a hexameric RNA, a hexameric ATPase gp16, and a dodecameric motor channel that only allows for the movement of dsDNA unidirectionally (4, 16, 29-34). Single molecule techniques have also been applied to study phi29 DNA packaging mechanisms. Motion of the DNA during packaging by a single phi29 motor was directly observed (30, 35). In addition, using optical tweezers, DNA packaging speed and force were measured for an individual motor complex (15, 36, 37). A mechanism of coordinative interaction among motor subunits was proposed to elucidate the packaging process (15). Concurrently, it has also been discovered that the motor utilizes a simple, yet novel revolution mechanism to translocate dsDNA, rather than the perceived rotational mechanism lending to undesirable coiling forces (4, 34).

Connector Portal Protein

As documented in many phage systems (2, 33, 38, 39), the ATPase, or terminase as it is called in many systems, plays a key role in transporting the DNA into the procapsid. However, the role of the connector in DNA translocation remained unidentified. The central channel of connector allows viral DNA to enter into the procapsid during maturation and exit during infection. Structural analysis showed that the connector contains three layers consisting of two hydrophilic layers separated by a hydrophobic layer. Utilizing this characteristic, phi29 connector was successfully embedded into a planar lipid membrane, and dsDNA translocation through the channel was studied by electrophysiological measurements (40-42). During translocation, DNA physically obstructs the connector channel, which shows up as a blockage of current. This new method has facilitated the proposal of a pump and valve mechanism for bacteriophage phi29 DNA packaging motor (38, 43) which has been validated in recent reports (41, 44, 45).

The successful insertion of the connector channel into bilayer lipid membrane made it possible to study dsDNA translocation through the channel using a single channel conductance assay (41, 42). Events of DNA translocation only occurred at one voltage polarity, demonstrated by numerous current blockades, while no events occurred at the other voltage polarity (41). Moreover, it was demonstrated that multiple channel insertions in the lipid membrane affects the frequency of DNA translocations due to their different orientation arrangements (41). These data demonstrate that phi29 connector only allows DNA trafficking in one direction. Furthermore, using antibody or gold particles to bind to the tag-conjugated C-terminal, the proper orientation of the connector for DNA translocation was probed to be from the N-terminus to C-terminus, the same direction that DNA traverses during packaging.

Previous findings showed that both partially and completely packaged phi29 dsDNA remained inside the viral procapsid during packaging (2, 46). In addition, the packaged DNA was able to remain inside the procapsid under high centrifugal force (41), in agreement with the one-way traffic mechanism of DNA translocation through the membrane embedded connector channel. This suggested that the phi29 DNA packaging is unidirectional against large internal forces and endorsed the pushing or injection model suggested previously (38). The connector may experience conformational change after the DNA packaging and restructure the channel to facilitate the DNA ejection during viral infection.

Moreover, the phi29 connector channel was found to be stable under even extreme pH conditions (40). Single pore conductance assays of membrane-embedded connector showed that the connector remains open with uniform channel conductance under extreme pH and both the conductance and the membrane insertion orientation of the channel are independent of the pH. While DNA translocation events were still observed at these extreme conditions, formation of

apurinic acid at pH 2 led to shorter current blockade events. Overall, the connector retains its stable channel properties under strong acidic or alkaline conditions despite the inherent effect on DNA structure. Furthermore, the mutation of the basic lysine residues inside the connector channel wall or the use of extreme pH, which alter the lysine charge, did not measurably impair DNA translocation or affect the one-way traffic property of the channel (40).

The structural study of the phi29 connector showed that there are 48 positively charged lysine residues in the inner channel (four 12-lysine rings from the twelve gp10 subunits). It was believed that these positively charged rings could play an important role in DNA translocation through the channel in that they may interact with the negatively charged phosphate backbone of dsDNA during DNA translocation (16). Different mutations were introduced to these lysine residues in order to study the effect of lysine rings. The effects on channel size, procapsid assembly, dsDNA translocation, and connector outer surface charge distribution were assessed through their interaction with the lipid membrane, by single-pore conductance, direction of dsDNA translocation, efficiency of DNA packaging, and the production of infectious virions. Furthermore, these assays were performed in both acidic and basic environments to investigate the role of the lysine residues in dsDNA translocation and dsDNA trafficking direction (44). These studies showed that the basic lysine residues were not involved in viral DNA packaging and did not affect the direction of DNA trafficking through the channel, with one exception when residue 234 was mutated from lysine to alanine. In this connector mutant, less virion production was observed, which can most likely be attributed to the DNA ejection step rather than packaging (44).

However, the mutations of lysine residue 200 and/or 209 to alanine (K200A, K209A, or both) were discovered to have low efficiency in procapsid assembly in which the connector acts

as a nucleating core (47-55). Additionally, connectors with single K200A and K209A mutations were competent, yet more difficult for insertion into the lipid membrane compared to wild-type connectors, and the double mutant K200A/K209A connector could not be inserted into the lipid membrane (44). The difficulty in membrane insertion indicates that these mutations may have altered the surface charge of the connector, which could affect the insertion efficiency. The other mutant K234A connector showed the same membrane insertion efficiency as the wild-type connector, indicating that the K234 mutation did not significantly alter the connector surface charge (44).

Lastly, the channel size of the lysine mutant connectors can be deduced from the single channel conductance assays. Upon connector insertion into the lipid membrane, discrete current jumps were observed under an applied voltage, representing the open-pore current amplitude. When DNA passes through the channel, the capacity of the electrolyte ion passage is reduced resulting in transient current blockade events. Since the diameter of dsDNA is 2 nm and the size of the narrowest region of the wild-type connector channel is 3.6 nm, the ratio of the cross-sectional area (represented by the ratio of the open-pore current and the current during the DNA blockade) can be used as a parameter to estimate the channel size at the narrowest point. From conductance measurements, the size of mutant connectors K200A and K209A were determined to be 3.7 nm and 3.6 nm respectively, which was similar to the wild-type connector. However, two different pore sizes were observed for the K234A mutant: 3.6 nm (diameter), which is similar to wild-type connector, and 3.0 nm (diameter), which is significantly smaller than wild-type. The reduced channel size of K234A in turn made it impossible for dsDNA translocation driven by electrical force and possibly affected dsDNA ejection in viral infection (44). The results indicated that the four lysine rings within the phi29 connector channel are not involved in

the active translocation of dsDNA and support the “Push through a One-way Valve” model of the dsDNA packaging mechanism.

Packaging RNA

Years of research have gone into determining the structure and function of pRNA as it is unique to phi29 bacteriophage. pRNA is 117 nucleotides (nt) in length and folds into a complex structure consisting of two major domains: the first domain is a helical region with an open 5'/3' end and the second component is an interlocking domain containing its core stability. In the center of pRNA is a thermo-stable three way junction (3WJ) motif (56, 57). The loops allow for intermolecular interactions between pRNA monomeric units and the creation of dimeric, tetrameric, and even hexameric rings (58).

pRNA (1, 30, 59) has been found to serve as a foothold for the ATPase gp16 (60). It is believed that pRNA dimers are the building blocks that form the completed ring. This pRNA was demonstrated to be indispensible in DNA packaging and viral assembly. It has been found that the pRNA mediates the binding of the motor ATPase, gp16, to procapsid, indicating the role of pRNA in motor function may be to serve as a hinge to connect motor components and thus gear the motor (60). Formation of the hexameric ring within the motor has been revealed through a series of experiments, including concentration-dependent curves (61); binomial distribution of mutant and wild-type pRNA (62); stoichiometric calculations showing a common factor of 2 and 3 (3); single molecule photobleaching (30); gold and ferritin labeling of pRNA (32); AFM imaging (4, 33, 34); and X-ray crystallography (63).

Analysis of the secondary structure of pRNA revealed that it contains two structural domains which could fold independently. Its central loop region contains two interlocking loops and is responsible for its intermolecular interactions to form a hexameric ring, as well as its

binding to the procapsid, while its double-helical 5'/3' paired region is essential in DNA packaging (64-68) and for the binding of the ATPase gp16 to bring it into proximity to the connector (60). It has also been revealed that pRNA contains an ATP-binding motif (69), However, pRNA itself does not display ATPase activity. It is expected that the ATPase active center is a complex of the entire motor and the ATPase action is a collective effort. Indeed, in the absence of pRNA, the ATPase activity of the ATPase gp16 is extremely low (2, 69, 69-72, 72).

Additionally, it was revealed that the C18C19A20 bulge in the double-helix domain is vital for DNA packaging; however, it is dispensable for procapsid binding (60, 67, 73). Further study on the role of the CCA bulge in DNA packaging revealed that the size and location rather than the sequence of the bulge are important for the proper orientation of the double-helical domain, which is hypothesized to be pertinent to making the correct contact between gp16 docked on pRNA and the genomic DNA. Lastly, the CCA bulge has been suggested to serve as the fulcrum in which the ATPase uses as a hinge to drive the motor (74).

Packaging ATPase gp16

As previously mentioned, it was recently determined that the packaging ATPase gp16 is a member of the classical AAA+ superfamily of proteins. When evidence of the pRNA hexamer was uncovered, it was proposed by Guo and co-workers (3) and subsequently supported by other authors (3, 16, 75) that viral DNA packaging is similar to the mechanism in DNA replication and RNA transcription, and that the mechanism responsible for those important phenomena can be correlated to the mechanism of viral DNA packaging. Moreover, like almost all DNA and RNA packaging motors, it was hypothesized that gp16, the ATPase in the phi29 packaging motor, belonged to the superfamily of AAA+ proteins (ATPases Associated with many cellular

Activities) (3, 60). Further sequence alignment and computer modelling revealed the critical Walker A (G/A-XXXXGK(T/S)) and Walker B motifs ((R/K)XXXXGXXXXLhhhhD), where G, A, K, T, S, R, L, and D denote glycine, alanine, lysine, threonine, serine, arginine, leucine, and aspartic acid residues respectively, X represents any of the 20 standard amino acids, and h denotes a hydrophobic amino acid. The phosphate-binding loop (P-loop) is typically identified as the ε-NH2 of lysine in the Walker A motif in which the phosphate group of ATP is bound. It was previously shown that any mutations to Walker A motif of phi29 gp16 abolished its ATPase and DNA packaging activity (2). The Walker B motif is typically a β-strand consisting of four hydrophobic acids with a conserved aspartate, which coordinates magnesium, and is usually followed immediately by a conserved glutamate, which is responsible for ATP hydrolysis.

All cellular and dsDNA viral initiators possess a common adenine nucleotide-binding fold belonging to the AAA^{+} family with a ubiquitous characteristic of coupling chemical energy from ATP hydrolysis to mechanical motion. The AAA+ family of ATPases assemble into oligomers, often hexamers, which form ring-shaped structures with a central channel. This large family of proteins are extremely diverse in function associated with a multitude of different cellular activities and implicated in many others. However, the common characteristic of this family is their ability to convert chemical energy from the hydrolysis of the gamma phosphate bond of ATP into a conformational change inside the protein. This change of conformation generates a loss of affinity for the substrate and a mechanical movement, which is used to make or break contacts between macromolecules, resulting in local or global protein unfolding, assembly or disassembly of complexes, or transport of macromolecules relative to each other. These activities underlie processes critical to DNA replication and recombination, chromosome secretion, membrane sorting, cellular reorganization, and many others (76).

In past years, models based on EM reconstruction have suggested gp16 exists as a pentameric structure (15, 77). However, recent biochemical studies on the oligomerization of g16, based on native gel electrophoresis, stoichiometric ratio binding assays, analytical ultracentrifugation, and mutant inhibition studies, have indicated that gp16 is a hexamer in solution (4), with an oligomerization pathway starting from the monomer to form a dimer which assembles into a tetramer and finally a hexamer (4) (Chapter 2). Furthermore, the sequential action among the ATPase and additional motor components is the most important event in force generation. It has been revealed that the contact of ATPase gp16 to ATP resulted in its conformational change to a higher binding affinity toward dsDNA (78). It was also found that ATP hydrolysis led to the departure of dsDNA from the ATPase/dsDNA complex, an action that might be the key step to push dsDNA to move along the connector channel (78) (Chapter 3).

Most recently, the cooperativity among the subunits of the motor ATPase has been revealed (Chapter 4). Hill constant calculations have revealed a sophisticated and coordinated action that involves revolution of the DNA around the gp16 subunits which ultimately contact the inner residues of the connector channel as well. It is believed this simple method of 'handing off' the DNA substrate around the motor ATPase leads to sequential steps of packaging. Furthermore, motion of the ATPase gp16 along the DNA has also been observed and is suggested to represent the force generation step in an active phage.

"Push Through a One-Way Valve" Revolution Mechanism for Viral DNA Packaging

DNA packaging into a preformed protein shell (procapsid) is a characteristic of dsDNA viruses in bacteriophages, herpesviruses, and adenovirues. Most viral procapsids are a few tens of nanometers in diameter, while the viral genomes are several micrometers in length. EM images revealed that the packaged viral DNA inside the small procapsid can be condensed to 500

mg/mL, comparable to near liquid crystalline density (79, 80). High internal pressure exists inside the procapsid during DNA packaging (36, 37, 81, 82), and this energetically unfavorable process is accomplished by packaging motors powered by ATP hydrolysis through a DNA and procapsid dependent ATPase (2, 5).

As stated previously, we have recently revealed that both the pRNA and the ATPase gp16 of bacteriophage phi29 DNA packaging motor are hexameric, and DNA packaging is accomplished via a "Push through One-way valve" mechanism. In this proposed model, the ATPase gp16 pushes dsDNA through the static connector channel section by section into the procapsid. The dodecameric connector channel functions as a valve that only allows the dsDNA to enter but not exit the procapsid during DNA packaging. Although the roles of the ATPase gp16 and the motor connector channel are separate and independent, pRNA bridges these two components to ensure the coordination of an integrated motor.

Our data indicates that ATP induces a conformational change in gp16, leading to its stronger binding to dsDNA. Furthermore, ATP hydrolysis led to the departure of dsDNA from the ATPase/dsDNA complex, an action used to push dsDNA through the connector channel. Many packaging models have been contingent upon the number of base-pair packaged per ATP relative to helical turns for B-type DNA. Both 2 and 2.5 base pairs per ATP have been used to argue for four, five or six discrete steps of DNA translocation. The "Push through One-way Valve" mechanism again raises the question of dsDNA packaging energy calculations and provides insight into the discrepancy between 2 and 2.5 bp per ATP as previously calculated. It is suggested that the number of base pairs per consumed ATP is directly related to not only the pushing action of gp16 but the contact of dsDNA with the interior channel of the connector.

Conclusions

In the next three chapters, it will become evident how the research presented lends to the hypothesis of the overall dissertation. In Chapter 2, the stoichiometry of the ATPase is thoroughly examined and determined empirically to be hexameric. Chapter 3 focuses on the sequential action of the ATPase with its two main ligands, DNA and ATP. Finally, Chapter 4 culminates all the data from the previous two chapters, provides new insights into the cooperativity of the ATPase, and suggests a simple mechanism for DNA translocation into the head of the phage.

Chapter 2. The Hexameric Fold of the Packaging ATPase

This chapter (with some modification) is in press at *Virology* under the title "The ATPase of the Phi29 DNA Packaging Motor is a member of the Hexameric AAA+ Superfamily". Special thanks to Dr. Gian Marco De Donatis for help in preparation of data for figures 2.3 and 2.4; Dr. Huaming Fang for help in preparation of data for figures 2.3 and 2.5; and Lei Lin for help in preparation of data for figure 2.2B.

Abstract

The AAA+ superfamily of proteins is a class of motor ATPases with variety of functions and typically exist as hexamers. The ATPase gp16 of phi29 DNA packaging motor has long been a subject of debate concerning stoichiometry and mechanism of action. Here, we confirmed the stoichiometry of phi29 motor ATPase as a hexamer and provide strong data to suggest that this ATPase is a member of the classical hexameric AAA+ superfamily. Native PAGE, EMSA, capillary electrophoresis , ATP titration, and binomial distribution assay revealed the stoichiometry of the ATPase as hexamer. Mutations to the consensus ATPase motifs validated our previous assumptions that the protein exists as another member of this AAA+ superfamily. Our data also supports the finding that the phi29 DNA packaging motor uses a revolution mechanism without rotation or coiling.

Introduction

The superfamily of AAA+ motors (ATPases Associated with diverse cellular Activities) plays a key role in several assorted functions, and many members of this clade of ATPases often fold into hexameric arrangements (24, 83). Despite their diversity, the common characteristic of this family is their ability to convert chemical energy from the hydrolysis of the γ-phosphate bond of ATP into a conformational change inside the protein. This change of conformation generates a loss of affinity to its substrate and a mechanical movement, which in turn is used to either make or break contacts between macromolecules, resulting in local or global protein unfolding, assembly or disassembly of complexes, or transport of macromolecules relative to each other. These activities underlie processes critical to DNA repair, replication, recombination,

chromosome segregation, dsDNA transportation, membrane sorting, cellular reorganization, and many others (22, 23).

DsDNA viruses package their DNA genome into a preformed protein shell called a procapsid, with the aid of a nanomotor (33, 38, 44, 84). Since 1978, it has been popularly believed that viral DNA-packaging motors run through a five-fold/six fold mismatch rotation mechanism (12). An RNA component (pRNA) was discovered on the phi29 DNA packaging motor (1), and subsequently, pRNA was determined to exist as a hexameric ring (3, 27). Based on this structure, it was proposed that the mechanism of the phi29 viral DNA packaging motor is similar to that used by other hexameric DNA tracking motors of the AAA+ family of proteins (3). A fervent debate subsequently developed concerning whether the RNA and ATPase of the motor exist as hexamers (3, 27, 30, 31, 33, 63, 85) or as pentamers (15, 86). The differing viewpoints have not yet been fully reconciled, but we have recently shown by X-ray diffraction, AFM imaging, and single molecule studies that the motor consists of three-coaxial rings geared by hexameric pRNA (63) (Figure 2.1). The force generation mechanism of the phi29 DNA packaging motor is still under scrutiny (15, 33, 41, 44, 45, 78, 87).

The phi29 DNA packaging motor reconstituted in the defined system over twenty years ago (5) is one of the most well-studied biomotor systems and has also proven to be one of the most powerful molecular motors (36, 37), capable of generating forces up to 57-110 pN. The DNA packaging mechanism has been scrutinized extensively and is still under fervent debate (3, 18, 19, 27, 28, 30, 36, 80, 87-100). The motor is composed of a dodecameric connector at the vertex of the procapsid, geared by a pRNA ring (1) which encircles the N-terminus of the connector (31, 101, 102) , and a ring of gp16 which functions as an ATPase to drive the motor (2, 72). The connector was recently revealed to only allow for unidirectional movement of

dsDNA (41), and a model using a "push through a one-way valve" mechanism was described (44, 78) which agrees nicely with the previously proposed ratchet (103) and compression (104, 105) models. This mechanism describes dsDNA as being pushed through the connector channel by the ATPase gp16 while the connector functions like a valve to prevent DNA from slipping out of the capsid during the packaging process (38, 39, 84, 106). This entropically unfavorable process is accomplished by a DNA-packaging motor that uses ATP as an energy source.

The ATPase gp16 is the most pivotal part of the phi29 DNA packaging motor. It provides energy for the motor by hydrolyzing ATP, converting energy obtained from breaking a chemical bond into physical motion. This enzyme possesses the typical Walker A and Walker B motifs (2) as in many other well-characterized AAA+ proteins (107, 108). The protein has been shown to bind to the 5'/3' paired helical region of pRNA (60, 109), and furthermore, its ATPase activity could be stimulated by both pRNA and DNA (2, 70-72). Intermediates in DNA packaging have been isolated (36, 46, 109, 110), and models of gp16 supercoiling dsDNA have been proposed (13, 109).

Here, the oligomeric state of the ATPase has been extensively investigated in order to better understand the DNA translocation mechanism. We conclusively determined that the motor ATPase forms a hexamer in a concentration dependent manner and upon binding to its substrate dsDNA. Furthermore, the major motifs of the ATPase have now been identified and we have shown through mutation analysis that the phi29 ATPase is a member of the hexameric AAA+ superfamily.

Materials and Methods

Cloning, mutagenesis and protein purification

The engineering of eGFP-gp16 and the purification of gp16 fusion protein have been reported previously (111). The eGFP-gp16 mutants G27D, E119A, and D118E E119D were constructed by introducing mutations to the gp16 gene (Keyclone Technologies, Cincinnati, OH).

Measurement of gp16 ATPase activity

Enzymatic activity *via* fluorescent labeling was described previously (70). Simply, a phosphate binding protein conjugated to a fluorescent probe which senses the binding of phosphate was used to assay ATP hydrolysis.

In vitro virion assembly assay

Purified *in vitro* components were mixed and subjected to the virion assembly assay as previously described (112). Briefly, newly assembled infectious virions were inoculated with *Bacillus* bacteria and plated. Activity was expressed as the number of plaques formed per volume of sample (pfu/mL).

Statistical analysis and data plotting.

Most statistical analysis was performed using Sigmaplot 11. The Hill coefficient was determined by nonlinear regression fitting of the experimental data to the following equation: $E= E_{max}*(x)^n/(k_{app} +(x)^n)$, where E and E_{max} refer to the concentration of the gp16/DNA complex, X is the concentration of ATP or ADP, K_{app} is the apparent binding constant, and n is the Hill coefficient.

CE experiments to determine ratio of gp16 to bound dsDNA

CE (capillary electrophoresis) experiments were performed on a Beckman MDQ system equipped with double fluorescent detectors (at 488 nm and 635 nm excitation wavelength). A bare borosilicate capillary with a total length of 60 cm and a 50 μm inner diameter was used. The method used consisted of a 20 min separation at 30 kV constant polarity. Assay conditions contained separation buffer of 50 mM Tris-HCl 100 mM borate at pH 8.00, 5 mM $MgCl_2$, 10% PEG 8000 (w/v), 0.5% acetone (v/v), 3 μM eGFP-gp16 monomer, and variable amounts of ATP/ADP and DNA.

Native PAGE of eGFP-gp16

Increasing amounts of eGFP-gp16 were loaded onto a 6% tris-glycine polyacrylamide gel in conjunction with the Native PAGE Mark kit (Invitrogen, Grand Island, NY). This commercially available Native PAGE Mark .uses a non-denaturing detergent to mildly solubilize and coat the protein with a negative charge. Thus, the expectation of the gel is to separate solely on the basis of mass. The gel was imaged using a Typhoon gel image scanner at an excitation wavelength of 488 nm.

Atomic Force Microscopy (AFM) imaging

APS mica was obtained by incubation of freshly cleaved mica in 167 nM 1-(3-aminopropyl) silatrane. The details of APS mica surface modification are described elsewhere (113, 114). The native PAGE purified RNA samples were diluted with 1xTMS buffer to a final concentration of 3-5 nM. Then, 5-10uL of pRNA was immediately deposited on APS mica. After 2 min incubation on the surface, excess samples were washed with DEPC treated water and dried under a flow of Argon gas. AFM images in air were acquired using MultiMode AFM NanoScope

IV system (Veeco/Digital Instruments, Santa Barbara, CA) operating in tapping mode. Two types of AFM probes were used under tapping mode imaging in air: (1) regular tapping Mode Silicon Probes (Olympus from Asylum Research, Santa Barbara, CA) with a spring constant of ~42 N/m and a resonant frequency between 300-320 kHz. (2) non-contact NSG01_DLC probes (K-Tek Nanotechnology, Wilsonville, OR) with a spring constant of about 5.5 N/m and a resonance frequency between 120-150 kHz.

Electrophoretic Mobility Shift Assay (EMSA)

The engineering of eGFP-gp16 and the purification of gp16 fusion protein have been reported previously (111). The fluorescently tagged protein that facilitates detection and purification was shown to possess similar assembly and packaging activity as compared to wildtype (78, 111).

Cy3-dsDNA (40 bp) was prepared by annealing two complementary DNA oligos containing a Cy3 label (Integrated DNA Technologies, Coralville, Iowa) at its 5' ends and purified by a 10% polyacrylamide gel. Samples were prepared in 20 μl buffer A (20 mM Tris-HCl, 50 mM NaCl, 1.5% glycerol, 0.1 mM Mg^{2+}). Specifically, 1.78 μM eGFP-gp16 was mixed with 7.5ng/μl of 40bp Cy3-DNA in the presence or absence of ATP and γ-S-ATP. Samples were incubated at ambient temperature for 20 min and then loaded onto a 1% agarose gel (44.5 mM Tris, 44.5 mM boric acid) and electrophoresed at 4°C for 1 hr at 8 V/cm. The eGFP-gp16 and Cy3-DNA samples were analyzed by a fluorescent LightTools Whole Body Imager using 488 nm and 540 nm excitation wavelengths for GFP and Cy3, respectively.

Results

Phi29 DNA packaging motor contains three coaxial rings

The phi29 DNA packaging motor consists of three major structural components: the connector, pRNA, and ATPase gp16 (Figure 2.1). Extensive studies (27, 30, 31, 62, 85, 115-117) of the pRNA and recent crystal structure (63) has revealed that pRNA exists as a hexamer, as also confirmed by AFM (58). This demonstrated that the three coaxial rings are connected to each other with appropriate stoichiometry.

Native PAGE, EMSA, and CE Reveal Hexameric ATPase

Fusion of eGFP to the N-terminus of gp16 resulted in fluorescent gp16 (eGFP-gp16) that showed similar biological activity as native gp16 (111). eGFP-gp16 produced six distinct fluorescent bands on a native PAGE gel, indicative of six monomers oligomerizing to form a hexameric quaternary complex (Figure 2.2A). In this experiment, we used the commercially available Native PAGE Mark from Invitrogen, which uses a non-denaturing detergent to mildly solubilize and coat the protein with a negative charge. Thus, the expectation of the gel is to separate solely on the basis of mass. In our gel of eGFP-gp16, the monomer and all even numbered oligomer bands had a higher intensity than the trimer and pentamer, suggesting that the assembly sequence is monomer to dimer to tetramer, and finally to hexamer, and that the final gp16 oligomeric state is likely a trimer of dimers, as seen in other ATPases (118, 118-120). In addition, as the concentration of gp16 was increased, the intensity of the hexamer band increased significantly, while the intensity of smaller oligomers remained fairly constant. This also suggests that a hexamer is the final oligomeric state. The presence of eGFP-gp16 hexamer was further confirmed by stoichiometric ratio assays.

Electrophoretic mobility shift assays (EMSA) were employed with the fluorescent eGFP-gp16 and with a short 40 bp dsDNA fragment conjugated with a cy3 fluorophore. The two components were mixed together, along with ATP and a non-hydrolyzable ATP analog (γ-S-ATP) (Figure 2.2B). It was evident that the ATPase preferred tight binding to the dsDNA upon addition of γ-S-ATP (Figure 2.2B, lane 6) as observed previously (78). Furthermore, after addition of ATP to the gp16:DNA complex, two distinct ATPase bands were present in the gel (Figure 2.2B, lanes 7,8).

The EMSA was used again with increasing amounts of ATPase and a fixed amount of dsDNA to determine the stoichiometry of the ATPase bound to dsDNA. As the molar concentration ratio of gp16:dsDNA reached 6:1, free dsDNA (bottom band, Figure 2.3A Cy3 channel) shifted nearly entirely to the bound state (top yellow band, lane 6). Furthermore, capillary electrophoresis was used to validate the qualitative EMSA data. In this case, the amount of gp16 remained constant, mainly due to the stickiness of the protein in the small capillary, and the dsDNA was increased sequentially in the reaction mixture. The fluorescent peak corresponding to DNA bound to protein was quantified for a range of dsDNA concentrations. The quantified peaks were then plotted for bound DNA against total amount of DNA. The plot reached a plateau at a bound DNA concentration of 0.5 μM, representing a concentration 6 times less than the total ATPase concentration (Figure 2.3B).

Mutations to known motifs suggest that phi29 gp16 is a member of the AAA+ Superfamily of ATPases

Gp16 shares the common ATP binding domain typical of all AAA+ proteins. This domain contains very well-conserved motifs responsible for ATP binding (Walker A and

Arginine finger) and ATP hydrolysis (Walker B). Previously (2), the walker A motif has been identified, but the walker B motif remained elusive. Sequence alignment to other known AAA+ proteins was subsequently performed to identify this ambiguous motif. From the alignment, the position of the walker B motif (residues 114-119) was identified. The sequences correlated well with the known consensus sequence for these motifs. Gp16 follows the normal walker B configuration hhhhDE identified as TIVFDE.

To confirm the results of the sequence alignment, relevant amino acids of both motifs were subsequently mutated. In the walker B motif, two mutations were generated: E119A single mutant and D118E/E119D double mutant, as it is known that the most important residues are the Asp for its role in magnesium ion binding and the glutamate responsible for the activation of a water molecule to perform a nucleophilic attack on the gamma phosphate of ATP. Both mutants were tested for their ability to hydrolyze ATP and to bind DNA.

In Figure 2.4A, both mutants were subjected to the ATP hydrolysis assay previously described (70). Only the wildtype ATPase was capable of hydrolyzing ATP to ADP and inorganic phosphate as the Walker A mutant is incapable of binding ATP while the Walker B mutant can bind, but not hydrolyze the substrate. We expanded our testing of the mutations in terms of DNA binding. Again using the same capillary electrophoresis as in our previous assay of wildtype ATPase, we quantified the DNA bound peak of both mutants. In the presence of γ-S-ATP, the wildtype and Walker B mutant displayed similar DNA binding affinity. However, upon addition of ATP, the wildtype no longer remains bound to DNA as previously shown (78), but the Walker B mutant retains its DNA binding capability, suggesting that this identified motif is in fact responsible for the catalytic step which pushes dsDNA away from gp16 upon hydrolysis.

Lastly, we attempted to validate our findings using EMSA (Figure 2.4C). Again, the wildtype ATPase exhibits high affinity to dsDNA with addition of γ-S-ATP (lane 3), but diminished affinity with ATP or no phosphate analog (lanes 2,4). The Walker A mutant has diminished binding affinity in all cases (lanes 5-7), albeit higher affinity with addition of γ-S-ATP, as this mutant is incapable of binding ATP which stabilizes the interaction between gp16 and dsDNA. Finally, the Walker B mutant which previously has been shown to be incapable of hydrolyzing ATP, was incapable of binding without ATP (lane 8), but exhibited high affinity with both ATP and γ-S-ATP (lanes 9,10). Both the capillary electrophoresis quantification and the EMSA confirmed our hypothesis that the recently discovered Walker B motif of phi29 ATPase is responsible for ATP hydrolysis.

Binomial Inhibition Functional Mutant Assays Validate Hexameric ATPase

Formation of gp16 as an active hexameric complex in phi29 DNA packaging was further demonstrated using a Walker B mutant gp16, and was analyzed by binomial distribution (62, 117). A mutant eGFP-gp16 (amino acid residues D118 and E119 were mutated to E and D, respectively) was found to be completely inactive in DNA packaging. The mutant was mixed with wild-type eGFP-gp16 in different ratios ranging from 10% to 90%, and the activity of the complex was assayed using the *in vitro* viral assembly system (Figure 2.5) (112). The dominant inhibitory activity of the Walker B mutant allowed an independent means of determining the stoichiometry of the ATPase (62).

In our trials, we assumed that the stoichiometry, Z, of the ATPase gp16 in the complex was between 1 and 12. Then, different concentrations of wildtype gp16 were mixed with the inactive Walker B mutant and used for *in vitro* assembly reactions. We used a binomial

distribution of $(p+q)^z$, where p and q represent the ratio of wildtype and mutant subunits within the gp16 oligomer, respectively (62). Following the expansion of the binomial, we generated 12 theoretical curves corresponding to the stoichiometry of 1 to 12 using the plot of motor activity (in this case, production of phi29 virion against the ratio of the Walker B mutant. The empirical data almost perfectly overlapped with the theoretical curve in slope and shape representative of a stoichiometry of 6, thereby confirming that the motor complex is hexameric (Figure 2.5).

Discussion

Similar to the AAA+ motor proteins that undergo a cycle of conformational changes during their interaction with ATP and adaptation of two distinct states, the phi29 motor ATPase also exists in either a high or low affinity state for DNA substrate. Recently, it has been qualitatively demonstrated *via* EMSA (78) that the ATPase gp16 is capable of binding to dsDNA in the presence of γ-S-ATP. Fusion of a fluorescent tag on the ATPase did not affect its function or activity (111), but provided a marker for binding assays. In the previous report, a small amount of Cy3-dsDNA was bound by eGFP-gp16 using the EMSA. However, stronger binding of gp16 to dsDNA was observed when gp16 was incubated with γ-S-ATP and dsDNA (78). To further validate the finding, two different assays were utilized. Forster Resonance Energy Transfer (FRET) analysis revealed an increase in energy transfer from eGFP-gp16 to Cy3-dsDNA when γ-S-ATP was included, as compared to the sample in the absence of γ-S-ATP. Furthermore, when γ-S-ATP was added to the mixture, sedimentation studies utilizing a 5-20% sucrose gradient revealed that the gp16-dsDNA complex was highly prevalent, as indicated by the overlap of the peak locations for the eGFP and Cy3 signals. These results suggest that the gp16/dsDNA complex is stabilized through the addition of the non-hydrolyzable ATP substrate.

The data confirmed that gp16 possesses both a DNA binding domain and a Walker-A motif with which to bind ATP (78).

However, the Walker B motif has previously been unidentified. By sequence homology and point mutation analysis, this motif has now been shown to be responsible for ATP hydrolysis in the ATPase of phi29. As expected, all the mutants were severely impaired in ATP hydrolysis activity and were similar to the Walker A mutant G27D, proving that the Walker A motif is responsible for binding of ATP. Regarding the ability to bind to DNA in the presence of γ-S-ATP, mutations in the walker A motif displayed a limited ability to bind DNA compared with the wild-type (Figure 2.4B,C), most likely due to their impaired affinity for γ-S-ATP. On the contrary, the walker B mutants retained their binding affinity for DNA in the presence of γ-S-ATP and were also sufficient to bind DNA in the presence of ATP, confirming that the Walker B mutation only affects the ability to hydrolyze ATP but not the binding to the nucleotide.

Our data shows that in the absence of ATP, or its derivative γ-S-ATP, the binding of gp16 to DNA is nearly undetectable. However, after the addition of γ-S-ATP the binding efficiency of gp16 to DNA increased significantly (Figure 2.4B,C). This suggests that ATP induces a conformational change in gp16 that causes it to assume a high affinity conformation for dsDNA binding. The conformational change was abolished after introducing a mutation to the Walker A motif in which the ATPase activity was undetectable due to the inability of the Walker A mutant to bind ATP. More significantly, when ATP was added to the gp16-γ-S-ATP-dsDNA complex, rapid ATP hydrolysis was observed (78) and gp16 departed from the dsDNA. This indicates that after hydrolysis, gp16 undergoes a further conformational change that produces an external force against the dsDNA that pushes the substrate away from the motor complex by a power stroke. This phenomenon can be seen in Figure 2.2B in which the ATPase

exists as two states after addition of ATP: DNA bound or expelled. However, introducing a mutation to the Walker B motif eliminated the catalytic force step. The data correlates nicely with other reports that Walker B mutants do not hydrolyze ATP, but bind strongly to DNA.

Previously, it was determined that gp16 is a DNA-dependent ATPase of the phi29 DNA packaging motor (2, 70, 72), providing energy to the motor through the reaction in which ATP is hydrolyzed into ADP and inorganic phosphate. As aforementioned, non-hydrolyzable γ-S-ATP stalled and fastened the gp16/dsDNA complex. It has been found that the hydrolysis of ATP leads to the release of dsDNA from gp16. After ATP was added to the gp16/dsDNA/γ-S-ATP complex, the band representing the gp16/dsDNA complex disappeared (78). ADP has a lesser effect on dsDNA release, whereas AMP is unable to release dsDNA from gp16. The release of dsDNA from the gp16/dsDNA/γ-S-ATP complex by ATP and ADP was also demonstrated by sucrose gradient sedimentation. The binding of eGFP- gp16 to dsDNA was evidenced with a shift in the DNA profile in the presence of γ-S-ATP, and in the absence of ATP. But, with low concentrations of ATP, gp16 and dsDNA existed as free molecules in solution with slower sedimentation rates (78). To investigate the mechanism further, the gp16/dsDNA/γ-S-ATP complex was purified using a sucrose gradient and subjected to an ATP hydrolysis kinetic assay. The hydrolysis of ATP to ADP and inorganic phosphate was confirmed when the purified gp16/dsDNA/γ-S-ATP hydrolyzed ATP after the addition of ATP to the purified complex. These results suggested that hydrolysis of ATP leads to the release of dsDNA from the gp16, forcing the DNA substrate away from the interior pocket of the ATPase, and lending to physical motion of genomic DNA towards the capsid.

Our data combining the stoichiometry of the ATPase and the sequential action previously elucidated (78), allows us to build upon our previous “push through a one-way valve” DNA

packaging model. We propose in Figure 6 that the hexamer formation is dependent upon ATP and the concentration of the ATPase. After binding to ATP, the ATPase undergoes a conformational change which significantly increases its affinity to dsDNA. An additional conformational change of the ATPase after release of inorganic phosphate causes gp16 to perform a power stroke to push dsDNA into the one-way valve of the portal protein.

The stoichiometry of the phi29 DNA packaging has long been a subject of debate; however, both camps believe that the ATPase and pRNA exist in a 1:1 stoichiometric ratio. Substantial cryo-EM data has been published suggesting a pentameric symmetry, but a significant amount of quantification and sequence alignment have suggested the hexameric fold (see Introduction). Here we show further biochemical data proving that the ATPase gp16 consists of six subunits in a concentration dependent manner (Figure 2.2A), upon binding to dsDNA (Figure 2.3), and on the active phi29 motor (Figure 2.5). Furthermore, we have identified the classical Walker motifs typical of the hexameric AAA+ superfamily, and found that phi29 DNA packaging motor uses a revolution without rotation and coiling or generation of torque (34). We show that the ATPase "hands off" the substrate dsDNA in a sequential action manner lending to revolution around the ATPase and connector protein (34). Our data leads to the conclusion that the hexameric stoichiometry and the mechanism of revolution for phi29 DNA packaging motor are in accordance with FtsK of the hexameric AAA+ superfamily, and we expect that most phages follow this "push through a one-way valve" via revolution mechanism (34).

Acknowledgements

We would like to thank Dr. Guo-Min Li for his valuable comments; Yi Shu, Luda Shlyakhtenko, and Yuri Lyubchenko for the AFM images of pRNA hexamer; Zhengyi Zhao,

Emil Khisamutdinov, and Hui Li for their diligent work on the animation figures; and Jeannie Haak for editing this manuscript. The work was supported by NIH grants R01 EB012135, and U01 CA151648 to PG, who is a co-founder of Kylin Therapeutics, Inc, and Biomotor and Nucleic Acids Nanotech Development, Ltd.

Figures

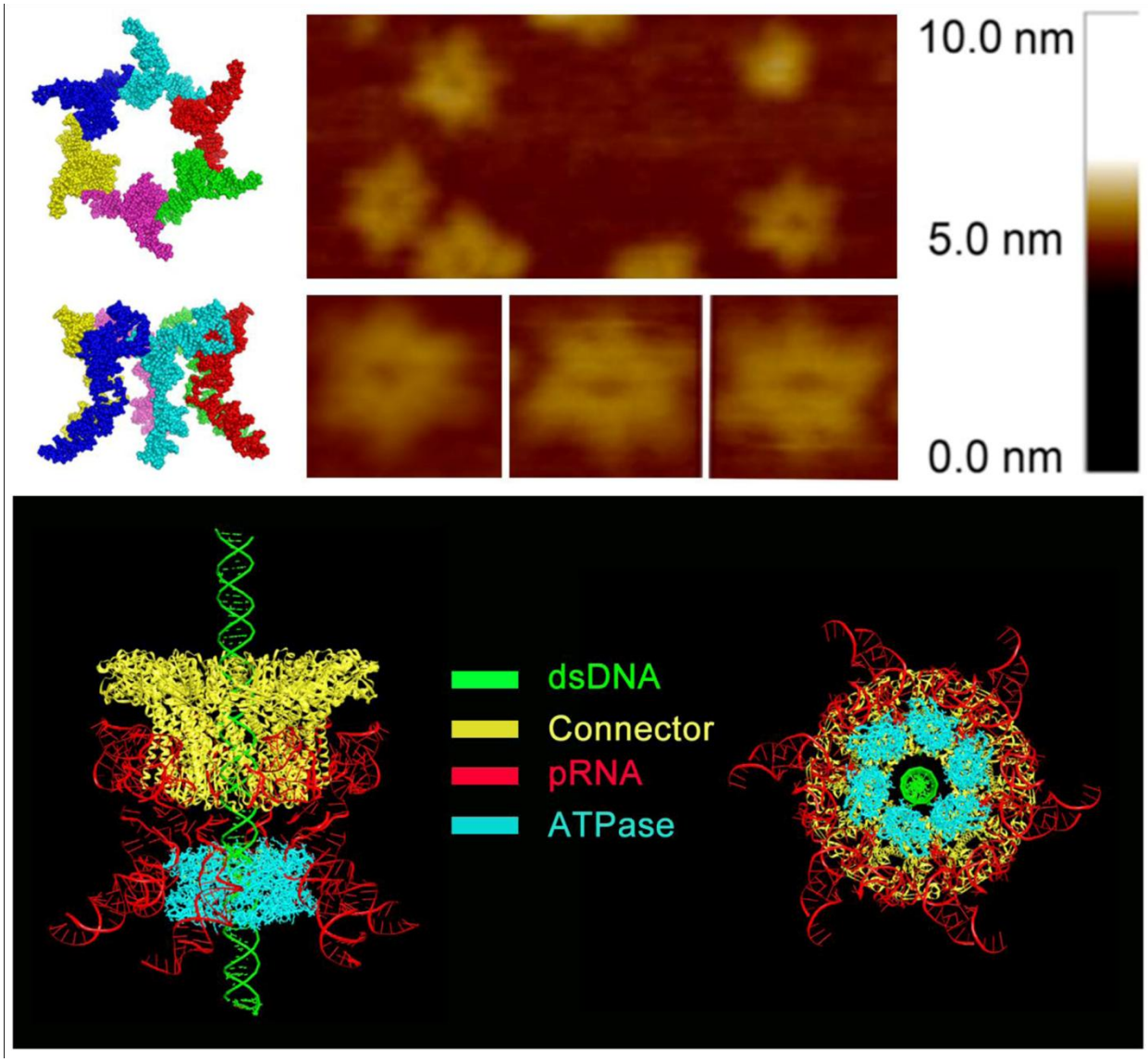

Figure 2.1. Depiction of the phi29 DNA-packaging motor structure and function. A schematic of hexameric pRNA (left, top) and AFM images of loop-extended hexameric pRNA (top, right). Illustrations of the phi29 DNA packaging motor and a pRNA hexamer: Side view (bottom, left) and bottom view (bottom, right).

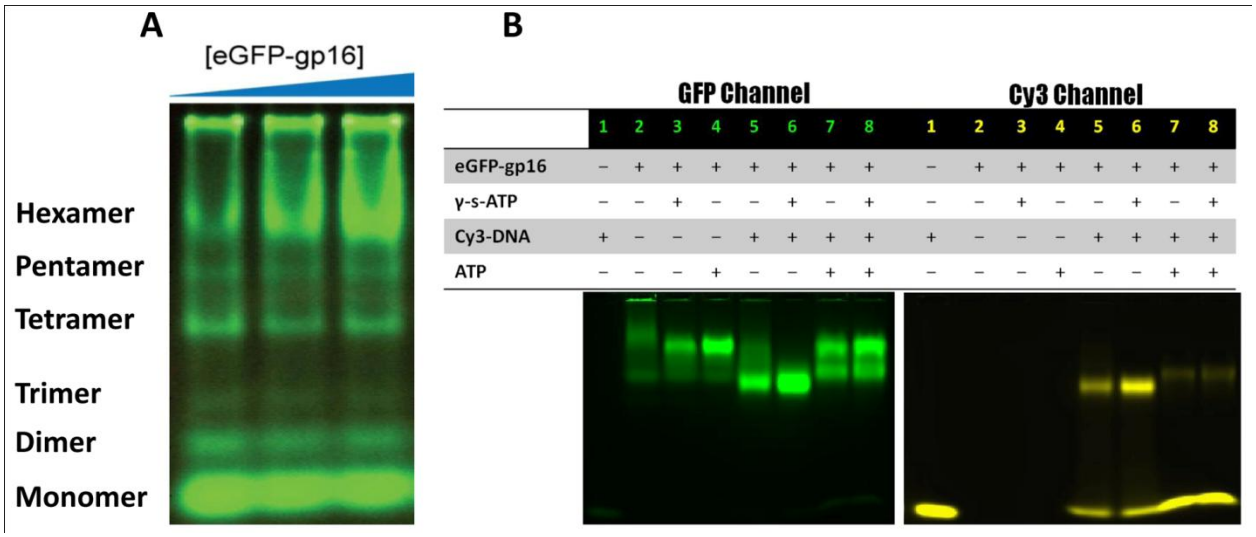

Figure 2.2. Native electrophoresis of eGFP-gp16. (**A**) 6% native PAGE reveals distinct bands characteristic of six oligomeric states; the top, hexameric band increased as the concentration of protein is increased. Oligomeric states were assigned based on the mobility of marker proteins in the Native PAGE Mark kit. (**B**) EMSA of native eGFP-gp16 with short, 40 bp Cy3-dsDNA and ATP or γ-S-ATP. The GFP channel (left) shows migration of the ATPase, whereas the Cy3 channel (right) indicates the migration of the dsDNA. Two distinct states of ATPase exist after addition of ATP to the gp16:DNA complex.

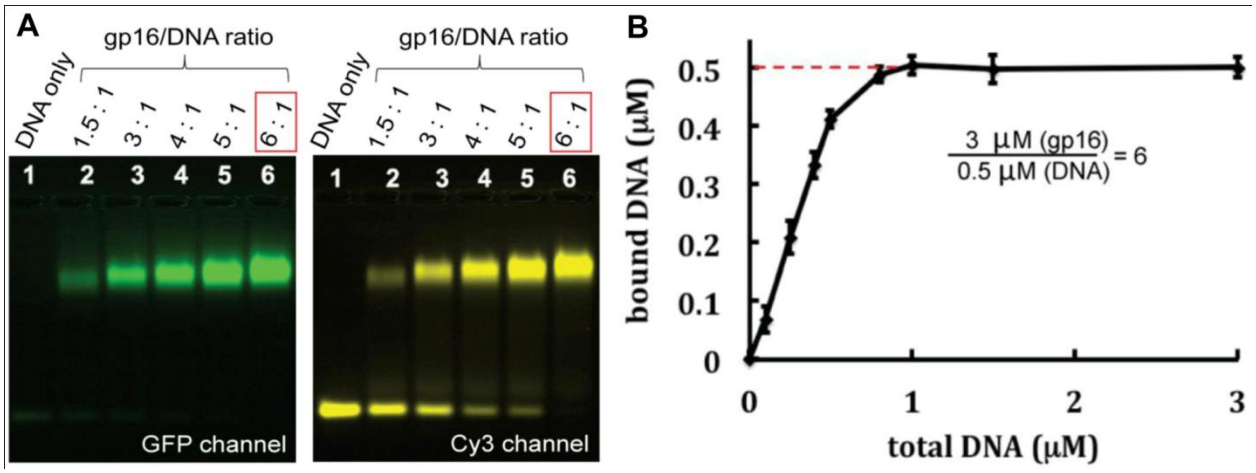

Figure 2.3. ATPase gp16 binds to DNA in a 6:1 molar ratio. Titration using EMSA of gp16 into dsDNA mixture (**A**) where free dsDNA band disappears (bottom right) as the molar ratio of gp16:dsDNA reaches 6:1. Titration of dsDNA into gp16 mixture using capillary electrophoresis (**B**) where peaks were quantified and plotted as a ratio of total DNA versus bound DNA. The plot plateaus at 0.5 μM despite addition of more dsDNA, a concentration 6 times less than the fixed molar concentration of ATPase gp16.

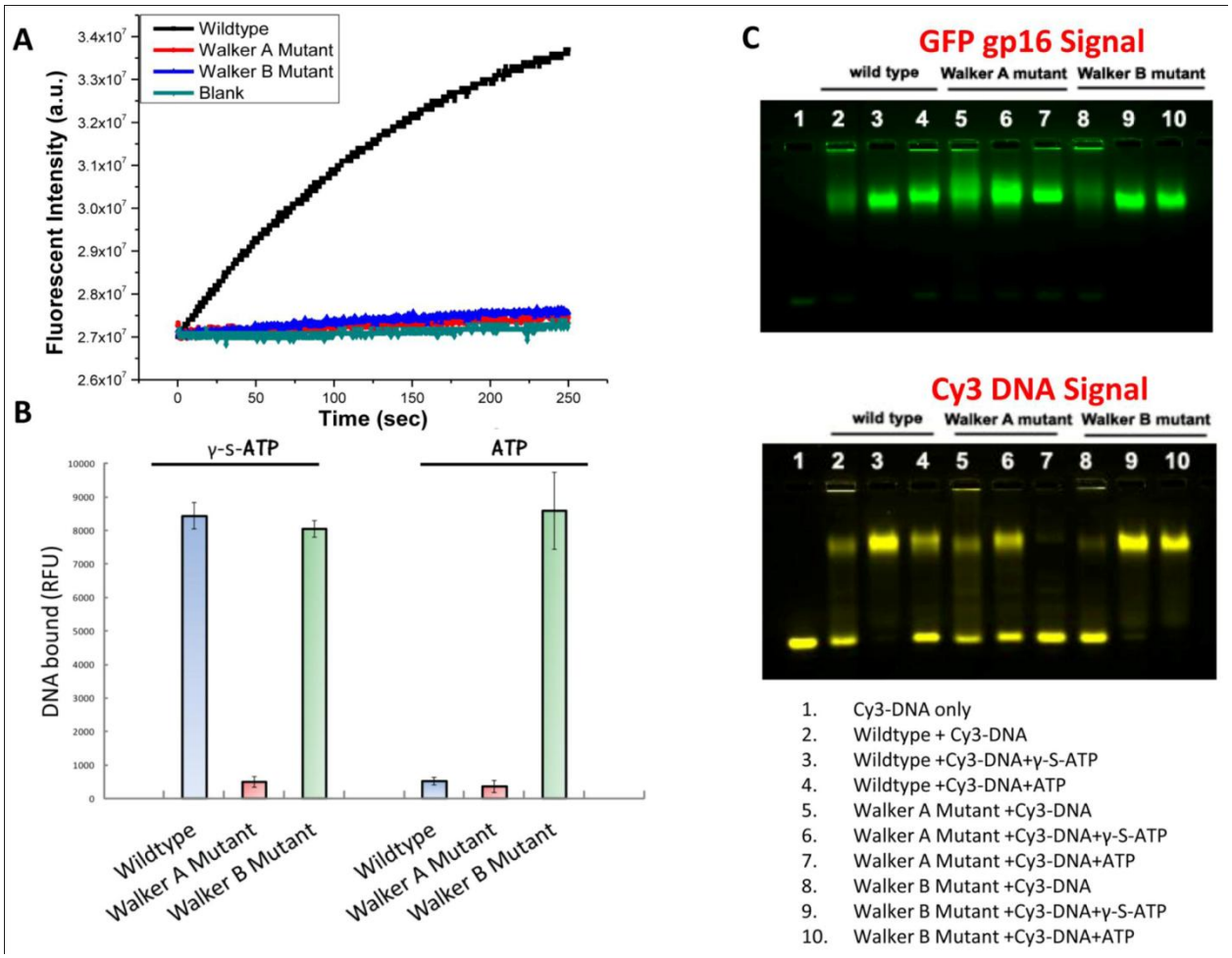

Figure 2.4. ATPase gp16 contains a typical Walker A and Walker B motif of the AAA+ family. Assay of ATPase gp16 for ATPase activity as described previously (70) (**A**). Mutations to the Walker A and Walker B motif terminate the ability of the ATPase to hydrolyze ATP. Capillary electrophoresis quantification of dsDNA binding to mutated and wildtype ATPase gp16 (**B**). Walker B mutant retains binding capability to dsDNA despite addition of ATP. EMSA of mutated and wildtype ATPase **(C**). DNA binding is diminished with mutations to the Walker A motif but is retained in the Walker B mutant with addition of ATP or γ-S-ATP.

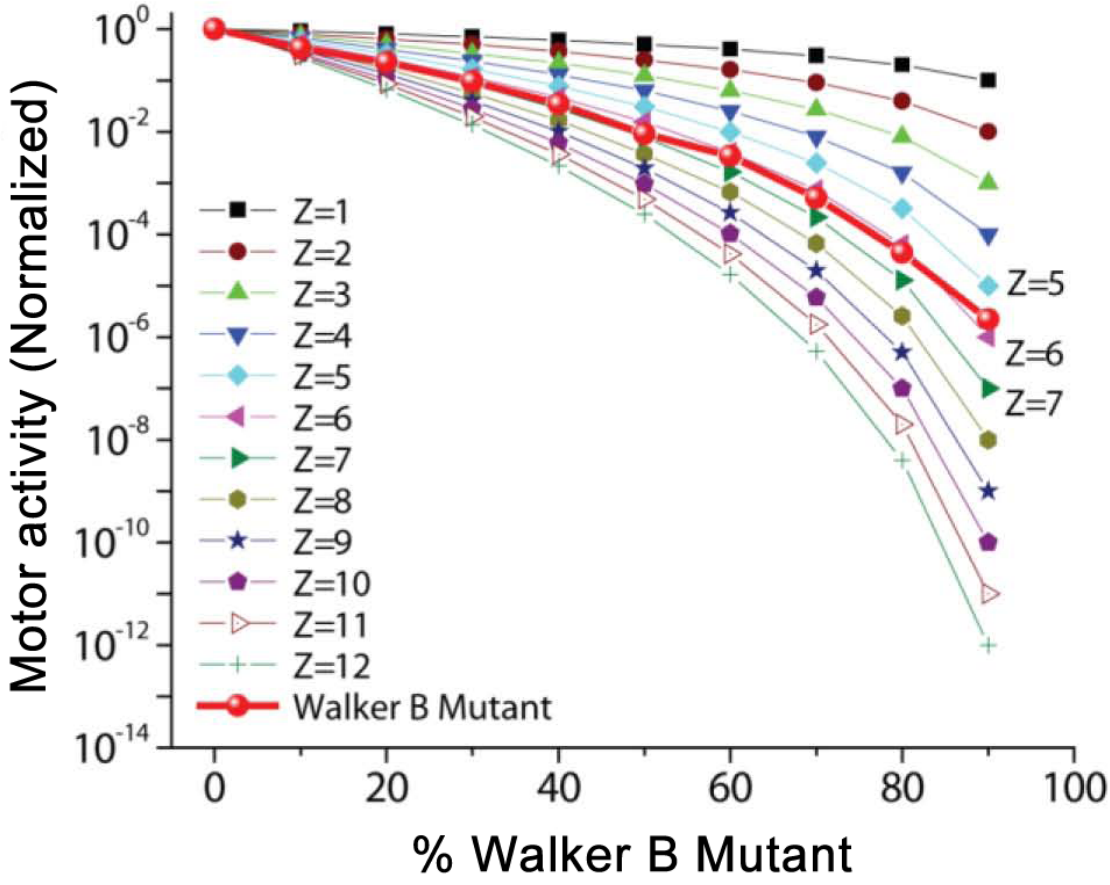

Figure 2.5. Viral assembly inhibition assay using a binomial distribution revealing that gp16 possesses a 6-fold symmetry in the DNA packaging motor (62)**.** Theoretical plot of percent Walker B mutant gp16 versus yield of infectious virions in *in vitro* phage assembly assays. Predictions were made with equation

$$(p+q)^Z = \binom{Z}{0}p^Z + \binom{Z}{1}p^{Z-1}q + \binom{Z}{2}p^{Z-2}q^2 + \cdots + \binom{Z}{Z-1}pq^{Z-1} + \binom{Z}{Z}q^Z = \sum_{M=0}^{Z}\binom{Z}{M}p^{Z-M}q^M ,$$

where p is the percentage of wild type eGFP-gp16 based on the molar concentration in solution; q is the percentage of eGFP-gp16/ED; Z, is the total number of eGFP-gp16 per procapsid or gp3-DNA; M is the theoretical number of mutant eGFP-gp16 in the phi29 DNA packaging motor; and p+q=1 (62).

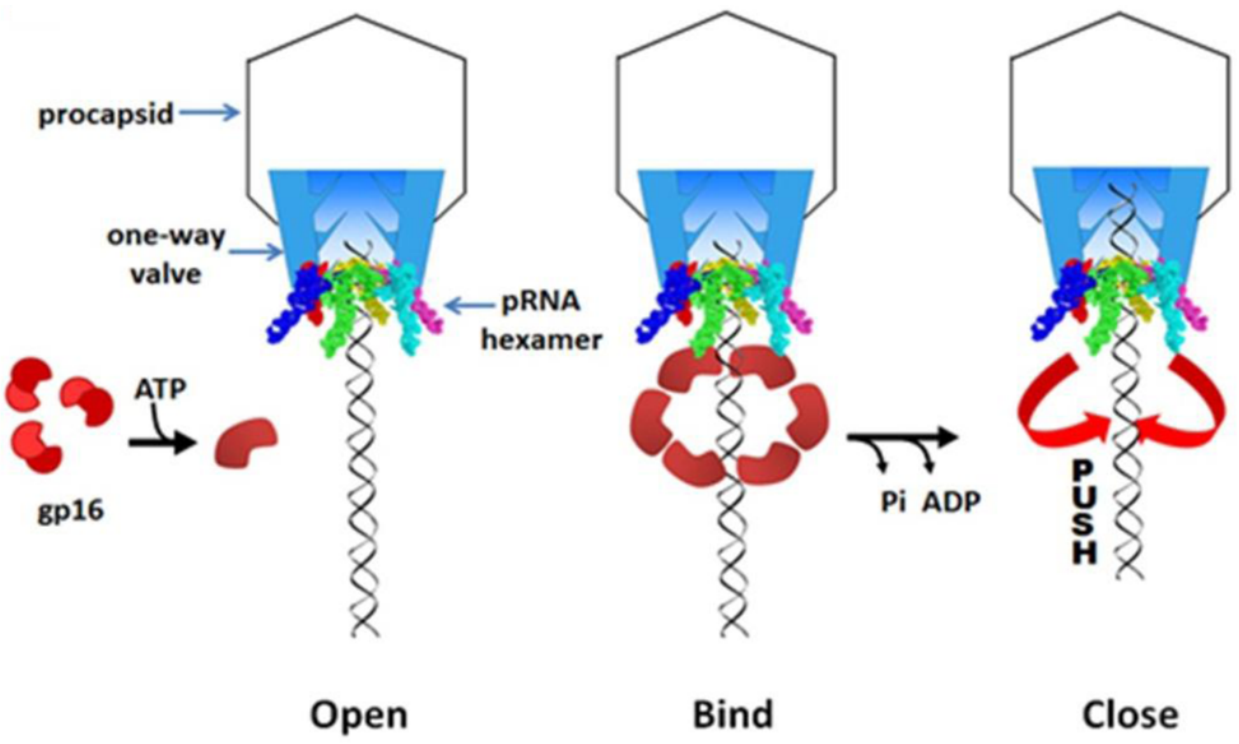

Figure 2.6. Hexameric Push through a One-Way valve mechanism (78). A conformational change in the hexameric ATPase occurs subsequently after binding to ATP which confers an increase in binding affinity to dsDNA. Release of inorganic phosphate from the ATPase complex results in a power-stroke to push the genomic dsDNA through the one-way valve of the connector portal protein into the capsid shell.

Chapter 3. Sequential Action of Motor ATPase

This chapter (with some modification) was published at *Nucleic Acids Research*, 2012, 40 (6): 2577-2586. Special thanks to Dr. Huaming Fang for help in preparation of data for figures 3.1A, 3.2, 3.4, and 3.5A.

Abstract:

Many cells and dsDNA viruses contain an AAA+ ATPase that assembles into oligomers, often hexamers, with a central channel. The dsDNA packaging motor of bacteriophage phi29 also contains an ATPase to translocate dsDNA through a dodecameric channel. The motor ATPase has been investigated substantially in the context of the entire procapsid. Here we report the sequential action between the ATPase and additional motor components. It is suggested that the contact of ATPase to ATP resulted in its conformational change to a higher binding affinity toward dsDNA. It was found that ATP hydrolysis led to the departure of dsDNA from the ATPase/dsDNA complex, an action that is speculated to push dsDNA to pass the connector channel. Our results suggest that dsDNA packaging goes through a combined effort of both the gp16 ATPase for pushing and the channel as a one-way valve to control the dsDNA translocation direction. Many packaging models have previously been proposed, and the packaging mechanism has been contingent upon the number of nucleotides packaged per ATP relative to the 10.5 bp per helical turn for B-type dsDNA. Both 2 and 2.5 base pairs per ATP have been used to argue for four, five or six discrete steps of dsDNA translocation. Combination of the two distinct roles of gp16 and connector renews the perception of previous dsDNA packaging energy calculations and provides insight into the discrepancy between 2 and 2.5 bp per ATP.

Introduction

Most cells and dsDNA viruses contain at least one AAA+ (ATPases Associated with Diverse Cellular Activities) protein that possesses a common adenine nucleotide-binding fold. A typical characteristic of the AAA+ family is the coupling of chemical energy by the ATPase, derived from ATP hydrolysis to mechanical motion using force exerted on a substrate, such as dsDNA. This process usually requires a conformational change on the AAA+ protein that assembles into oligomers, often hexamers, forming a ring-shaped structure with a central channel (23) (121) (122) (123) (124) (125) (108).

Double stranded DNA (dsDNA) viruses package their genomic dsDNA into a preformed protein shell, deemed procapsid, during maturation (for review, see (38, 126)). This entropically unfavorable process is accomplished by a nanomotor which also uses ATP as an energy source (2, 6, 127, 128). In general, the dsDNA packaging motor involves a protein channel and two packaging molecules, with the larger molecule serving as part of the ATPase complex and the smaller one being responsible for dsDNA binding and cleavage (2, 3). Besides the well-characterized connector channel core, the motor of bacterial virus phi29 involves an ATPase protein gp16 (2, 60, 70-72, 110, 129, 130) and a hexameric packaging RNA ring (1, 3, 30). In 1998, Guo *et. al.* first proposed that the mechanism of the intriguing viral dsDNA packaging motor resembles the action of other AAA+ proteins which form a hexameric ring to translocate dsDNA using ATP as an energy source (see discussion in (3)). This motor is of particular interest to nanotechnology in that it is both simple in structure and can be assembled *in vitro* using purified components. The elegant design of the 30-nm nanomotor, one of the strongest motors (36) assembled *in vitro* to date (5), has instigated the reengineering of an imitative packaging motor for several applications. Previous reports indicate that phi29 nanomotor

possesses packaging efficiencies up to 90% and the ability to switch off packaging through the addition of a non-hydrolyzable ATP derivative, γ-S-ATP (2, 109, 110). The latter attribute has enabled single-molecule measurements of motor velocities and force against an external load using an optical trap, contributing to the evidence of a stalling force up to 57 pN (36). Twenty years ago, Guo, Peterson, and Anderson determined that one ATP was used to package two base pairs of dsDNA (2), and later, the same group demonstrated the sequential action of motor components (14). Recently, Bustamante and coworkers confirmed the sequential action mechanism of motor components (15). They calculated that during this process each ATP that is hydrolyzed led to about 2.5 bp of dsDNA translocation (15). Clarification of such discrepancy will help to illuminate the mechanism of motor action.

The packaging of 19.3 kbp dsDNA into a confined procapsid is entropically unfavorable and requires a large amount of energy. The packaged dsDNA undergoes approximately 30-100 fold decrease in volume as opposed to pre-packaging (80). Previous results suggest that ATPase activity of gp16 is dsDNA-dependent and may be stimulated by pRNA (69-72). It has also been shown that maximal ATPase activity was generated in the presence of all packaging components, including the procapsid and all its constituents (2, 69, 72).

The dsDNA packaging motor is well characterized in bacteriophage phi29, however gp16 (the ATPase protein) has long been an enigma. This protein tends to form aggregates in solution, which has negative consequences including the hindrance of the study and application of the protein, as well as contributing to contradictory data regarding ATPase activity, ATP/dsDNA/pRNA binding location, and stoichiometry studies. Reengineering techniques have both increased the solubility of this protein (129, 130) as well as served to provide a fluorescent arm (111) that facilitates identification and application.

The mechanism of ATP hydrolysis is important and ubiquitous, but the mechanism of energy conversion from ATP hydrolysis to physical motion remains elusive. The mechanism in which gp16 uses ATP to drive the motor is still not well understood. However, it is well known that both pRNA and gp16 play roles in the packaging of 19.3 kbp of gp3-dsDNA into a preformed procapsid during maturation. Surprisingly, we also found that gp16 alone is capable of fastening itself to dsDNA and releasing this dsDNA through ATP hydrolysis, independent of pRNA and the procapsid. Furthermore, the sequence in which dsDNA binds to ATP was studied, revealing an important phenomenon in the packaging mechanism. Moreover, dsDNA passes through the portal protein during its translocation into the procapsid and it has been speculated that the channel plays a role in the process (45).

Materials and Methods:

Expression and Purification of eGFP-gp16 in E. coli

The engineering of eGFP-gp16 was published by Lee *et. al.* (111) . eGFP-gp16 was expressed and purified as described previously (60, 111, 130) with minor modifications. Briefly, the protein was over-expressed in *E.coli BL21(DE3)* with induction of 0.4mM IPTG. The bacterial cells were harvested and resuspended in His-binding buffer (20mM Tris-HCl,pH 7.9, 500mM NaCl, 15% glycerol, 0.5mM TECP and 0.1% Tween-20). The cells were then lysed by passing though French Press and the lysate was clarified by centrifugation. 0.1% PEI was added to the clarified lysate to remove nucleotides and other proteins. Homogeneous eGFP-gp16 was purified by one-step Ni-resin chromatography.

Electrophoretic Mobility Shift Assay (EMSA):

The samples were prepared in 20µl buffer A (20mM Tris-HCl, 50mM NaCl, 1.5% glycerol, 0.1mM Mg^{2+}). Typically, 1.78µM eGFP-gp16 was mixed with 7.5ng/µl 40bp Cy3-dsDNA at various conditions. The samples were incubated at ambient temperature for 20min and then loaded onto a 1% agarose gel (0.5TB: 44.5 mM Tris, 44.5mM Boric Acid) for electrophoresis for 2hr under 80V at 4°C. The eGFP-gp16 and Cy3-dsDNA in the gel was analyzed by fluorescent LightTools (Edmonton, Alberta, CA) Whole Body Imager using 488 nm and 540 nm wavelengths for eGFP and cy3 respectively.

Forster Resonance Energy Transfer (FRET):

FRET samples were analyzed using Horiba Jobin Yvon (Edison, NJ) FluoroHub at excitation wavelength of 480 nm and the emission spectra was scanned from 500-650 nm with 5 nm slits at both excitation and emission. Samples were prepared in an appropriate cuvette volume (typically 50 µl) and allowed to incubate at room temperature for at least 5 minutes prior to excitation in order to allow reaction to fully catalyze.

Sucrose Gradient Sedimentation:

Sucrose was diluted at 5% and 20% (w/v) using a dilution buffer (50 mM NaCl, 25 mM Tris pH 8.0, 2% glycerol, 0.01% Tween-20, 0.1 mM $MgCl_2$) and a gradient was made using protocols established by BioComp Gradient Maker. Samples were subsequently gently added to the top of the gradient as not to disrupt the formed gradient, balanced, and placed in Beckman Optima L Preparative Ultracentrifuge at 5.5 hours, 35000 rpm, 4°C. Samples were then fractionated directly from the bottom of the tube and analyzed by a Biotek Synergy 4 microplate reader at both GFP and cy3 wavelengths.

Kinetic Assay (MDCC-PBP):

The conversion of MDCC emission to an enzymatic kinetic equation has previously been reported (70).

Phage Assembly Activity Inhibition and Isolation of Partially Filled Procapsids:

The phage assembly assay has been previously described (112). To isolate the partially filled procapsid, γ-S-ATP was added to the packaging reaction buffer and the reaction was added to the top of a sucrose gradient and centrifuged for an extended period. The gradient was subsequently fractionated and variations of packaging components were again added to the individual fractions including ATP, ADP, or AMP. The fractions were then plated as performed in the phage assembly assay and tested for viral activity.

Connector Insertion into Lipid Bilayer and Electrophysiolgical Measurements:

Connector protein gp10 was inserted into a lipid bilayer and current traces were recorded after addition of dsDNA as previously described (41).

Results

γ-S-ATP , a non-hydrolyzable ATP analog, promotes binding of gp16 to dsDNA

The conditions in which gp16 interacted with dsDNA were investigated. It was immediately discovered that the ATPase was capable of binding to dsDNA in the absence of pRNA and other motor components. An electrophoretic mobility shift assay was employed to study the interaction. Fusion of an eGFP tag at the N-terminus of gp16 did not affect its biological activity (111), but provided a fluorescent marker for detection. In Figure 3.1A, the binding between eGFP-gp16, dsDNA, and γ-S-ATP was explored. Two different fluorescent

filters, FITC and cy3, were used to visualize the protein and dsDNA, respectively. It was hypothesized that γ-S-ATP would lock gp16 onto dsDNA and our results proved this phenomenon. dsDNA was bound by eGFP-gp16 in the absence of the nucleotide (Figure 3.1A, lane 3). However, stronger binding of gp16 to dsDNA was observed when gp16 was incubated with γ-S-ATP (Figure 3.1A, lane 4). To further validate the finding, two different assays were utilized. Förster Resonance Energy Transfer (FRET) analysis revealed an increase of energy transfer from eGFP-gp16 to Cy3-dsDNA when γ-S-ATP was included (Figure 3.1B, royal blue curve), to the sample in the absence of γ-S-ATP (green curve). FRET decreased significantly upon addition of excess ATP to the gp16/dsDNA/γ-S-ATP complex (teal curve). Furthermore, when γ-S-ATP was included in the mixture, sedimentation studies utilizing a 5-20% sucrose gradient revealed that gp16-dsDNA complex was highly prevalent as indicated by overlap in the eGFP and cy3 wavelength spectra (Figure 3.1C). These results suggested that the gp16/dsDNA complex is stabilized through addition of the non-hydrolyzable ATP substrate. Furthermore, the data suggested that gp16 possesses both a dsDNA binding domain and a motif to bind ATP.

ATP induced a conformational change in gp16 that led to increased binding affinity of gp16 to dsDNA

To continue with the previous findings, the mechanism of gp16 action in relation to ATP was studied. It has been extensively reported that gp16 is a dsDNA dependent ATPase (2, 70), that dsDNA stimulates the ATPase activity of gp16 (2, 70, 72), and that the phi29 dsDNA packaging motor uses one ATP to translocate 2 (2) or 2.5 (127) base pairs of dsDNA into the prohead. However, the interaction of gp16 with dsDNA or ATP and the sequential action of these three components was previously unidentified. To tackle this question, eGFP-gp16 was mixed with either dsDNA or γ-S-ATP and allowed to incubate. Subsequently, the remaining,

missing component was added to the mixture and again allowed to incubate. All samples were subjected to an EMSA and imaged. The band representative of gp16 in complex with dsDNA appeared significantly sharper when γ-S-ATP was incubated first (Figure 3.1D, lanes 6,7,8) than when dsDNA was initially added (Figure 3.1D, lanes 3,4,5). FRET and gradient sedimentation also revealed the same phenomenon (data not shown). All these data support the speculation that gp16 binds first to γ-S-ATP to increase the binding affinity to dsDNA, and that γ-S-ATP is capable of fastening gp16 to dsDNA to form a more stable complex.

Gp16 departed from dsDNA following ATP hydrolysis

It has been reported that gp16 is a dsDNA-dependent ATPase of the phi29 dsDNA packaging motor (2, 70, 72, 131), providing energy to the motor by hydrolyzing ATP into ADP and inorganic phosphate. For further applications, it is important to elucidate the mechanism in which ATP hydrolysis is related to the motion of motor components for the translocation of dsDNA.

As aforementioned, γ-S-ATP stalled and fastened the gp16/dsDNA complex. It was subsequently found that hydrolysis of ATP led to the release of dsDNA from gp16 (Figures 3.2 and 3.3). When increasing amounts of ATP was added to the gp16/dsDNA/γ-S-ATP complex, the band representing the gp16/dsDNA complex disappeared (Figure 3.2A). ADP had a lesser effect on dsDNA release (Figure 3.2B), whereas AMP was unable to release dsDNA from gp16 (Figure 3.2C). This same phenomenon was observed in the previous FRET assay (Figure 3.1B, teal curve).

The release of dsDNA from gp16/dsDNA/γ-S-ATP complex by ATP and ADP was also demonstrated by sucrose gradient sedimentation. Binding of eGFP-gp16 to dsDNA was

evidenced by a shift in the dsDNA profile in the presence of γ-S-ATP and in the absence of ATP (Figure 3.3A, black curve). With low concentrations of ATP however, gp16 and dsDNA existed as a free molecule in solution with slower sedimentation rates (Figure 3.3A, colored curves). To investigate the mechanism further, gp16/dsDNA/γ-S-ATP complex was purified using the sucrose gradient and subjected to an ATP hydrolysis kinetic assay. The hydrolysis of ATP to ADP and inorganic phosphate was confirmed by the demonstration that purified gp16/dsDNA/γ-S-ATP complex was able to hydrolyze ATP after addition of ATP to the purified complex (Figure 3.3B). Simply, a fluorescent molecule (MDCC-PBP) undergoes a conformational change after binding to inorganic phosphate which gives off fluorescence emission. The increase in fluorescence emission can be correlated to the hydrolysis of ATP to ADP with simple calculations. The results suggested that hydrolysis of ATP led to the release of dsDNA from the gp16.

Evaluation of the findings on γ-S-ATP, ATP, ADP, AMP and gp16 interaction using the active ATP-driven dsDNA packaging motor

All previous experiments involving the interaction between gp16 and ATP or its derivatives were carried out in the procapsid-free system. Even though the previous experiments were derived from precursor proteins of the active motor, it is important to relate this interaction to an active motor involving the procapsid. A dsDNA packaging and viral assembly assay was performed in which purified motor components were added together and allowed to form an active virion in the presence and absence of γ-S-ATP, ATP, ADP, AMP and gp16 imitating their interaction in the procapsid-free system. When γ-S-ATP was added with an increased ratio to ATP, dsDNA packaging and viral assembly was gradually blocked (Figure 3.4A). The data agrees perfectly with that from the procapsid-free system showing that γ-S-ATP blocked the

dissociation of dsDNA from gp16 (Figure 3.1A). The partially filled procapsids, incubated with optimal γ-S-ATP concentration, were then isolated in a sucrose gradient and subjected to addition of other motor components including ATP, ADP, and AMP in the phage assembly assay. The partially filled procapsids were able to be converted into infectious virion when ATP was added (Figure 3.4B, red curve), agreeing with the data from the procapsid-free system in which ATP promoted the departure of dsDNA from the fastened gp16/dsDNA complex (Figure 3.2A). When ATP was replaced by ADP or AMP, active phages were not produced (Figure 3.4B), again in accordance with the data from the procapsid-free system showing that ADP and AMP did not allow easy departure of dsDNA from the gp16/dsDNA complex (Figure 3.2B & C). After adding further eGFP-gp16, pRNA, gp9-14, and ATP, the partially filled procapsids were able to recommence packaging and form an assembled, active bacteriophage.

Inorganic phosphate inhibited gp16 binding to dsDNA and elicited dsDNA discharge

Now that we have provided conclusive evidence that hydrolysis of ATP by gp16 to ADP and inorganic phosphate is the catalytic step leading to the translocation of dsDNA, the question remains as to which of the two resulting products, ADP and Pi, departs and which component remains bound to gp16? That is, does the gp16 conformational change result from a departure of ADP or Pi from gp16?

Inorganic phosphate is one of the products of the energy-producing reaction when ATP is hydrolyzed to ADP. A gel retardation assay revealed that in the presence of high concentrations of phosphate, dsDNA was released from the gp16/dsDNA/γ-S-ATP complex (Figure 3.5A, lane 4). It was also found that the presence of inorganic phosphate prevented the formation of gp16/dsDNA complex, either in the presence of γ-S-ATP or ATP. The gp16/dsDNA/γ-S-ATP

complex was incubated with the phosphate analog sodium vanadate, which also proved to inhibit binding of gp16 to dsDNA (Figure 3.5A, lane 6). A sucrose sedimentation gradient assay revealed concurring results. 50 mM phosphate was able to completely inhibit the formation of gp16/dsDNA complex or dissociate the complex into free gp16 and dsDNA, as evidenced by the shift of the dsDNA peak in the sucrose gradient (Figure 3.5B). It is interesting to find that ADP also stimulated the release of gp16 from the gp16/dsDNA complex (Figure 3.2B). All these results questioned whether the inorganic phosphate by itself can compete with the ATPase center for ATP binding and whether the gp16/Pi or gp16/ADP complex remains as the final product after gp16 propels dsDNA forward.

Discussion

EMSA, sucrose gradient sedimentation, FRET, and kinetic studies provided evidence to support the hypothesis that gp16 first interacts with ATP or the ATP analog γ-S-ATP and then with dsDNA. eGFP-gp16 was first incubated with either γ-S-ATP or short cy3-dsDNA and subsequently incubated with the third component, either dsDNA or γ-S-ATP (Figure 3.1D). The mixtures were then subjected to a low percentage agarose gel to evaluate the gp16/dsDNA complex. A significantly sharper cy3 band was detected corresponding to gp16/dsDNA complex in samples in which γ-S-ATP was added first. This data indicated that more gp16/dsDNA complex had formed under those conditions.

To further study the γ-S-ATP function in fastening gp16 to dsDNA, we carried out three different experiments. Gp16 was incubated with dsDNA and γ-S-ATP. The sample was then applied to a 5-20% sucrose gradient, fractionated, and analyzed for eGFP (representing gp16) and cy3 (representing dsDNA) signal (Figure 3.1C). Profile-overlay analysis indicated that, in

the presence of γ-S-ATP, gp16 tightly bound to dsDNA despite large centrifugal force and dilution factor. Similar samples from agarose gel electrophoresis revealed a much stronger gp16/dsDNA complex band when γ-S-ATP was present. Finally, FRET was applied to measure the energy transfer and distance between eGFP-gp16 (donor fluorophore) and cy3-dsDNA (acceptor fluorophore). Our data illustrated that higher energy transfer was present with the addition of γ-S-ATP, which provided indirect evidence that the protein formed a complex with dsDNA. In combination, these assays contributed to the principle that the motor complex can be stalled by addition of a non-hydrolyzable ATP substrate (70, 110) but more importantly, they expanded our understanding of the phi29 packaging mechanism.

After gp16/dsDNA complex was formed through addition of γ-S-ATP, it was critical to understand what compounds were capable of dissociating gp16 from dsDNA. Again using an EMSA, gp16-dsDNA complex was allowed to form by incubating eGFP-gp16, cy3-dsDNA, and γ-S-ATP together, but this time, adenosine monophosphate, adenonsine diphosphate, and adenosine triphosphate were subsequently added before electrophoresis. Figure 3.2 clearly shows the concentration of tri-, di-, and monophosphate at which the complex dissociates. ATP had the highest efficiency in promoting the kicking away of dsDNA from gp16, ADP had a lesser effect, but AMP had no effect. The same concept was used in Figure 3.3A in which gp16/dsDNA complex was preformed and subsequently incubated with varying concentrations of ATP. The samples were then added on top of a linear sucrose gradient and centrifuged for an extended period of time. In the absence of ATP, complex formed, but even in low concentrations of ATP, gp16 is released from its dsDNA substrate. Furthermore, a kinetic study was applied in which ATP was added to a gp16/dsDNA complex previously purified by a sucrose gradient. A fluorescent substrate was used to detect the release of inorganic phosphate in

solution after ATP was hydrolyzed and the maximum velocity and Michaelis-Menten constant were calculated after varying concentrations of ATP were assayed. The curve is representative of all kinetic enzymes and again proves that ATP can be hydrolyzed and released even after gp16/dsDNA complex has formed.

To relate the above observed phenomena to a functional phage, an assay was performed in which the partially filled procapsids formed via incubation with γ-S-ATP was isolated in a sucrose gradient and subjected to a phage assembly assay with addition of either ATP, ADP, and AMP. A similar assay has previously been performed (46). The results are consistent with the data from the procapsid-free syste and provide indirect support for the conclusion that γ-S-ATP enhanced the binding of gp16 to dsDNA and that ATP hydrolysis promoted the departure of dsDNA from the gp16/dsDNA complex.

The dsDNA packaging mechanism is a universal biological phenomenon for dsDNA viruses including herpes viruses, poxviruses, adenoviruses, and other dsDNA bacteriophages. The mechanism of packaging has provoked interest among virologists, bacteriologists, biochemists, and especially researchers involved in nanotechnology; however, the actual mechanism remains elusive. In the past, many models have been proposed to interpret the mechanism of motor action including the 1) Gyrase-driven supercoiled and relaxation (7); 2) Force of osmotic pressure; 3) Ratchet mechanism (103); 4) Brownian motion (11); 5) Five-fold/six-fold mismatch connector rotating thread (12); 6) Supercoiled dsDNA wrapping (13); 7) Sequential action of motor components (14, 15); 8) Electro-dipole within central channel (16); and, 9) Connector contraction hypothesis (17, 132), 10) dsDNA torsional compression translocation mechanism (6, 8). Based on our results, a hypothesis has been developed to describe the mechanism of dsDNA packaging. We coined the "Push through a One-way Valve"

mechanism described as a combined effort between the gp16 ATPase which provides energy for pushing and the connector channel for one-way control. We believe that gp16 possesses at least four binding motifs for pRNA, dsDNA, adenosine and phosphate (the P loop). In our theory, at any given time, gp16 alone is able to bind to dsDNA but with low affinity. Upon binding to adenosine triphosphate or derivatives (ATP, γ-S-ATP) however, gp16 undergoes a conformational change which promotes the binding to dsDNA. In this conformation, gp16 tightly binds to dsDNA in order to eliminate slipping in the packaging process. However, in order to generate energy, gp16 cleaves the gamma phosphate of ATP, producing a force from which gp16 switches to a relaxed conformation propelling the dsDNA unidirectionally into the procapsid using pRNA as a fulcrum. In this relaxed form, the binding site is unoccupied until a new ATP molecule is introduced to gp16 to restart the cycle (Figure 3.6).

In many packaging motors, the ATPase acts to rid itself of the phosphate but continues to clutch the ADP (127, 133). The data shown in this report clearly shows that both ADP and phosphate can release gp16 from its substrate dsDNA. Our results suggest that ADP competes for the binding pocket better than inorganic phosphate, so it is assumed that gp16 has higher affinity for ADP than inorganic phosphate. This dictates that inorganic phosphate is expelled first, as observed in other phages, but also suggests that ADP is released from the pocket to allow the cycle to restart. The data is unable to clarify which expulsion step catalyzes the motor action, but that both steps are required to generate a new cycle.

Recently, our group discovered that the channel of phi29 dsDNA packaging motor exercises a one-way traffic mechanism of dsDNA translocation from the N-terminal external end to the C terminal internal end, but blocked dsDNA to exit (41). Therefore we concluded that phi29 dsDNA packaging went through a schematic marching mechanism via a unique

mechanism by pushing through a one-way channel valve of the dsDNA packaging motor (Figure 3.6). The mechanism of providing force through a one-way valve agrees with Black *et. al.* finding in bacteriophage T4 that dsDNA was compressed if the portal entrance was blocked at the front end (104, 105, 134). The authors interpreted that the force for the compression is due to the torsional force from coiled dsDNA, but relates to our idea that dsDNA is rotated into the portal (135). Our suggested mechanism is also validated through the discovery in T4 in which it was determined that both ends of dsDNA remain in the portal of the procapsid during the packaging process (104, 105). If the motor functioned by pulling dsDNA within the procapsid rather than pushing by gp16, one end of dsDNA would be required to be internalized for packaging to commence. Finally, this mechanism agrees with Bustamante *et. al.* who clearly confirmed that dsDNA is processed by an unknown dsDNA-contacting component in one strand (136).

The stoichiometry of gp16 has not been fully addressed in this proposed mechanism, but in 1998, Guo *et. al.* (3) proposed that the mechanism of dsDNA packaging is similar to the hexameric AAA+ ATPase family that has many functions but also acts to translocate dsDNA during dsDNA replication and repair. Many well-characterized dsDNA tracking motors (26, 137-139) and other ATPases within the AAA+ family (135) possess an even-numbered protein structure. Furthermore, such phages as phi12 (140, 141) and others have proved to possess a hexameric ATPase. Since the pRNA of phi29 has been determined to be hexameric (3, 30) (31), this raises speculation that gp16 might be similar to the AAA+ family and also exist as a hexamer.

Twenty years ago, Guo *et. al.* (2) determined that one ATP was used to package two base pairs of dsDNA. The stoichiometry of one ATP for two base pairs of dsDNA was also

subsequently confirmed by the T3 system (142). This information has been utilized substantially by biochemists and biophysicists to interpret the mechanism of motor action (103, 126, 127, 141, 143, 144). Recently, Bustamante and coworkers reported the packaging of 2.5 base pairs per ATP using single molecule analysis through tweezer based experiments (15). Many packaging models have previously been proposed, and the packaging mechanism has been contingent upon the number of nucleotides packaged per ATP. Currently, the motion mechanism is interpreted based on structural and biophysical properties of the dodecameric channel and the B-type dsDNA linking number of 10.5 bp per helical turn. It is logical that a specific number of ATP is required to translocate a definite number of dsDNA if gp16 and connector are an integrated, concrete motor structure. From our results, it was revealed that the dsDNA packaging task is carried out by two different steps by two separate components: gp16 for active pushing and the channel serving as a one-way valve to control the direction. Currently, the debate is whether 2 (2) or 2.5 (15) base pairs are packaged per ATP and whether the motor ATPase is a tetramer, pentamer, or hexamer for four (144), five (134), or six (2) discrete steps of motor action. The calculation of ATP and dsDNA ratio related to the linking number of B-type dsDNA would have been useful to interpret the motor mechanism if only one motor protein, either gp16 or connector, plays a determinative role in dsDNA translocation speed. However, as reported here, the pushing force is from the ATPase gp16, but the dsDNA translocation speed is most likely also affected by the connector channel. Temporary pause and motion steps have been reported to occur during translocation (86, 87, 127). The calculated translocation rate resulted from two uncoordinated force generating factors, gp16 and connector, will make it impossible to obtain a definitive and reproducible number of base pairs per ATP consumed. The translocation rate generated by gp16 is altered by the channel valve since the temporary pause or slide of the

dsDNA during translocation through the channel will negatively affect the speed. The newly demonstrated mechanism of dsDNA packaging demonstrated here can address the discrepancy between the 2 and 2.5 base pair per consumed ATP debate. The difference depends on the experimental conditions that can be varied. Finding of the combination of the two distinct roles of gp16 and connector renews the perception of previous dsDNA packaging energy calculations and provides insight into the mechanism of motor action (Figure 3.6).

Funding:

This work was supported by NIH grant GM059944 and EB012135.

Acknowledgements:

We would like to thank Mathieu Cinier and Jia Geng for help in preparation of figures; Gian Marco De Donatis and Farzin Haque for their helpful insight.

Figures

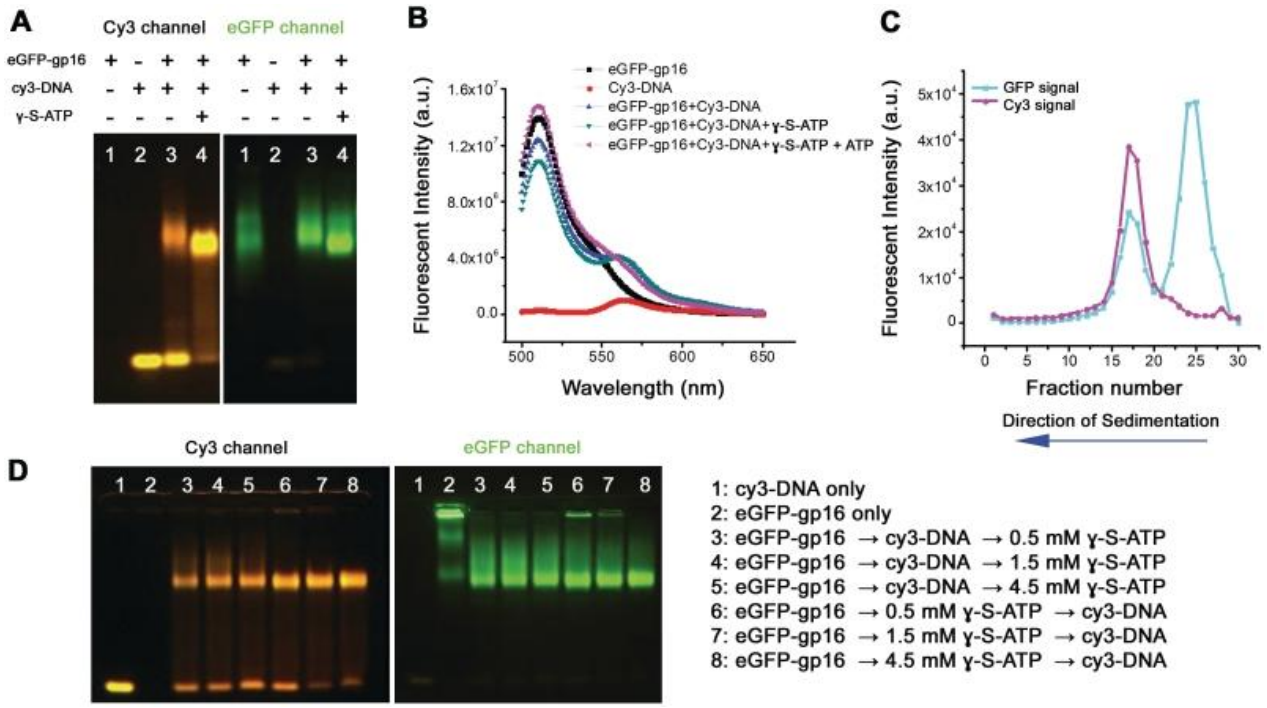

Figure 3.1. **Demonstration of gp16 fastening to fluorescent dsDNA after incubation with non-hydrolyzable ATP derivative** through A) Electrophoretic Mobility Shift Assay, B) FRET, and C) Sucrose Gradient Sedimentation; D) EMSA to demonstrate efficiency of binding when ATP substrate is added before dsDNA.

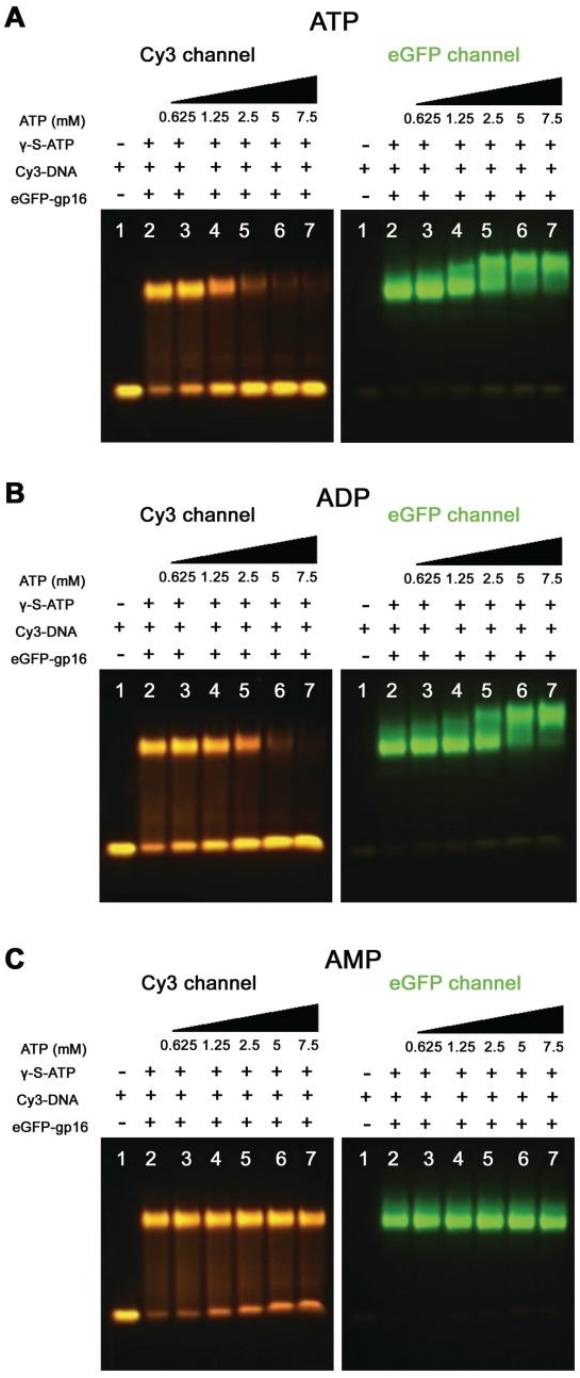

Figure 3.2. **Electrophoretic Mobility Shift Assay showing release of dsDNA from gp16** after addition of increasing amounts of A) ATP and B) ADP; C) AMP is unable to release gp16 from dsDNA

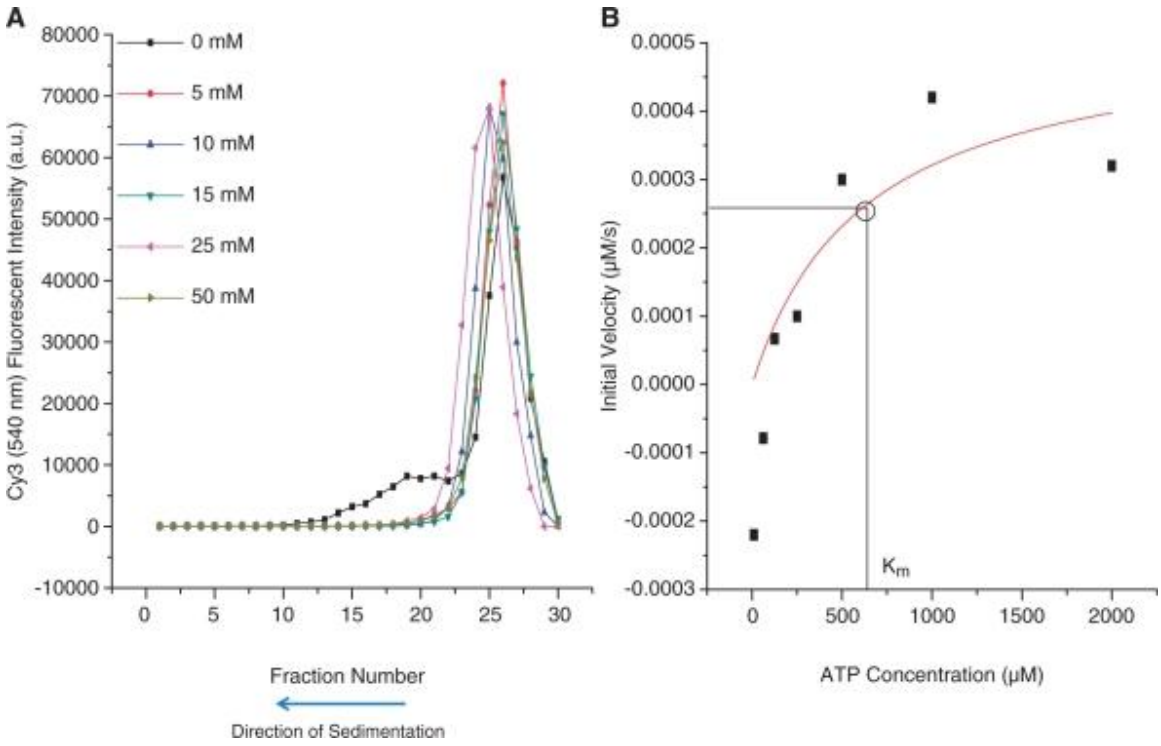

Figure 3.3. **Effect of ATP on Gp16/dsDNA/γ-S-ATP complex.** Complex was formed and subjected to increasing amounts of ATP and assayed by A) sucrose gradient sedimentation and B) fluorescent assay using an inorganic phosphate binding substrate to determine kinetics of ATP hydrolysis.

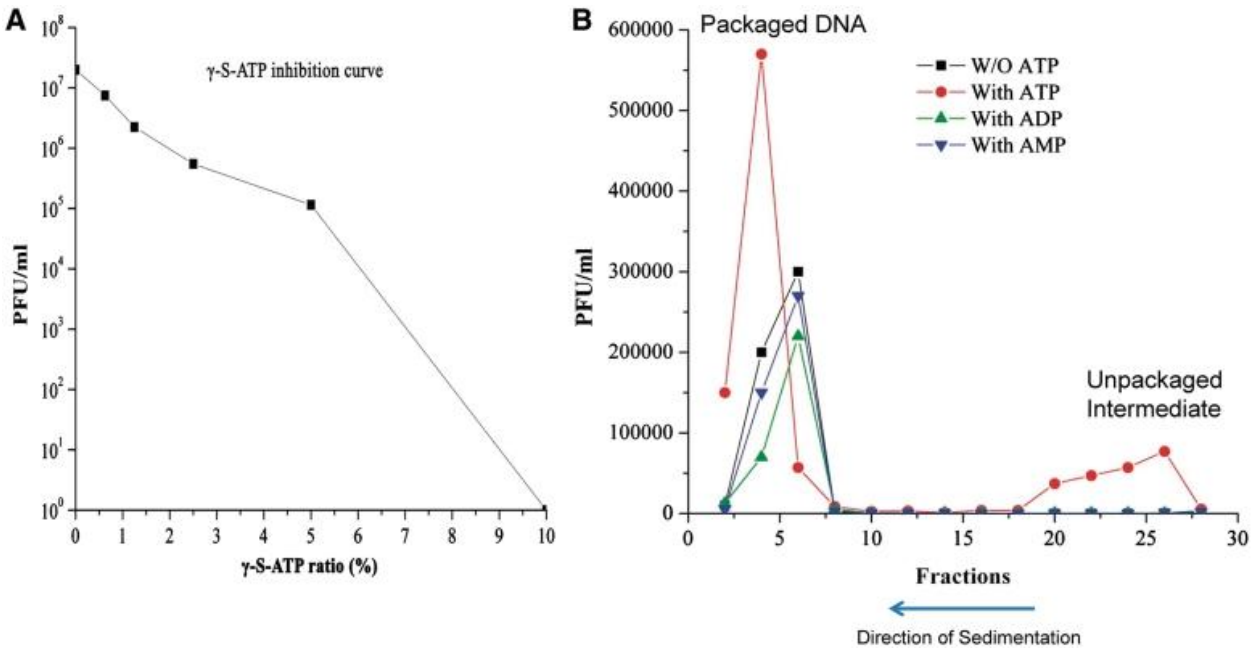

Figure3.4. **Isolation of the Partially Filled Procapsid to Determine Effect of ATP, ADP, and AMP on Viral Assembly.** A) Decrease of phage assembly activity by introduction of non-hydrolyzable ATP derivative. B) Activity of isolated partially filled procapsids after sucrose gradient sedimentation.

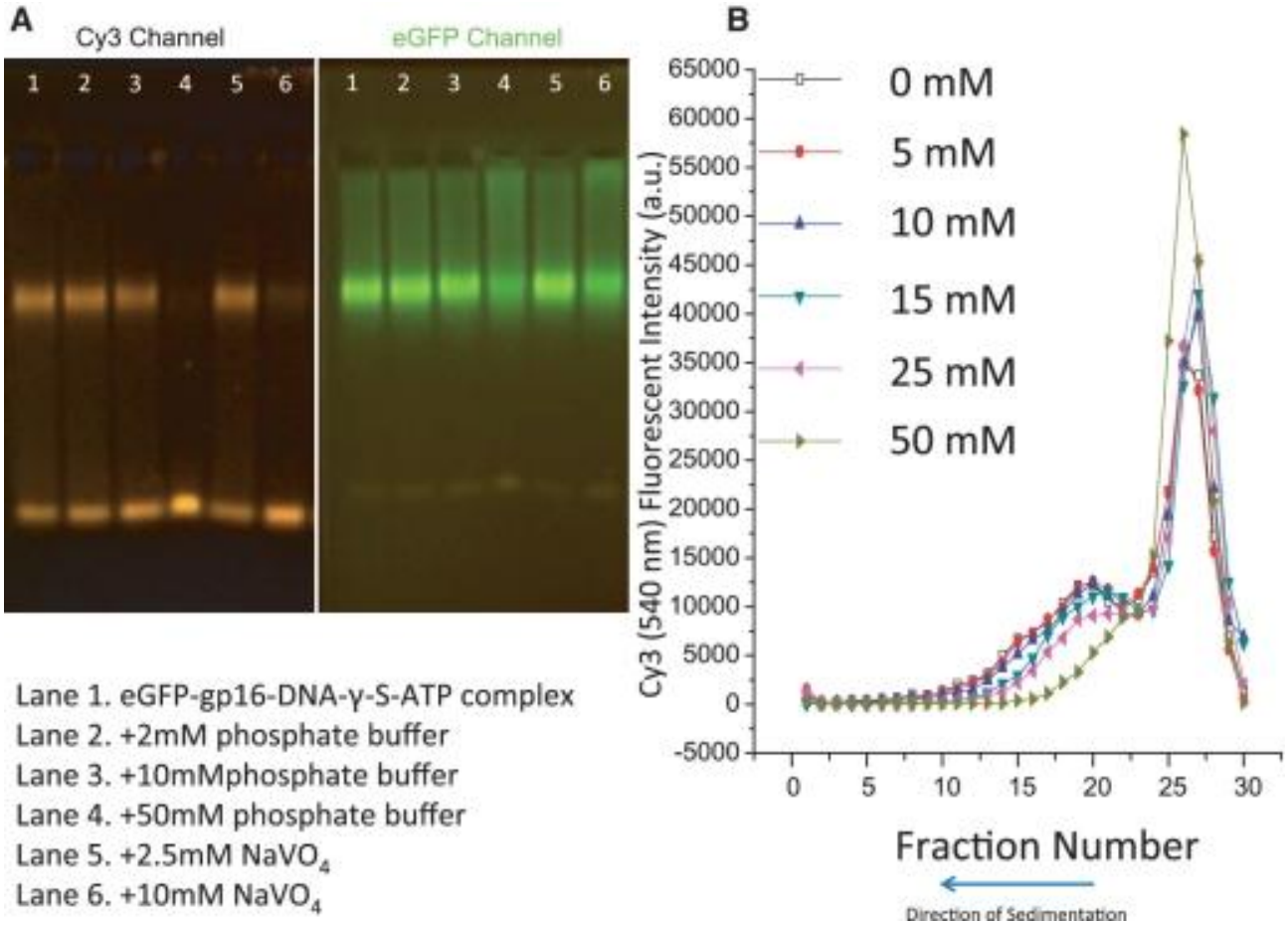

Figure 3.5. **Effect of Phosphate and Phosphate Derivative Sodium Vanadate on gp16/dsDNA/γ-S-ATP complex formation.** Release of eGFP-gp16 from dsDNA complex by adding excess amounts of phosphate (A, lanes 2-4, and B). Decrease in gp16 binding to dsDNA using phosphate derivative sodium vanadate (lanes 5,6).

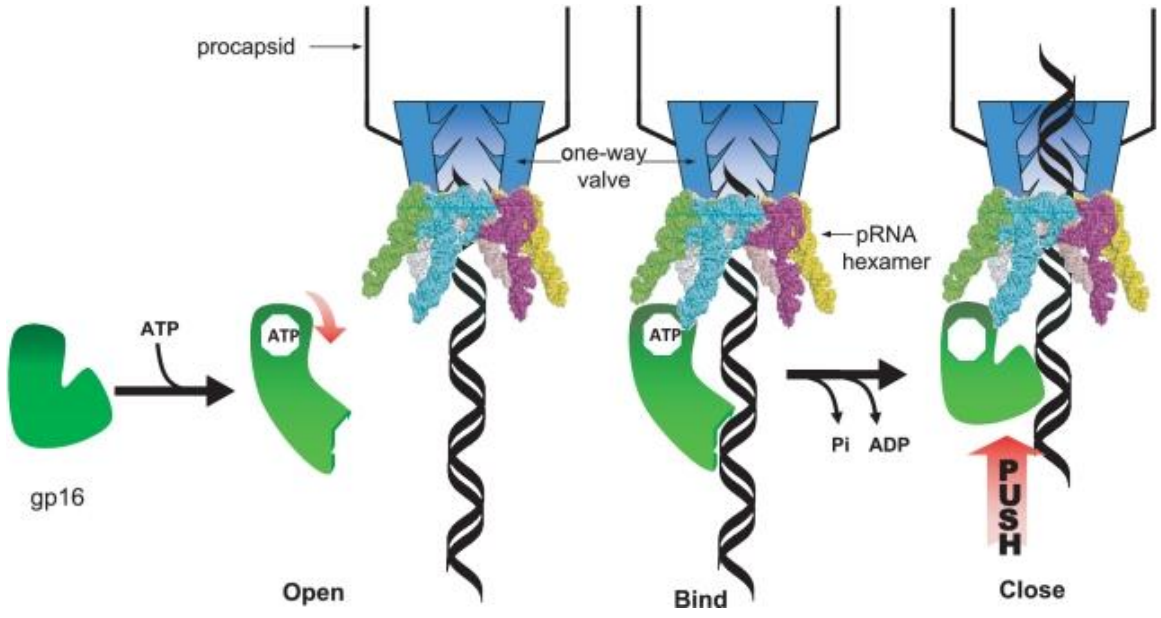

Figure 3.6. **The "Push through a One-way Valve" mechanism in phi29 dsDNA packaging.** Schematic of dsDNA packaging mechanism termed "push through a one-way valve". ATP binds to gp16, promoting gp16 binding to dsDNA. ATP hydrolysis induced a force or conformational change to push dsDNA translocation into the connector channel, which is a one-way valve that only allows dsDNA to enter but not exit the procapsid during dsDNA packaging.

Chapter 4. Mechanism of Revolution of ATPase for Viral DNA Packaging

This chapter (with some modification) is under submission at *Virology* under the title "Revolution rather than rotation of AAA+ hexameric phi29 nanomotor for viral dsDNA packaging without coiling". Special thanks to Dr. Gian Marco De Donatis for help in preparation of data for figures 4.5 and 4.6; Dr. Huaming Fang for help in preparation of data for figures 4.3 and 4.4; Dr. Yi Shu for help in preparation of data for figure 4.1D; and Hui Zhang for help in preparation of data for 4.8.

Abstract

It has long been believed that the DNA-packaging motor of dsDNA viruses utilizes a rotation mechanism. Here we report a revolution rather than rotation mechanism for the bacteriophage Phi29 DNA packaging motor. Analogously, the Earth "rotates" along its own axis resulting in cycles of day and night; however, it "revolves" around the sun every 365 days. It has been found that the Phi29 motor contains six copies of the ATPase gp16 (4). ATP binding to one ATPase subunit stimulates the ATPase to adopt a conformation with a high affinity to bind dsDNA. ATP hydrolysis induces a new conformation with a lower affinity for dsDNA, thus pushing dsDNA away and transferring it to an adjacent subunit by a power stroke. DNA revolves unidirectionally along the hexameric channel wall, but neither the dsDNA nor the hexameric ATPase itself rotates. One ATP is hydrolyzed in each transitional step, and six ATPs are consumed for one helical turn of 360°. As demonstrated with Hill constant determination, binomial assay, cooperation and sequential analysis, transition of the same dsDNA chain along the channel wall, but at a location 60° different from the last contact, urges dsDNA to move forward 1.75 base pairs each step (10.5 bp/turn ÷ 6ATP = 1.75 bp/ATP). The 30°-tilted angle of each connector subunit that runs anti-parallel to the dsDNA helix facilitates the one-way traffic of dsDNA and coincides with the 12 subunits of the channel (360° ÷ 12 = 30°). The hexamer motor also caused four steps of pause due to the utilization of 4 lysine rings to facilitate the continuation of revolution (ACS Nano, In Press). Nature has evolved a clever machine to translocate DNA double helices that avoids the difficulties during rotation that are associated with DNA supercoiling. The discovery of the revolution mechanism might reconcile the stoichiometry discrepancy in many phage systems for which the ATPase was found to be present as tetramer, hexamer, and nonamers.

Introduction

The AAA+ (ATPases Associated with diverse cellular Activities) superfamily of proteins is a class of motor ATPases with a wide range of functions. Many members of this class of ATPases often fold into hexameric arrangements (24, 25, 145-149) and are involved in DNA translocation, tracking, and riding (26, 83, 122, 150, 151). Despite their functional diversity, the common characteristic of this family is their ability to convert chemical energy obtained from the hydrolysis of the γ-phosphate bond of ATP into a mechanical force, usually involving a conformational change of the AAA+ protein. This change of conformation generates both a loss of affinity for its substrate and a mechanical movement; which in turn is used to either make or break contacts between macromolecules, resulting in local or global protein unfolding, complex assembly or disassembly, or the translocation of DNA, RNA, proteins, or other macromolecules. These activities underlie processes critical to DNA repair, replication, recombination, chromosome segregation, DNA/RNA transportation, membrane sorting, cellular reorganization, and many others (22, 23, 26, 152, 153). Numerous biochemical and structural aspects of reactions catalyzed by AAA+ proteins have been elucidated, along with other interesting allosteric phenomena that occur during ATP hydrolysis. For instance, the crystal structure of the sliding clamp loader complex, a system that helps polymerases overcome the problem of torque generated during the extension of helical dsDNA, has revealed a spiral structure that strikingly correlates with the grooves of helical dsDNA; suggesting a simple explanation for how the loader/DNA helix interaction triggers ATP hydrolysis, and how DNA is released from the sliding clamp (154, 155).

In both prokaryotic and eukaryotic cells, DNA needs to be transported from one cellular compartment to another. As for dsDNA viruses, they translocate their genomic DNA into preformed protein shells, termed procapsids, during replication (for review, see (33, 38, 126, 156)). This entropically unfavorable process is accomplished by a nanomotor that uses ATP as an energy source (2, 6, 14, 69, 70, 78, 127, 128). The dsDNA packaging motor also consists of a protein channel and two packaging molecules with which it carries out its activities. Our discovery 25 years ago has resulted in the knowledge that the larger molecule serves as part of the ATPase complex, and the smaller one is responsible for dsDNA binding and cleaving (2, 3); this notion has now become a well-established definition (for review, see (33, 38, 126, 156)). Besides the well-characterized connector channel core, the motor of bacterial virus phi29 involves an ATPase protein gp16 (2, 60, 70-72, 110, 129, 130) and a hexameric packaging RNA ring (1, 3, 30, 63). The connector contains a central channel encircled by 12 copies of the protein gp10 that serves as a pathway for dsDNA translocation (16, 29, 157).

The cellular components that show the strongest similarity to viral DNA packaging motor include FtsK, an AAA+ DNA motor protein that transports DNA and separates intertwined chromosomes during cell division (108), and the SpoIIIE family (158), an AAA+ protein responsible for transportation of DNA from a mother cell into the pre-spore during the cell division of Bacillus subtilis (159). It has recently been revealed that the ATPase of phi29 gp16 is similar to these families in structure and function (3, 108). Both the FtsK and SpoIIE DNA transportation systems rely on the assemblage of a hexameric machine. FtsK proteins contain three components: one for DNA translocation, one for controlling of orientation, and one for anchoring it to the substrate (158). Extensive studies suggest that FtsK may employ a “rotary inchworm” mechanism to transport DNA (160). The FtsK motor encircles dsDNA by a

hexameric ring. During each cycle of ATP binding and hydrolysis within each FtsK subunit, one motif acts to tightly bind to the helix while the other progresses forward along the dsDNA. This process causes translational movement, a mechanism that is repeated by the subsequent transfer of the helix to the next adjacent subunit (160). Many other hexameric dsDNA tracking motors function in a similar fashion, including TrwB, which is used in DNA transport during bacterial conjugation (161); Rad54, an ATPase supporting viral DNA replication (162); and RuvB that plays a role in the resolution of the Holliday junction during homologous recombination (163).

Many intriguing packaging models have been proposed for the motor of dsDNA viruses (15, 86, 87, 156, 164). It has long been popularly believed that viral DNA packaging motors run through a rotation mechanism involving a five-fold/six fold mismatch structure (12). The best-studied bacteriophage Phi29 DNA packaging motor was constructed in 1986 (5) and has been shown to contain three co-axial rings (Figure 4.1) (1, 2, 60, 72). In 1987, an RNA component was discovered on the packaging motor (1), and subsequently, in 1998, this RNA particle was determined to exist as a hexameric ring (3, 27) (featured by *Cell* (28)). Based on this structure, it was proposed that the mechanism of the Phi29 viral DNA packaging motor is similar to that used by other hexameric DNA tracking motors of the AAA+ family (3). This notion has caused a fervent debate concerning whether the RNA and ATPase of the motor exist as hexamers or as pentamers. Many laboratories have persisted to prove the pentameric model (77, 86, 165), despite the solid finding of the presence of hexameric folds in the motor, as revealed by biochemical analysis (3, 4, 27, 28); single molecule photobleaching (30); gold labeling imaged by EM (30-32); nano-fabrication (166); and RNA crystal structure (63). Due to strong supporting data in favor of the motor hexamer, the pentamer-supporters have proposed alternatives to reconcile the pentamer and hexamer debate. One theory is that a pRNA hexamer is first

assembled on the motor, after which one of the subunits leaves, resulting in the final pentameric state (18, 77, 167). This proposition was countered by findings showing that the motor intermediates isolated during the active DNA packaging process also contain a hexamer (30). Due to the discrepancy in their data, another group proposed an alternative theory in which one of the subunits in the pentamer ring is inactive during each cycle and the other four pentamer subunits function sequentially during the DNA packaging process (15, 86). We provide conclusive data that confirms that the ATPase motor is in fact a hexamer (34), that it is a relative of the hexameric AAA+ DNA translocase, and that the motor mechanism of DNA translocation involves revolution without a counter force, rather than a rotational mechanism that involves a coiling force, as has been popularly believed.

Materials and Methods

Cloning, mutagenesis and protein purification.

The engineering of eGFP-gp16 and the purification of gp16 fusion protein have been reported previously (111). eGFP-gp16 mutants G27D, E119A, R146A, and D118E E119D were constructed by introducing mutations to the gp16 gene (Keyclone Technologies).

Measurement of gp16 ATPase activity.

Enzymatic activity *via* fluorescence was described previously (70).

In Vitro virion assembly assay

Purified *in vitro* components were mixed and subjected to virion assembly assay, as previously described (112).

Statistical analysis and data plotting.

Most statistical analysis was performed using Sigmaplot 11. Determination of the Hill coefficient was obtained by nonlinear regression fitting of the experimental data to the following equation: $E= E_{max}*(x)^n/(k_{app} +(x)^n)$, where E and E_{max} refer to the concentration of gp16/DNA complex, X is the concentration of ATP or ADP, K_{app} is the apparent binding constant, and n is the Hill coefficient.

CE experiments to determine ratio of gp16 to bound dsDNA:

CE (Capillary electrophoresis) experiments were performed on a Beckman MDQ system equipped with double fluorescent detectors (488nm and 635nm excitation). The capillary used was a bare borosilicate capillary 60 cm in total length and a 50 µm inner section. The method consisted of a 20 min separation at 30 KV normal polarity. Typical assay conditions contained 50 mM Tris-HCl, 100 mM borate at pH 8.00, 5 mM $MgCl_2$, 10% PEG 8000 (w/v), 0.5% acetone (v/v), 3 µM eGFP-gp16 monomer and variable amounts of ATP/ADP and DNA.

Sucrose gradient sedimentation of gp16/prohead:

Ultra-pure proheads were incubated with eGFP-gp16 and pRNA at room temperature for an extended period. The samples were loaded on top of a 5-20% sucrose gradient dissolved in buffer that mimicked *in vivo* conditions; 200 µl 60% sucrose was used as a cushion. The samples were then sedimented at 35000 rpm for 4 hr, fractionated, and the fluorescent signal was captured using a Synergy IV microplate reader.

Electrophoretic Mobility Shift Assay (EMSA):

The engineering of eGFP-gp16 and the purification of gp16 fusion protein (111), as well as the gp16 and dsDNA binding assay (78), have been reported previously. Cy3- or Cy5-dsDNA (40 bp) was prepared by annealing two complementary DNA oligos containing Cy3 or Cy5 labels at their 5' ends (IDT). The annealed product was purified from 10% polyacrylamide gel. The samples for EMSA assay were prepared in 20 μl buffer A (20 mM Tris-HCl, 50 mM NaCl, 1.5% glycerol, 0.1 mM Mg^{2+}). 1.78 μM eGFP-gp16 was mixed with 7.5 ng/μl 40bp Cy3-DNA at various conditions in the typical fashion. The samples were incubated at ambient temperature for 20 min and then loaded onto a 1% agarose gel (44.5 mM Tris, 44.5mM boric acid) for electrophoresis for 1 hr under 80 V at 4°C. The eGFP-gp16 and Cy3-DNA in the gel was analyzed by fluorescent LightTools Whole Body Imager using 488 nm and 540 nm excitation wavelengths for GFP and Cy3, respectively.

Observation of gp16 motion:

Double-stranded lambda DNA (48kbp) was stretched by forming a tightrope between two polylysine coated silica beads (168). The dsDNA was tethered between beads by back-and-forth infusion of DNA over the beads for 10 min; the tethering was formed as a result of charge-charge interactions. The stretched DNA chain was lifted above the surface by the 4 μm silica beads. The incident angle of the excitation beam in objective-type TIRF (total internal reflection fluorescence) was adjusted to a sub-critical angle in order to image the samples a few microns above the surface with low fluorescence background (168). To-Pro-3 was used to confirm the formation of the DNA tightropes. After the DNA tightrope was formed, a mixture of 1 nM Cy3-gp16 with 100 nM unlabeled gp16 in buffer B (25 mM Tris, pH 6.1, 25 mM NaCl, 0.25 mM

$MgCl_2$) was infused into the sample chamber for binding to the stretched DNA. After 30 min incubation, a solution containing anti-photobleaching mixture (30) was infused into the chamber to detect binding. Movies were taken after the chamber was washed with buffer C (25 mM Tris, pH 8, 25 mM NaCl, 0.25 mM $MgCl_2$). A comparison was made of washings with buffer C, with and without 20 mM ATP. Sequential images were acquired with a 0.2 sec exposure time at an interval of 0.22 sec, with a laser of 532 nm for excitation. The movies were taken for about 8 min, or until the Cy3 fluorophores lost their fluorescence due to photobleaching. Image J software was utilized to generate kymographs to show the displacement of the Cy3-gp16 spots along the DNA chains.

Results

The structure of the hexameric motor

The essential components of the Phi29 DNA packaging motor include the dodecameric channel (also known as the connector) and the ATPase gp16 geared by a ring of RNA. The crystal structure of the three-way junction (3WJ) of the pRNA (56), one of the motor components, has recently been solved (63) and the hexameric pRNA ring has been constructed (Figure 4.1A). AFM images revealed an elaborate, ring-shaped structure consisting of six distinct arms representing the six subunits of pRNA (Figure 4.1D).

Sliding of gp16 out of dsDNA verified by addition of steric blocks to the end of dsDNA

When Cy3-dsDNA was mixed with eGFP-gp16, a transfer of energy from the donor fluorophore (eGFP) to the acceptor fluorophore (Cy3) was observed, indicating that the protein fluorophore is at a close proximity to the dsDNA fluorophore. However, after addition of ATP, the Förster Resonance Energy Transfer (FRET) efficiency decreased significantly (Figure 4.2),

suggesting that the protein had walked off of the DNA after ATP hydrolysis. In contrast, the binding of gp16 to dsDNA was significantly enhanced in the presence of non-hydrolyzable ATP analogue, γ-S-ATP, as shown in both gel shift and binding assays. These data support our recent report that ATP induces a conformational change in gp16 resulting in a higher binding affinity for dsDNA (78). To further verify whether the discharge of gp16 from DNA is simple dissociation or a process by which gp16 walks along DNA, we exploited a streptavidin hindrance test (Figure 4.3). Two biotin moieties were conjugated to the 3'-ends of the two strands of the dsDNA (Figure 4.3). The terminally biotinylated DNA was incubated with streptavidin, which binds to biotin and provides a blockade for gp16's departure. If gp16 dissociates from the DNA such that binding is an "on and off" manner, instead of tracking or walking along DNA, streptavidin would not be able to block the gp16 discharge and would essentially render the addition of the streptavidin useless. However, if gp16 formed a ring and slid along the dsDNA helix, streptavidin will effectively block the departure of gp16 from dsDNA. Our results revealed that the gp16/DNA/γ-S-ATP complexes remained stable in the presence of ATP when the terminally biotinylated Cy3 DNA was pre-incubated with streptavidin, but binding was not retained in the presence of ATP and absence of streptavidin.

Binomial quantification assay revealing one Walker B mutant completely blocks motor function

The Walker A motif of AAA+ proteins has previously been shown to be responsible for ATP binding, and the Walker B motif the initiation of ATP hydrolysis (169). The Walker A motif has previously been identified in Phi29 ATPase gp16 (2) and recently we have confirmed the presence of the Walker B motif in gp16 by introducing mutation to both motifs and performing functional assays (34). With the cloned mutants to the Walker B motif, the Hill

constant was evaluated using capillary electrophoresis of DNA binding affinity to distinguish between a sequential or concerted action mechanism.

In order to elucidate the mechanism of the DNA packaging motor, we had to empirically determine the number of copies of inactive Walker B mutant within the hexameric ring that are required to block the entire DNA packaging process. This will partially explain whether the action of motor component is sequential or concerted. The minimum number (y) of mutant gp16 needed to block the packaging within the hexameric ring was predicted with the equation

$$(p+q)^6 = \binom{6}{0}p^6 + \binom{6}{1}p^5q^1 + \binom{6}{2}p^4q^2 + \binom{6}{3}p^3q^3 + \binom{6}{4}p^2q^4 + \binom{6}{5}p^1q^5 + \binom{6}{6}q^6,$$

where p and q represent the ratio of wildtype and Walker B mutant gp16, respectively, and p + q = 1 (Figure 4.4). Using this expanded binomial, each term represented a different mixed hexamer where the exponents of p and q were indicative of the copy numbers of wildtype and mutant in each mixed hexamer, respectively. For example, the term $\binom{6}{3}p^3q^3$ indicates that the hexameric gp16 contains a perfect mix of 3 wildtype and 3 Walker B mutant monomers. Our empirical data almost perfectly overlapped with the theoretical curve corresponding to the term $\binom{6}{0}p^6q^0$, indicating that when y is greater than or equal to 1, the entire complex becomes inactive, suggesting that one copy of the Walker B mutant is capable of completely abolishing motor activity.

Motor ATPase tightly clinched dsDNA after binding to ATP and subsequently pushed the dsDNA away after ATP hydrolysis

Similar to the AAA+ motor proteins that undergo a cycle of conformational changes during their interaction with ATP and adaptation of two distinct states, Phi29 motor ATPase also

exists in either a high or low affinity for the DNA substrate. Recently, it has been qualitatively demonstrated *via* electrophoretic mobility shift assays (EMSA) (78) that the motor ATPase gp16's affinity towards dsDNA increases in the presence of γ-S-ATP, but remains low in the presence of ADP, AMP, or no nucleotide. To get quantitative information about the different binding states of gp16, we utilized a CE assay that allowed for direct quantification of the amount of DNA bound to gp16. At increasing concentrations of γ-S-ATP, the amount of bound DNA increased progressively, indicating that gp16 transitioned from a state in which binding to DNA was unfavorable to one in which binding was preferred (Figure 4.5A). The regression plot of dissociation constant (K_d) for dsDNA versus concentration of γ-S-ATP indicated that the affinity of gp16 for substrate increased 40 fold in saturating amounts of γ-S-ATP (Figure 4.5B). This significant increase strongly suggests that the species that binds to DNA is the gp16-ATP complex and the gp16 binds first to ATP and secondly to DNA, as also suggested in the previous report (78). However, adding ADP, even at non-physiological conditions (up to 6 mM), failed to promote an increase in dsDNA binding affinity (Figure 4.5C). Furthermore, the amount of DNA bound to g16 was comparable to the situation in which no nucleotide was added. These observations indicate that gp16 cycles through states of ATP binding/DNA loading and ATP hydrolysis/DNA release or pushing. The conclusion was also supported by the finding that addition of normal ATP to the gp16/DNA/γ-S-ATP complex promoted the departure of the dsDNA from the complex (Figure 4.7).

Only one molecule of ATP is sufficient to generate the high affinity state for DNA in the ring of the motor ATPase.

Next, we sought the answer to how many nucleotides were required for gp16 to generate the high affinity state for dsDNA; in other words, how many subunits need to bind to ATP in

order for the gp16 hexamer to stably associate to dsDNA. This information is useful to understand how the hexameric complex of gp16 utilizes the substrate in order to generate unidirectional DNA translocation. AAA+ proteins are typically organized into a homo-oligomeric assembly where each component contains the recognition motifs required for binding of the substrate. In principle, one can imagine that each subunit can bind to the substrate independently from the others; however, such an arrangement can lead to futile cycles of ATP consumption. Two major configurations can be hypothesized to avoid the above described scenario. Firstly, it may be possible that the binding sites for the substrate consist of the same recognition motifs in all the subunits, and in this case, all subunits can bind at the same time to the substrate. In this hypothetical situation, it is intuitive to imagine that a form of coordination among the subunits must also exist at the level of ATP hydrolysis, since the most effective mechanism of translocation would allow all subunits to hydrolyze at the same time corresponding to an exodus of the dsDNA substrate. The second possibility is that DNA is bound at any given time to only one subunit of the oligomer, and after the cycle of ATP hydrolysis is terminated in the specific subunit that binds DNA, the substrate is then passed to the next subunit in the high ATP affinity state in order to initiate another cycle of hydrolysis. To distinguish between these two scenarios, we analyzed the amount of DNA bound to gp16 by keeping the concentration of gp16 and DNA constant and varying the concentration of γ-S-ATP in the reaction mixture (Figure 4.5D). If more than one γ-S-ATP per oligomer of gp16 is required to generate the high affinity state for DNA in the protein, the plot would show a cooperativity profile, with the Hill coefficient representing the amount of γ-S-ATP required to be bound to gp16. Our data exhibits no cooperativity in binding (Hill coefficient = 1.5) indicating that all of the subunits of gp16 are not required to be bound to γ-S-ATP to stabilize binding to DNA.

In principle, a Hill coefficient close to one indicates that only one γ-S-ATP-activated subunit in the oligomer is required for DNA binding or that the binding of DNA is progressively increased with the number of subunits that are bound to γ-S-ATP. To overcome this argument, we performed an experiment similar to the CE assay described above. The complex of gp16-DNA was assembled in the presence of saturating conditions of γ-S-ATP. After the complex formed, increasing amounts of ADP were added in order to compete with γ-S-ATP for the active sites of gp16 and to ultimately promote the release of DNA. The results exhibited a remarkably cooperative behavior (Figure 4.5E,F). From the fractional inhibition plot we extrapolated a Hill coefficient close to 6, indicating that 6 molecules of ADP must be bound to gp16 before dsDNA can be released from the protein. This indicates that only one ATP bound subunit is able to stably bind DNA and prevent ADP mediated release. Furthermore, our results indicate that gp16 most likely binds to dsDNA at only one subunit per round of ATP hydrolysis. As mentioned above, a Hill coefficient close to one indicates that binding of DNA is progressively increased with the number of subunits that are bound to γ-S-ATP. However, the 3.6-nm diameter of the motor channel, as measured from the crystal structure (16, 29), suggests that only one dsDNA can be bound within the channel; indicating that dsDNA shifts to a subsequent gp16 subunit upon release of the former. In combination with the finding that one Walker B mutant gp16 was found to be sufficient to block the motor for DNA packaging, these results support the model that the motor ATPase works sequentially, and upon ATP hydrolysis the subunit of the ATPase gp16 assumes a new conformation and pushes dsDNA away from the subunit and transfers it to an adjacent subunit (Figure 4.7).

Mixed oligomer between wildtype and mutants display negative cooperativity and communication between the subunits of gp16 oligomer

The fact that dsDNA only binds to one gp16 subunit at a time suggests that gp16 undergoes cooperativity during translocation. To verify this hypothesis we analyzed ATPase activity by studying the effect on the oligomerization of gp16 when mutant subunits were introduced (62, 117). If we assume communication between the subunits of the ATPase, the effect on the ATPase activity mediated by one inactive subunit should be higher than the simple sum of the ATPase activity of the single subunit. When the ATPase activity was measured in the absence of dsDNA, increasing amounts of Walker B mutants added to the overall oligomer of gp16 failed to provide any significant effect on the rate of hydrolysis (Figure 4.6A,C), suggesting that each subunit of gp16 is able to hydrolyze ATP independently. On the contrary, when saturating amounts of dsDNA were added to the reaction, we observed a strong negative cooperative effect with a profile that mostly overlapped with the one predicted for the case in which one single inactive subunit is able to inactivate a whole oligomer (Figure 4.6B,D); a predicted case calculated from a binomial distribution inhibition assay (62, 117). The results suggest that in the presence of dsDNA, a rearrangement occurs within the subunits of gp16 that enables them to communicate between each other and "sense" the nucleotide state of the reciprocal subunit. The fact that dsDNA needs to be present in the reaction indicates that dsDNA binds to the inactive subunit during the catalytic cycle and remains bound to it, which generates a stalled ATP hydrolysis cycle. This observation supports the idea that only the subunit that is binding to the substrate at any given time is the one that is permitted to hydrolyze ATP, thus performing translocation while the other subunits are in a type of 'stalled' or 'loaded' state. The scenario suggests an extremely high level of coordination on the function of the protein, which is

likely the most efficient process to couple energy production with DNA translocation *via* ATP hydrolysis. An effective mechanism of coordination is apparent between gp16 and dsDNA using the hydrolysis cycle as means for regulation.

Direct observation of multiple ATPase gp16s lining up in queue along dsDNA as the initiation step in DNA packaging

The standard notion derived from extensive investigation of viral packaging motors is that the ATPase binds to the procapsid to form a procapsid/ATPase complex as the first step of motor action in DNA packaging (110, 170). To investigate the sequence of interaction between motor components during DNA packaging, a fluorescent Cy3-conjugated gp16 was used to visualize the protein. Interestingly, we found that the first step in DNA packaging was the binding of multiple gp16 queued along the dsDNA, as observed by single molecule imaging (Figure 4.8 Part I) and by binding affinity studies. Moreover, negatively stained electron microscopy images have been taken of a multimeric gp16 complex along long genomic DNA (Figure 4.8 Part II), lending further support to our conclusions.

DNA tightropes were constructed (168), which not only generated a straight DNA chain, but also lifted the DNA a few microns away from the surface of the slide within the sample chamber. Background fluorescence from non-specific binding of Cy3-gp16 to the surface of the slide was therefore eliminated when the focus of the imaging plane was at the Cy3-gp16 molecules on the DNA chains. A string of multiple Cy3 spots representing Cy3-gp16 complexes were bound along the DNA chains (Figure 4.8 Part I A-C, E, F). In the absence of DNA, a Cy3 signal was not observed between the polylysine beads (Figure 4.8 Part I D), indicating that the queued Cy3 signals were truly from the multiple Cy3-gp16 bound to the DNA chains. The

results suggest that ATPase gp16 lines up in a queue along dsDNA as the initiation step in DNA packaging. This data is in accordance with another study whose results showed that when complexes of procapsid containing partially packaged dsDNA were isolated by sucrose sedimentation, conversion of the complexes to complete the DNA packaging process required ATPase gp16, but not pRNA (46). The same publication also indicated that multiple gp16, but only a single hexameric pRNA, was required for packaging (46).

It has been previously reported that the terminases of viral DNA packaging motors bind to procapsids, although with an extremely low affinity and efficiency (17, 60, 110, 170-172). Our finding that gp16 binds to dsDNA first and then moves along dsDNA before reaching and binding to the procapsid is not contradictory to previous findings, rather a further refinement of the previous understanding. We hypothesize that gp16 contains two domains, one for dsDNA binding and one for connector/procapsid binding. In the absence of genomic DNA, gp16 will bind to procapsid, albeit at a lower affinity. The key to understanding the sequence of interaction is based on the relative affinity of the protein for its substrate. Gp16 has a higher binding affinity for genomic DNA compared to that of the procapsid (Figure 4.9). In the absence of dsDNA, gp16 and other terminases bind to the procapsid (110). However, in the presence of genomic DNA, gp16 and other terminases prefer to bind to genomic DNA and track along it until reaching their final destination, the components of the procapsid, and translocated.

To confirm this hypothesis, we further investigated the interaction of ATPase gp16 with the procapsid (Figure 4.9). We discovered that gp16 had the tendency to bind to all kinds of substrate, including nonspecifically to the procapsid. No significant difference was observed during the formation of the procapsid/gp16 complex in the presence or absence of pRNA (Figure 4.9), which has been reported to serve as the bridge for gp16 binding to procapsid (60). The

estimated dissociation constant was calculated and gp16 was found to have a 10-fold higher affinity for dsDNA than for the prohead/pRNA complex. Although the ATPase is hypothesized to contain both dsDNA and procapsid binding domains, it is suggested that the ATPase prefers to bind to the procapsid only after tracking along the genomic DNA; that is, gp16 prefers to bind to genomic DNA first before reaching the procapsid.

Direct observation of ATP-dependent motion of gp16 along dsDNA in real-time by single molecule fluorescence imaging

The motion of gp16 along the lifted dsDNA tightrope was observed by single molecule fluorescence imaging. Sequential images were taken after washing with different buffers to illustrate the displacement of Cy3-gp16 over time. When the sample was washed with a buffer, a total of 195 Cy3-gp16 spots were studied. In the absence of ATP, the vast majority of these Cy3-gp16 spots did not show any motion along the DNA chain. After 20 mM ATP was added to the washing buffer, active motion of eGFP-gp16 along the dsDNA was observed, as shown by the sequential images (Figure 4.8 Part I G) and kymographs (Figure 4.8 Part I H).

Translocation of dsDNA helix by revolution without involvement of coiling or tension force

It has previously been demonstrated that the connector is a one way valve (41, 44, 78) that only allows dsDNA to move into the procapsid, but does not allow movement in the opposite direction. Gp16, which is bridged by pRNA to associate with the connector, is expected to be the pushing force (Figure 4.10A). The binding of ATP to one subunit stimulates gp16 to adapt a conformation with high affinity for dsDNA, while ATP hydrolysis forces gp16 to assume a new conformation with lower affinity for dsDNA, thus pushing dsDNA away from the subunit and transferring it to an adjacent subunit (Figure 4.10). Since the contact of the connector with

dsDNA chain is transferred from one point on the phosphate backbone to another, rotation of the hexameric ring or the dsDNA is not required. One ATP is hydrolyzed in each transitional step, and six ATPs are consumed for one cycle to translocate dsDNA one helical turn of 360° (10.5 base pairs). The binding of gp16 to the same phosphate backbone chain, but at a location 60° different from the last subunit, urges dsDNA to move forward 1.75 base pairs (10.5 bp per turn ÷ 6 ATP = 1.75 bp/ATP), agreeing with the 2 bp/ATP(2) or 1.8 bp/ATP previously quantified empirically(142).

Translocation of dsDNA helix by revolution through the 30°-tilted connector subunits facilitated by anti-parallel displacement between dsDNA helix and the connector portal protein

Extensive research has also been undertaken to understand the role of the connector during packaging, especially after the crystal structure of the connector had been elucidated. An interesting phenomenon was observed. All 12 subunits of the connector protein tilt at a 30° angle, in a configuration anti-parallel to the dsDNA helix during packaging, to form the channel (16, 29). The anti-parallel arrangement can be visualized from an external viewpoint in which dsDNA propels through the connector potentially making contact at every 30° subunit (Figure 4.11). This anti-parallel arrangement tends to argue against the bolt and nut mechanism. This structural arrangement greatly facilitates controlled motion, supporting the conclusion that dsDNA revolves through the connector channel without producing a coiling or torsion force, and touching each of the 12 connector subunits in 12 discrete steps of 30° transitions for each helical pitch (360° ÷ 12 = 30°) (Figure 4.11D). Moreover, the 30° angle of each connector subunit coincides nicely with the crystal structure of the spiral cellular clamp loader and the grooves of dsDNA (154, 173). Nature has created and evolved a clever rotating machine to reduce the

torque force and to translocate the DNA double helix which actually avoids the difficulties associated with rotation such as DNA supercoiling seen in many other processes.

Discussion

A rotation mechanism of viral DNA packaging motor has long been proposed (12) and is well-liked by the scientific community. However, studies combining the methods of single-molecule force spectroscopy with polarization-sensitive single-molecule fluorescence trap (19) have suggested that the connector does not rotate. The suggestion of non-rotation by the connector was further supported by the experiment in which the connector was covalently linked to the capsid protein of the procapsid (20, 21). When the connector and the procapsid protein were fused to each other, rotation of the connector within the procapsid was not possible. However, the motors were still active in packaging, implying that connector rotation is not necessary for DNA packaging. Furthermore, since the connector does not rotate, there is no reason to believe that gp16 will rotate since the gp16 ring is tightly bound to the pRNA ring (60) that is immobilized to the external end of the stationary connector. The finding that phi29 DNA packaging motor utilizes a revolution instead of rotation mechanism is in a good agreement with all data reported in the history. Since the revolution mechanism is independent of stoichiometry and motors with different oligomeric ATPase subunits all can execute the revolution mechanism the discovery of the revolution mechanism might reconcile the stoichiometry discrepancy among many phage systems for which the ATPase was found to be present as tetramer(164), hexamer (3, 27, 28, 30, 30-32, 63, 166), and nonamers (174).

The connector was recently revealed to only allow for unidirectional movement of dsDNA (41), and a model using a “push through a one-way valve” mechanism was described

(44, 78) which is in accordance with the previously proposed ratchet (103) and compression (104, 105) models. This mechanism describes dsDNA being pushed by the ATPase gp16 through the connector which functions as a valve to prevent DNA from reversing out of the capsid during the packaging process (38, 39, 84, 106). The finding of a revolution hexamer mechanism is seemingly contradictory to the publications reporting the existence of four bursts of translocation per helical turn of genomic B-type dsDNA (15, 86). Although there was much discrepancy in step size and pulse, the data for the four step pause looks quite strong. To address the inconsistencies, we investigated the mechanism of the generation of the four pause steps and found that the four steps of pauses were caused by the dsDNA revolving through the four lysine rings (175) (conditionally accepted). Connector crystal analysis (16, 29) has revealed that the dominantly negatively charged phi29 connector interior channel surface is decorated with 48 positively charged lysine residues existing as four 12-lysine rings derived from the 12 protein subunits that enclose the channel. It has been proposed that these electropositive lysine residues interact with the electronegative phosphate backbone of DNA during DNA translocation through the channel (16, 29). Although the lysine residues were not found to be essential for DNA entry(33, 44), the four positively charged residues have been shown to influence more or less the DNA translocation speed (44, 176, 177).

Based on the crystal structure (16, 29), the length of the connector channel is ~7 nm. The interior of the channel is negatively charged and four lysine rings (K200, K209, K234, and K235) are scattered as four rings inside the channel. Vertically, these four lysine layers fall within a 3.7 nm (16, 29) range and are spaced approximately ~0.9 nm apart ((~3.7 nm)/4=~0.9 nm). Since lysine residues K234 and K235 lie in the inner loop of the connector between residues 229 to 246, of which the residues were missing in the crystal structure, the two residues

close to the boundary of the inner loops were used to estimate their location. Since B-type dsDNA has a pitch of 0.34 nm per base pair as a rise along its axis, 0.9 nm ÷ 0.34 nm.bp^{-1} = ~2.6 bp per rise. This value agrees with the aforementioned finding that DNA packages in four 2.5 bp steps for each helical turn (15, 86). We suggest that the four distinct, alternating positively and negatively charged property of the channel wall alters the speed of DNA translocation and results in four steps of pause during revolution advancement (175). Thus the revolution mechanism is not contradictory to the finding of four steps of pause. However, the authors interpreted their solid findings of pauses as five motor subunits with one subunit inactive resulting in four steps of burst, a model that is seemly novel but does not exist.

Acknowledgements

We would like to thank Dr. Guo-Min Li for his valuable comments, Zhengyi Zhao, Emil Khisamutdinov, and Hui Li for their diligent work on the animation figures, Drs. Bruce Maley and Mary Gail Engle for EM images, and Jeannie Haak for editing this manuscript. The work was supported by NIH grants R01 EB003730, R01 EB012135, and U01 CA151648 to PG, who is a co-founder of Kylin Therapeutics, Inc, and Biomotor and Nucleic Acids Nanotech Development, Ltd.

Figures

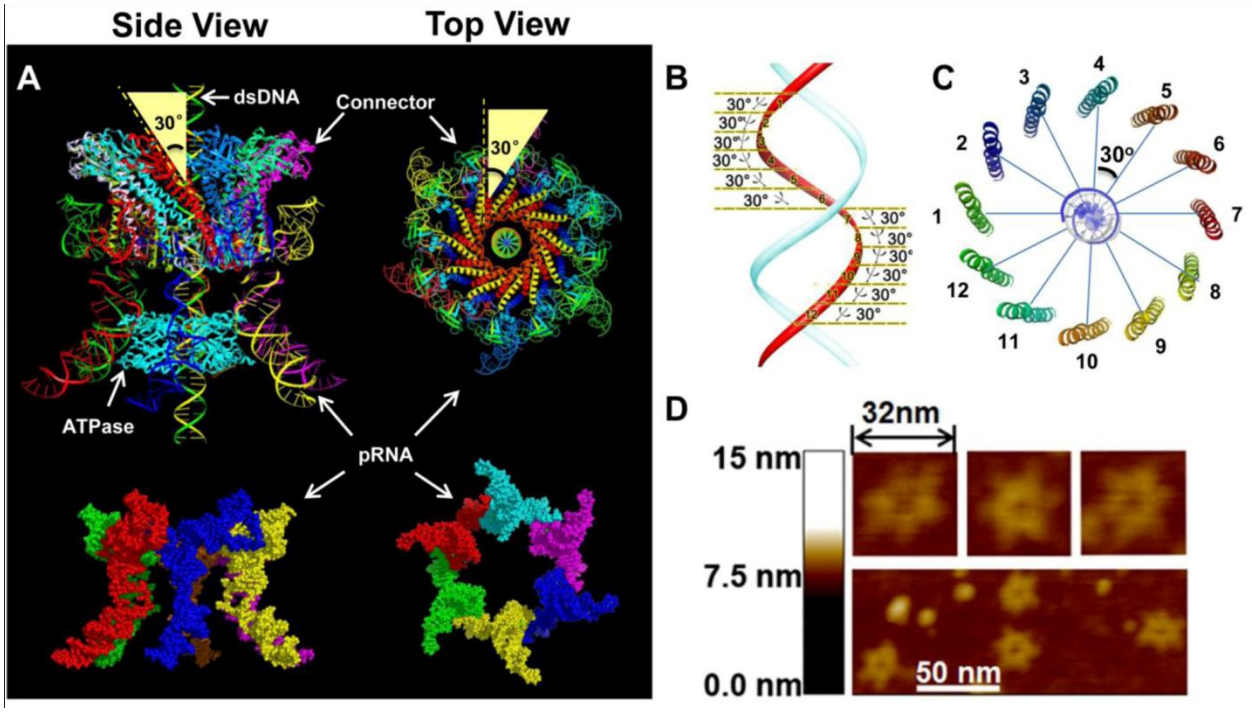

Figure 4.1. Depiction of structure and function of phi29 DNA-packaging motor. (A) Model of hexameric pRNA based on crystal structure and the 30° tilting of the channel subunits of the connector; (B) DsDNA showing the change of 30° angle between two adjacent connector subunits; (C) Connector showing the change of 30° angle between two adjacent connector subunits; (D) AFM images of the hexameric pRNA with 7-nt loops.

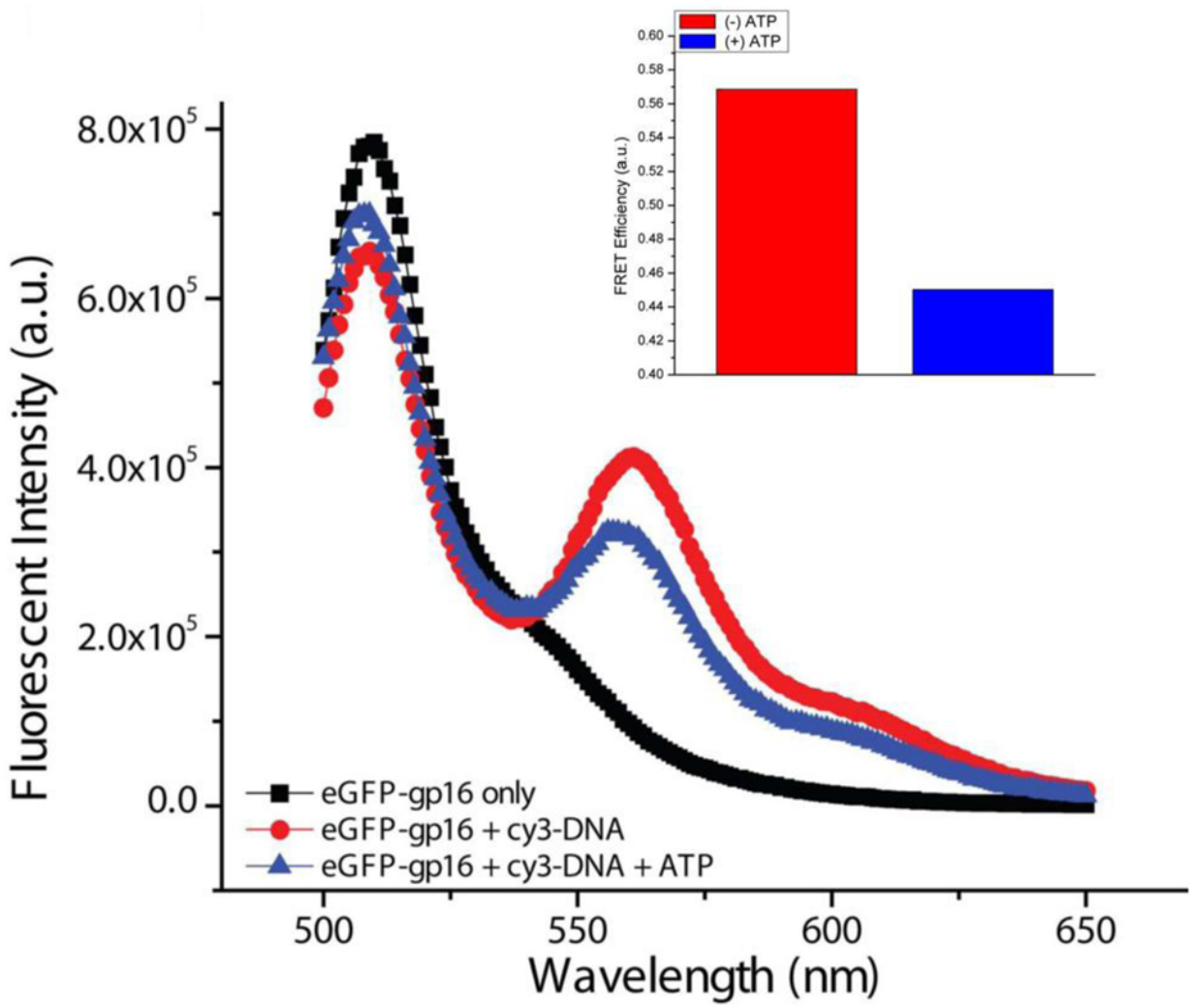

Figure 4.2. FRET Assay of fluorogenic ATPase and short dsDNA. eGFP-gp16 was incubated with Cy3-DNA and with (blue line) and without ATP (red line) and excited at 480 nm. Energy transfer occurs between the two fluorophores indicating the gp16 and DNA are in close proximity.

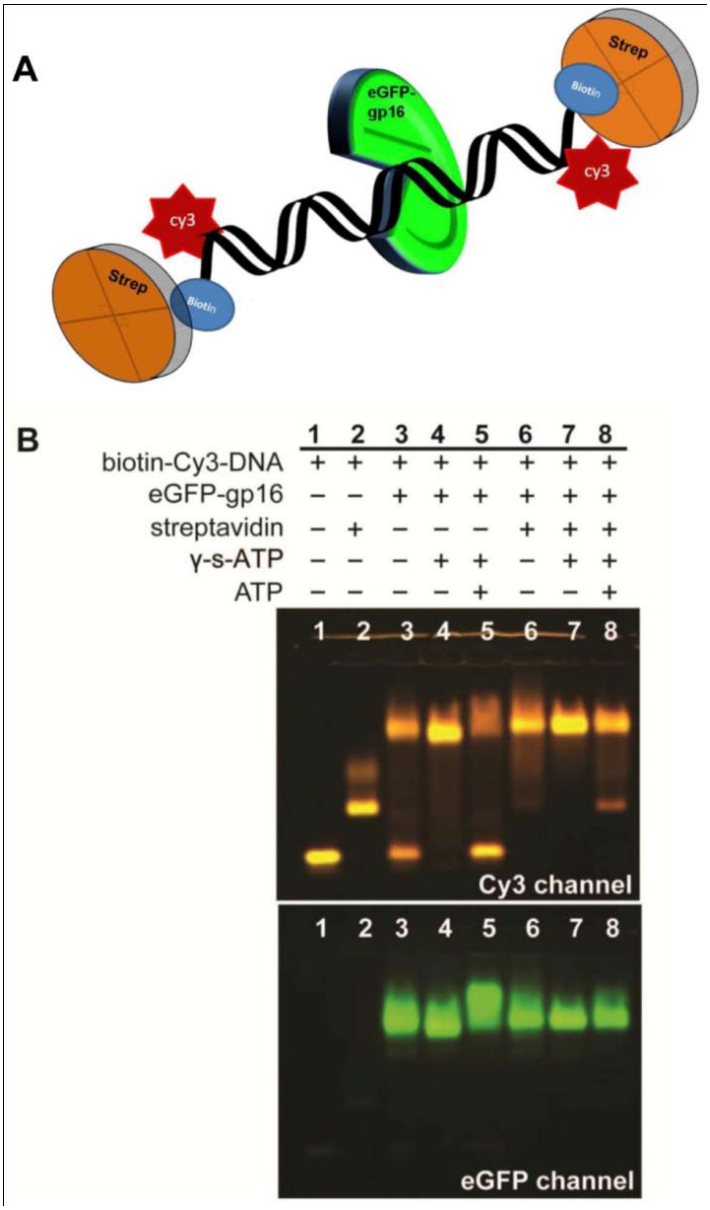

Figure 4.3. Differentiation of gp16 walking along or dissociating from dsDNA by EMSA using terminally-hindered short dsDNA with two biotin at both ends. Fluorogenic Cy3-dsDNA was incubated with GFP-gp16, non-hydrolyzable γ-S-ATP and streptavidin in different combinations. The complexes were then electrophoresed through an agarose gel and scanned for Cy3 fluorescence of DNA and GFP fluorescence of gp16.

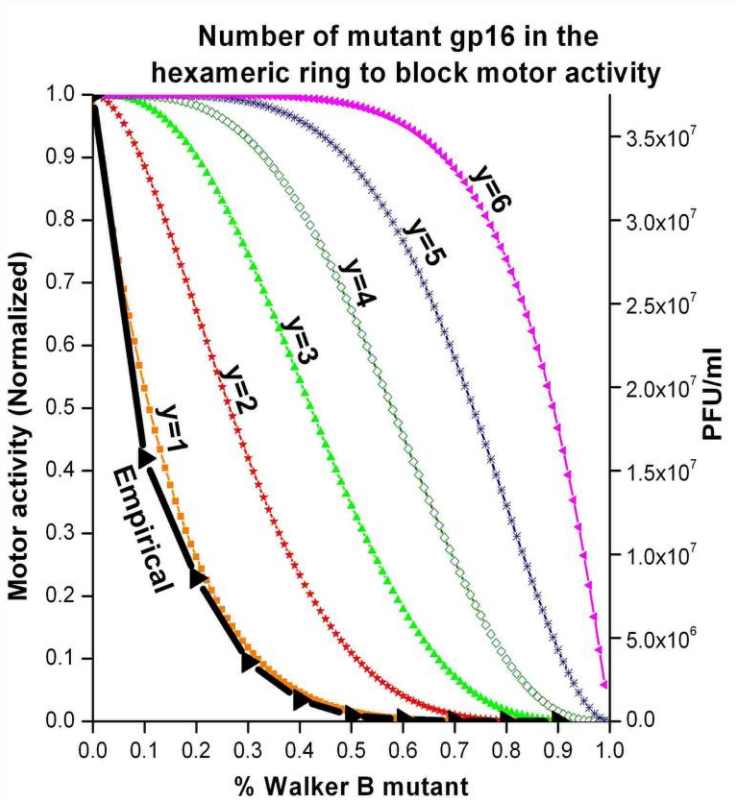

Figure 4.4. Binomial distribution assay to determine the minimum number (y) of Walker B mutant eGFP-gp16 in the hexameric ring to block the motor activity. The equation $(p+q)^6 = \binom{6}{0}p^6 + \binom{6}{1}p^5q^1 + \binom{6}{2}p^4q^2 + \binom{6}{3}p^3q^3 + \binom{6}{4}p^2q^4 + \binom{6}{5}p^1q^5 + \binom{6}{6}q^6$ is used, where p and q represent the ratio of wild type and mutant eGFP-gp16 respectively, and p+q=1. If y=1, then the motor activity will be $\binom{6}{0}p^6$; if y=2, then the motor activity will be $\binom{6}{0}p^6 + \binom{6}{1}p^5q^1$; if y=3, then the motor activity will be $\binom{6}{0}p^6 + \binom{6}{1}p^5q^1 + \binom{6}{2}p^4q^2$; if y=4, then the motor activity will be $\binom{6}{0}p^6 + \binom{6}{1}p^5q^1 + \binom{6}{2}p^4q^2 + \binom{6}{3}p^3q^3$; if y=5, then the motor activity will be $\binom{6}{0}p^6 + \binom{6}{1}p^5q^1 + \binom{6}{2}p^4q^2 + \binom{6}{3}p^3q^3 + \binom{6}{4}p^2q^4$; if y=6, then the motor activity will be $\binom{6}{0}p^6 + \binom{6}{1}p^5q^1 + \binom{6}{2}p^4q^2 + \binom{6}{3}p^3q^3 + \binom{6}{4}p^2q^4 + \binom{6}{5}p^1q^5$.

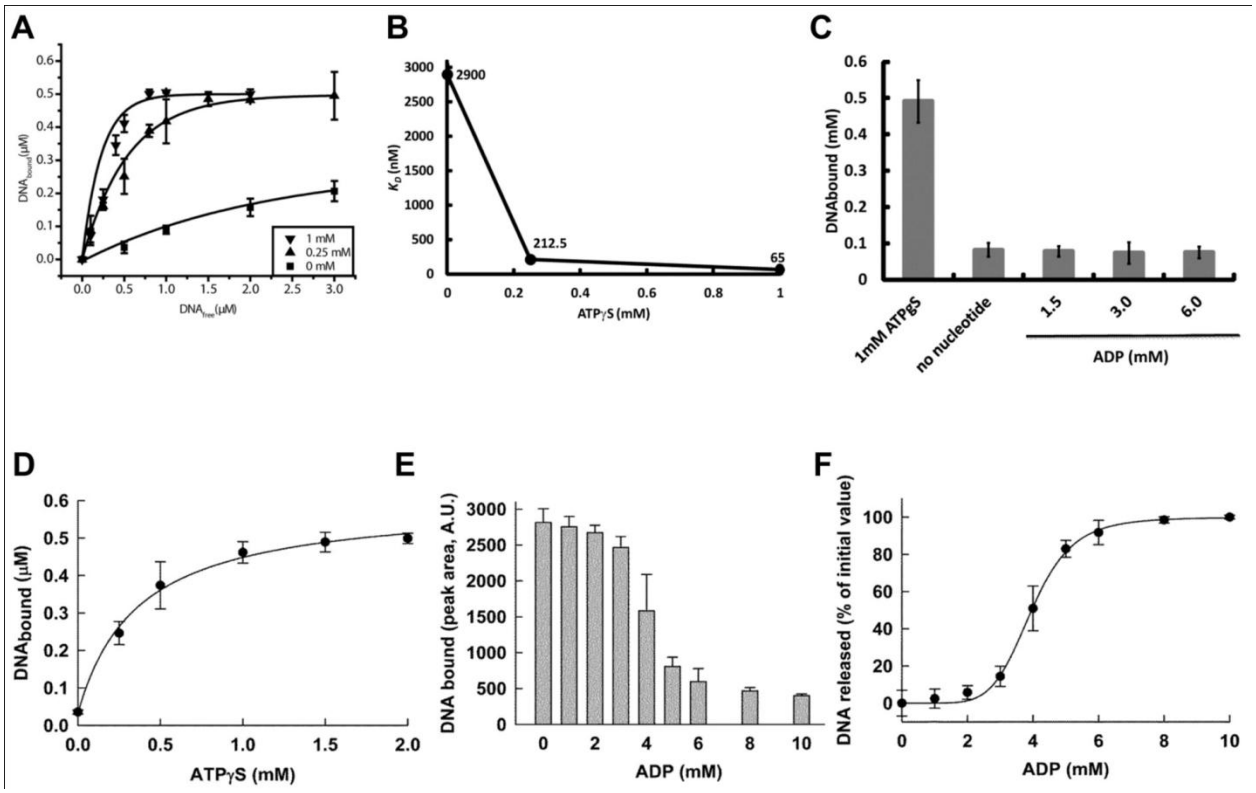

Figure 4.5. Data demonstrating only one γ-S-ATP is sufficient to bind to one subunit of the hexameric gp16 complex and promote a high affinity state for dsDNA. Sequential binding of gp16 for dsDNA substrate involves γ-S-ATP substep. (A) The K_d for dsDNA in the presence (triangles) and absence (squares) of γ-S-ATP. (B) The relative K_d of gp16 decreased 40-fold as the concentration of γ-S-ATP increased from 0 mM to 1 mM. (C) ADP, a derivative of ATP hydrolysis, was unable to promote binding and had the similar effect as no nucleotide addition. The hyperbolic curve (D) suggests a cooperativity factor of 1, indicating that one γ-S-ATP is sufficient to produce the high affinity state of gp16 for DNA. DNA releases from the complex DNA-gp16-γ-S-ATP mediated by ADP (E), forming a sigmoidal curve (F) with a cooperativity factor of 6 indicating that all 6 subunits of gp16 need to be bound to ADP to release DNA from the protein.

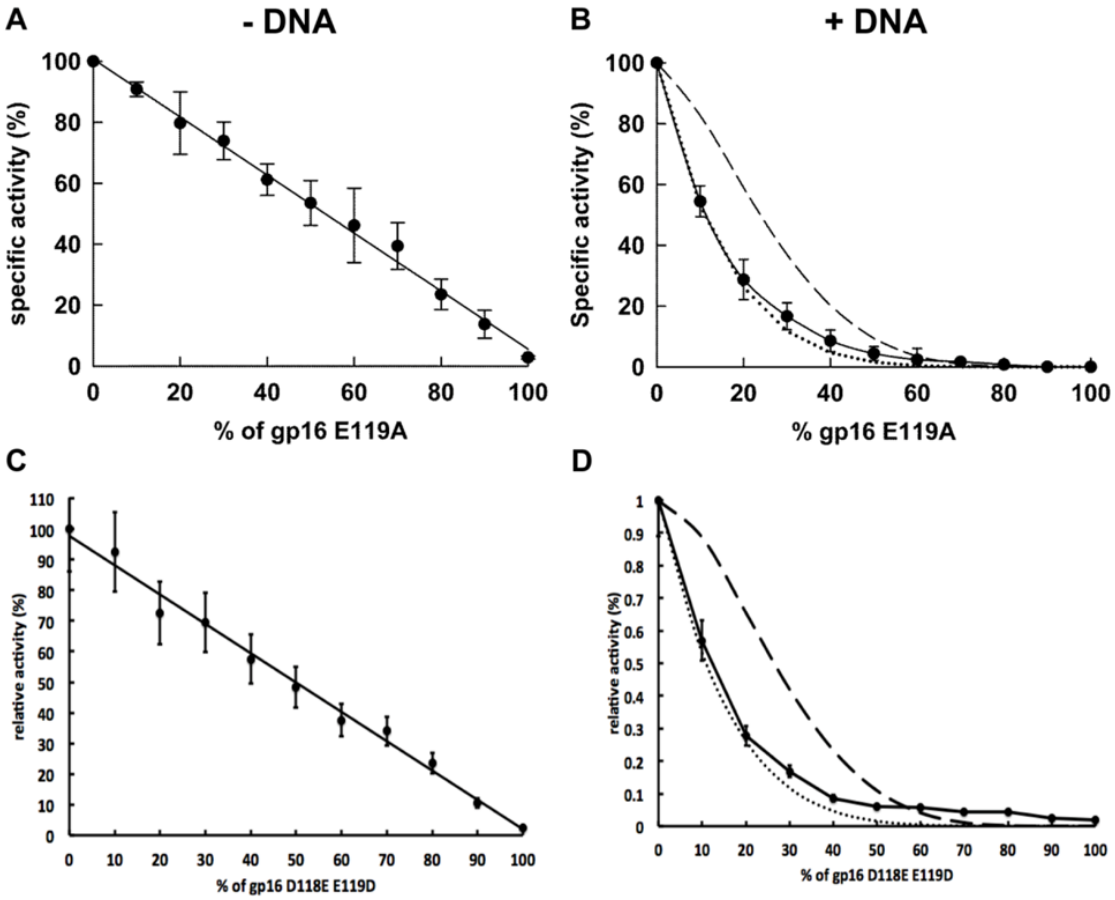

Figure 4.6. ATPase inhibition assay of Walker B mutants reveal complete negative cooperativity. The inhibition ability of the Walker B mutants E119A and D118E/E119D was assayed by ATPase activity to determine the theoretical model in the absence (left) and presence (right) of dsDNA. In the presence of DNA (right), the experimental data (solid line) overlapped with the theoretical curve indicating that one inactive subunits (dotted line) within the hexamer are able to completely block the activity of the hexameric gp16 and abolish gp16's ability to hydrolyze ATP, demonstrating negative cooperativity. The dashed line is the theoretical curve representing two inactive subunits are necessary for complete inhibition of the hexamer.

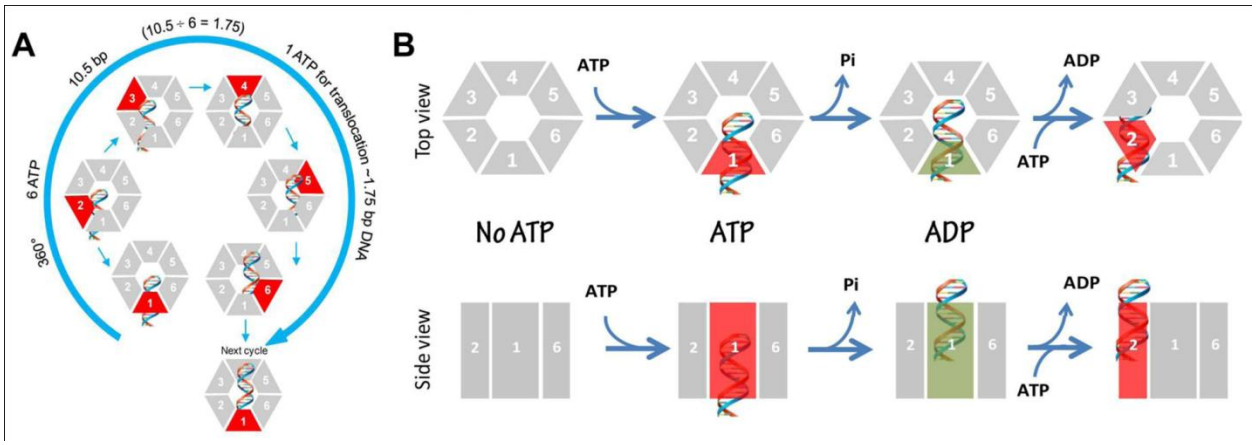

Figure 4.7. Schematic of gp16 binding to DNA and mechanism of sequential revolution in translocating genomic DNA. The connector is a one way valve that allows dsDNA to move into the procapsid, but does not allow movement in the opposite direction. Gp16, which is bridged by pRNA to associate with the connector, is the pushing force. The binding of ATP to one subunit stimulates gp16 to adapt to a conformation with a higher affinity for dsDNA. ATP hydrolysis forces gp16 to assume a new conformation with a lower affinity for dsDNA, thus pushing dsDNA away from the subunit and transferring it to an adjacent subunit. DsDNA moves forward 1.75 base pairs when gp16 binds at a location 60^{o} different from last subunit on the same phosphate backbone chain. Rotation of the hexameric ring or the dsDNA is not required since the dsDNA chain is transferred from one point on the phosphate backbone to another. In each transitional step, one ATP is hydrolyzed, and in one cycle, six ATPs are required to translocate dsDNA one helical turn of 360^{o} (10.5 base pairs).

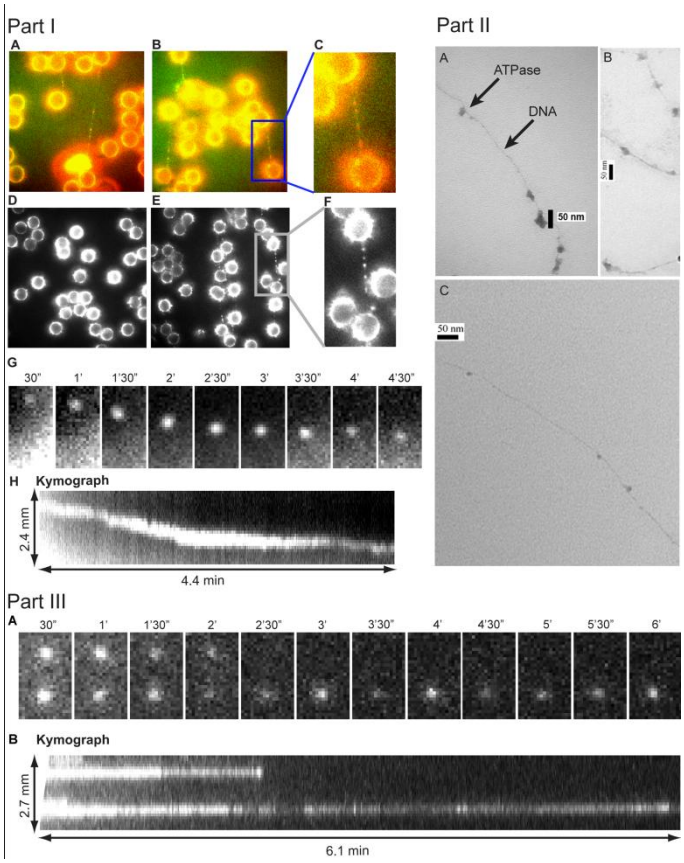

Figure 4.8. Direct observation of ATPase complex queued and moving along dsDNA. Part I. Cy3 conjugated gp16 was incubated with (A, B, E) and without (D) phi29 genomic dsDNA, tethered between two polylysine beads where (C, F) are magnified images of the framed regions of (B, E), respectively. (A-C) are overlapped pseudocolor images indicating the binding of Cy3-labeled gp16 along the To-Pro-3 stained dsDNA chain (Red: Cy3-gp16; Green: To-Pro-3 DNA). (G, H) The motion of the Cy3-gp16 spot was analyzed and a kymograph was produced to characterize the ATPase walking. **Part II. Negatively-stained transmission electron microscopy images of ATPase queued along dsDNA.** gp16 was bound to non-specific dsDNA in queue. **Part III. Recording of two Cy3-gp16/dsDNA complexes showing motionless gp16 spots in a buffer containing no ATP.** (A) Sequential images of the recording. (B) Kymograph of the two spots.

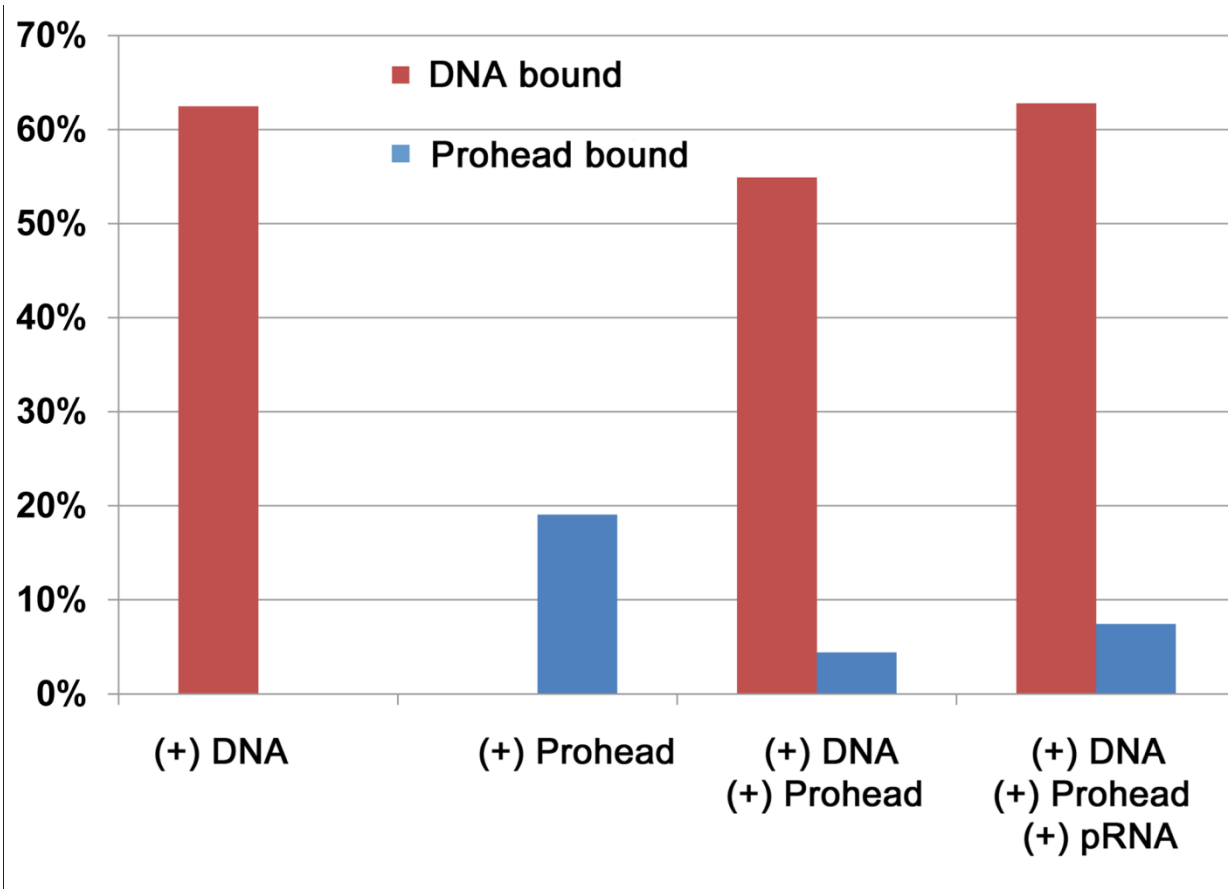

Figure 4.9. Comparison of binding affinity of gp16 to dsDNA and procapsid/pRNA complex using sucrose sedimentation. Ratio of prohead-bound and DNA-bound gp16 under different treatments where the percent of bound gp16 to total gp16 is expressed, showing gp16's affinity to DNA is much greater than to prohead/pRNA complex.

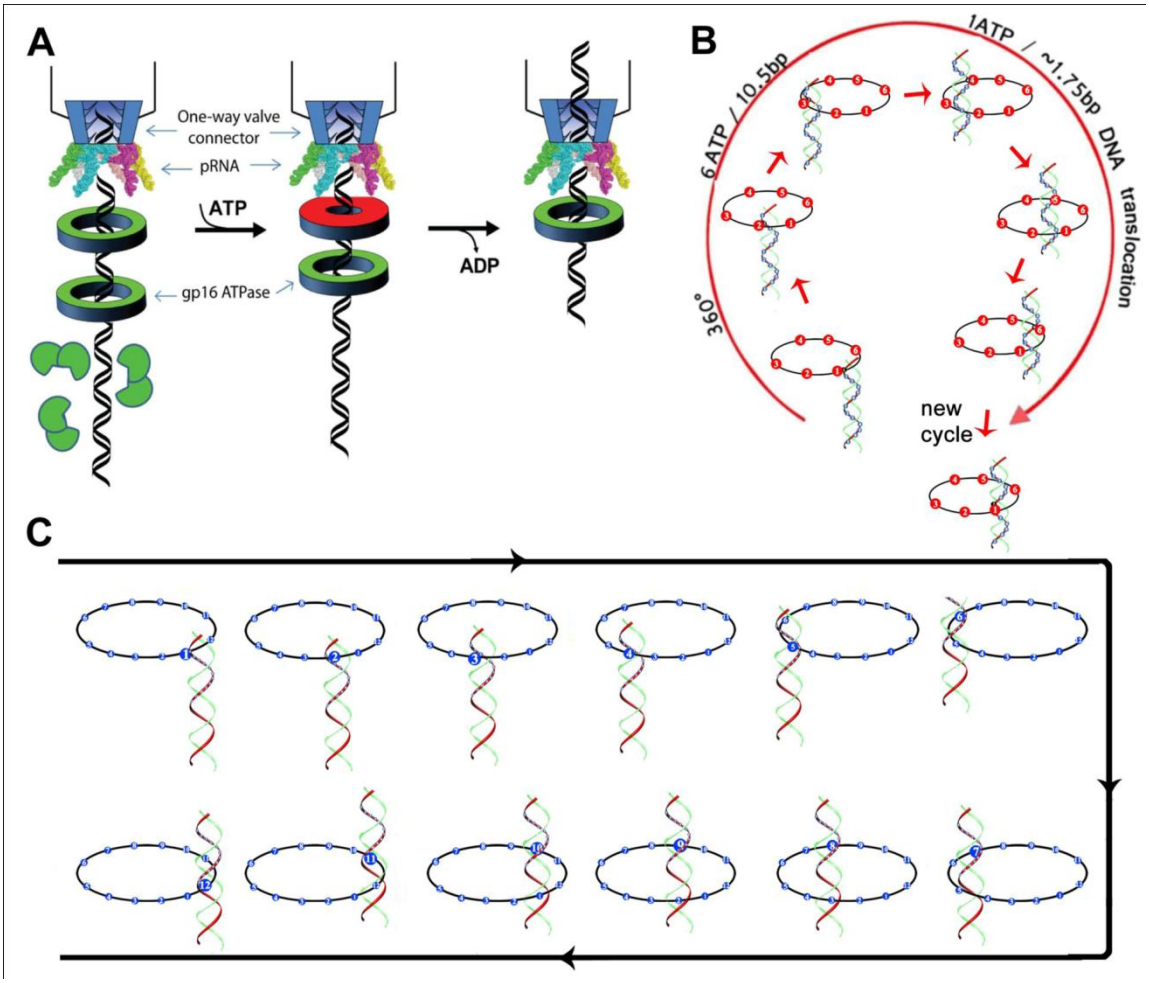

Figure 4.10. Mechanism of sequential revolution in translocating genomic DNA. Connector is a one way valve (12, 19, 112) that allows dsDNA to move into the procapsid but does not allow movement in the opposite direction. Binding of ATP to one gp16 subunit stimulates it to adapt a conformation with higher affinity for dsDNA. ATP hydrolysis forces gp16 to assume a new conformation with lower affinity for dsDNA, thus pushing dsDNA away from this subunit and transferring it to an adjacent subunit. Binding of gp16 to the same phosphate backbone chain but at a location 60° different from last subunit urges dsDNA to move forward 1.75 base pairs. Since the dsDNA chain is transferred from one point on the phosphate backbone to another point, the rotation of the hexameric ring or the dsDNA is not required. (C) The revolution of dsDNA along the 12 subunits of the connector channel.

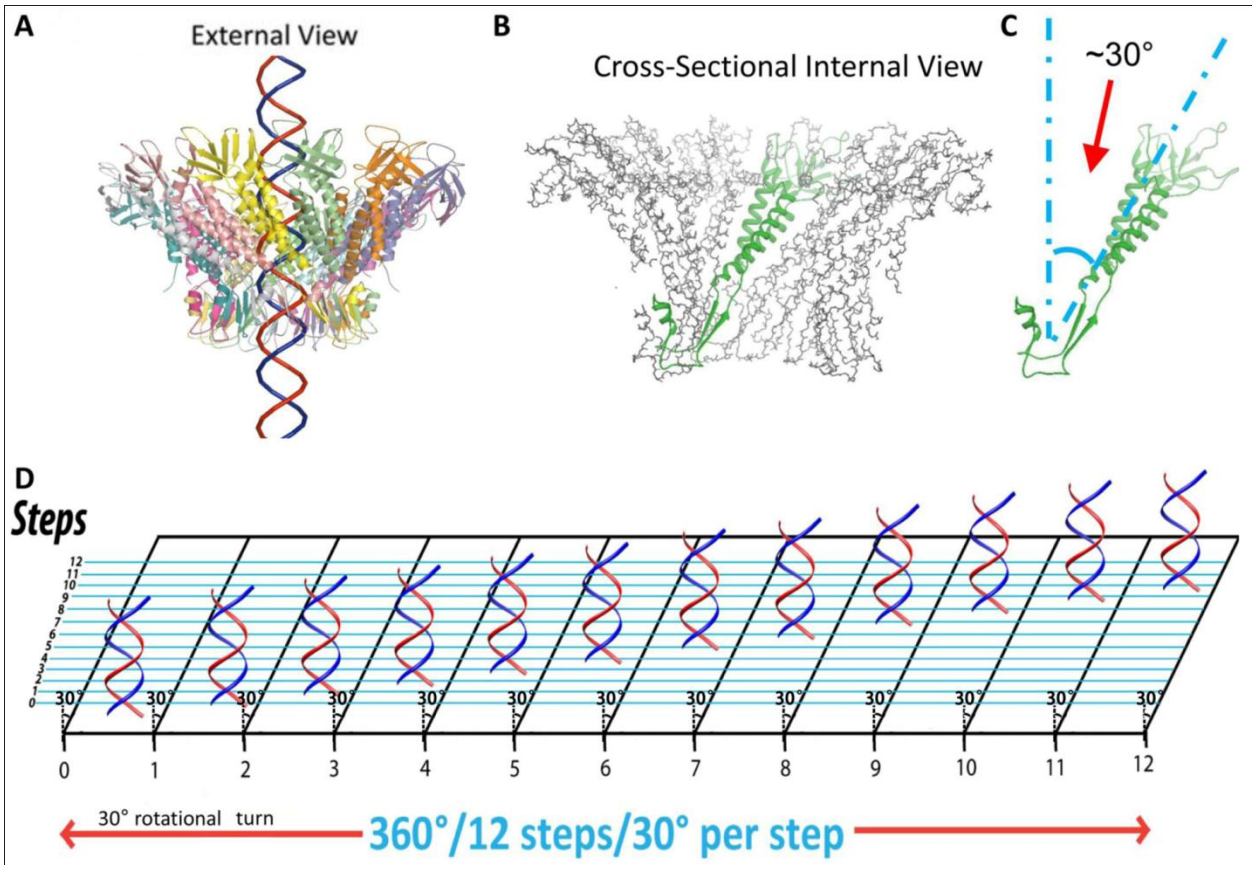

Figure 4.11. **DNA revolves and transports through 30° tilted connector subunits facilitated by anti-parallel helices between dsDNA helix and connector protein subunits.** The anti-parallel configuration can be visualized in an external view (A) in which DNA revolves through the connector making contacts at every 30° subunit (B,C). A planar view is suggested (D) in which DNA is advanced and travels along the circular wall of the connector channel with no torsion or coiling force through the connector channel touching each subunit translating to 12 discrete steps of 30° revolving turns for each step.

Chapter 5. Current State of DNA Packaging Field and Future Directions

Future Directions of Current Research

The mechanism of DNA packaging has been well-described throughout the duration of this thesis. However, it is imperative to determine whether this mechanism is ubiquitous among other phages and other members of the AAA+ superfamily of ATPase. In order to do this, similar experiments should be performed on the ATPases of such phages as T4, Spp1, T7, and others.

Furthermore, the experiments presented within this thesis should be verified using other techniques. Primarily, the full crystal structure of the ATPase should be examined. Despite continuing efforts, the ATPase has not been crystallized due to its insoluble nature and tendency to form different oligomers in solution. A pioneering approach is to co-crystallize the protein with DNA and the non-hydrolyzable ATP analog, γ-S-ATP. Crystallization has been at the forefront of determining the stoichiometry of biomolecules; however, recently, cryo-electron microscopy has been making a surge in this regard. Cryo-EM reconstructions of the phi29 ATPase have been elucidated on the vertex of the portal vertex (15); however, this technique assumes stoichiometry based on the five-fold stoichiometry of the vertex. It would be interesting to use cryo-EM on the ATPase in solution rather than complexed with the rest of the phage.

Another approach to determine cooperativity in ATP and DNA binding is to use surface plasmon resonance (SPR). This technique allows for simple quantification of the dissociation constant between two biomolecules. With this approach, the calculated dissociation constant obtained from capillary electrophoresis quantification can be verified in relation to the Walker A and Walker B mutants with and without addition of DNA. This will confirm the existence of cooperativity in the ATPase and validate our revolution "push through a one-way valve" mechanism of DNA translocation.

State of DNA Packaging Field

The field of DNA packaging has thrived for over 40 years and many advances in the basic science have been achieved. Major components have been identified and mechanisms have been determined. However, advances that translate to medicinal and technology purposes have yet to be reached. There are many potential areas in which the science could translate to application such as targeted gene therapy and viral assemblyinhibition.

Over the years, studies on the DNA packaging motor have primarily focused on fundamental aspects including structure, biological/biochemical function, and mechanical or physical behaviors of the viral motor or its components for genome packaging. More recently, these powerful viral motors have inspired novel biomimetic designs that have opened up possibilities for building artificial nanomotors operable outside their natural environment for use in nanodevices, and nanomedicine, including the sensing of ions, chemicals, or DNA/RNA (16, 40-42, 45, 136, 178), and targeted gene delivery or drug loading (179, 179, 180, 180-185). A thorough understanding of how the motor components interact with each other during the packaging process and how the energy from ATP hydrolysis is transferred into physical motion would provide valuable insights into fundamental phenomena and the development and application of nanomotor biomimetics. In addition, possible novel targets for antiviral therapy could be discovered based on the studies of the viral DNA packaging mechanism (186-189). Utilizing motor components in nanotechnology and/or disease treatments has also been actively pursued (40-42, 45, 179-185). To continue research on DNA packaging into the future and advance medicine in the future, these approaches should be better targeted.

References

1. Guo P, Erickson S, & Anderson D (1987) A small viral RNA is required for *in vitro* packaging of bacteriophage phi29 DNA. *Science*236: 690-694.

2. Guo P, Peterson C, & Anderson D (1987) Prohead and DNA-gp3-dependent ATPase activity of the DNA packaging protein gp16 of bacteriophage f29. *J Mol Biol*197: 229-236.

3. Guo P, Zhang C, Chen C, Trottier M, & Garver K (1998) Inter-RNA interaction of phage phi29 pRNA to form a hexameric complex for viral DNA transportation. *Mol. Cell.*2: 149-155.

4. Schwartz C, De Donatis GM, Fang H, & Guo P (2013) The ATPase of the phi29 DNA-packaging motor is a member of the hexameric AAA+ superfamily. *Virology*In press.

5. Guo P, Grimes S, & Anderson D (1986) A defined system for *in vitro* packaging of DNA-gp3 of the *Bacillus subtilis* bacteriophage phi29. *Proc. Natl. Acad. Sci. USA*83: 3505-3509.

6. Sabanayagam CR, Oram M, Lakowicz JR, & Black LW (2007) Viral DNA packaging studied by fluorescence correlation spectroscopy. *Biophys. J*93: L17-L19.

7. Khan SA, Hayes SJ, Wright ET, Watson RH, & Serwer P (1995) Specific single-stranded breaks in mature bacteriophage T7 DNA. *Virology*211: 329-331.

8. Oram M, Sabanayagam C, & Black LW (2008) Modulation of the Packaging Reaction of Bacteriophage T4 Terminase by DNA Structure. *J Mol Biol*381: 61-72.

9. Leforestier A, Brasiles S, de FM, Raspaud E, Letellier L, Tavares P, & Livolant F (2008) Bacteriophage T5 DNA ejection under pressure. *J. Mol. Biol.*384: 730-739.

10. Fujisawa H & Morita M (1997) Phage DNA packaging. *Genes Cells*2: 537-545.

11. Astumian RD (1997) Thermodynamics and kinetics of a Brownian motor. *Science*276: 917-922.

12. Hendrix RW (1978) Symmetry mismatch and DNA packaging in large bacteriophages. *Proc. Natl. Acad. Sci. USA*75: 4779-4783.

13. Grimes S & Anderson D (1997) The bacteriophage phi29 packaging proteins supercoil the DNA ends. *J Mol Biol*266: 901-914.

14. Chen C & Guo P (1997) Sequential action of six virus-encoded DNA-packaging RNAs during phage phi29 genomic DNA translocation. *J. Virol.*71: 3864-3871.

15. Moffitt JR, Chemla YR, Aathavan K, Grimes S, Jardine PJ, Anderson DL, & Bustamante C (2009) Intersubunit coordination in a homomeric ring ATPase. *Nature*457: 446-450.

16. Guasch A, Pous J, Ibarra B, Gomis-Ruth FX, Valpuesta JM, Sousa N, Carrascosa JL, & Coll M (2002) Detailed architecture of a DNA translocating machine: the high-resolution structure of the bacteriophage phi29 connector particle. *J. Mol. Biol.*315: 663-676.

17. Morita M, Tasaka M, & Fujisawa H (1995) Structural and functional domains of the large subunit of the bacteriophage T3 DNA packaging enzyme: importance of the C-terminal region in prohead binding. *J. Mol. Biol.*245: 635-644.

18. Simpson AA, Tao Y, Leiman PG, Badasso MO, He Y, Jardine PJ, Olson NH, Morais MC, Grimes S, Anderson DL *et al.* (2000) Structure of the bacteriophage phi29 DNA packaging motor. *Nature*408: 745-750.

19. Hugel T, Michaelis J, Hetherington CL, Jardine PJ, Grimes S, Walter JM, Faik W, Anderson DL, & Bustamante C (2007) Experimental test of connector rotation during DNA packaging into bacteriophage phi29 capsids. *Plos Biology*5: 558-567.

20. Baumann RG, Mullaney J, & Black LW (2006) Portal fusion protein constraints on function in DNA packaging of bacteriophage T4. *Mol Microbiol.*61: 16-32.

21. Maluf NK & Feiss M (2006) Virus DNA translocation: progress towards a first ascent of mount pretty difficult. *Mol Microbiol.*61: 1-4.

22. Martin A, Baker TA, & Sauer RT (2005) Rebuilt AAA + motors reveal operating principles for ATP-fuelled machines. *Nature*437: 1115-1120.

23. Ammelburg M, Frickey T, & Lupas AN (2006) Classification of AAA+ proteins. *J Struct Biol*156: 2-11.

24. Wang F, Mei Z, Qi Y, Yan C, Hu Q, Wang J, & Shi Y (2011) Structure and mechanism of the hexameric MecA-ClpC molecular machine. *Nature*471: 331-335.

25. Grainge I, Lesterlin C, & Sherratt DJ (2011) Activation of XerCD-dif recombination by the FtsK DNA translocase. *Nucleic Acids Res.*39: 5140-5148.

26. Lowe J, Ellonen A, Allen MD, Atkinson C, Sherratt DJ, & Grainge I (2008) Molecular mechanism of sequence-directed DNA loading and translocation by FtsK. *Mol. Cell*31: 498-509.

27. Zhang F, Lemieux S, Wu X, St.-Arnaud S, McMurray CT, Major F, & Anderson D (1998) Function of hexameric RNA in packaging of bacteriophage phi29 DNA in vitro. *Mol. Cell.*2: 141-147.

28. Hendrix RW (1998) Bacteriophage DNA packaging: RNA gears in a DNA transport machine (Minireview). *Cell*94: 147-150.

29. Badasso MO, Leiman PG, Tao Y, He Y, Ohlendorf DH, Rossmann MG, & Anderson D (2000) Purification, crystallization and initial X-ray analysis of the head- tail connector of bacteriophage phi29. *Acta Crystallogr D Biol Crystallogr*56 (Pt 9): 1187-1190.

30. Shu D, Zhang H, Jin J, & Guo P (2007) Counting of six pRNAs of phi29 DNA-packaging motor with customized single molecule dual-view system. *EMBO J.***26**: 527-537.

31. Xiao F, Zhang H, & Guo P (2008) Novel mechanism of hexamer ring assembly in protein/RNA interactions revealed by single molecule imaging. *Nucleic Acids Res*36: 6620-6632.

32. Moll D & Guo P (2007) Grouping of Ferritin and Gold Nanoparticles Conjugated to pRNA of the Phage phi29 DNA-packaging motor. *J Nanosci and Nanotech (JNN)*7: 3257-3267.

33. Zhang H, Schwartz C, De Donatis GM, & Guo P (2012) "Push Through One-Way Valve" Mechanism of Viral DNA Packaging. *Adv. Virus Res*83: 415-465.

34. Schwartz C, De Donatis GM, Zhang H, Fang H, & Guo P (2013) Revolution rather than rotation of AAA+ hexameric phi29 nanomotor for viral dsDNA packaging without coiling. *Virology*In Press.

35. Chang C, Zhang H, Shu D, Guo P, & Savran C (2008) Bright-field analysis of phi29 DNA packaging motor using a magnetomechanical system. *Appl. Phys. Lett.*93: 153902-153902-3.

36. Smith DE, Tans SJ, Smith SB, Grimes S, Anderson DL, & Bustamante C (2001) The bacteriophage phi29 portal motor can package DNA against a large internal force. *Nature*413: 748-752.

37. Rickgauer JP, Fuller DN, Grimes S, Jardine PJ, Anderson DL, & Smith DE (2008) Portal motor velocity and internal force resisting viral DNA packaging in bacteriophage phi 29. *Biophysical Journal*94: 159-167.

38. Guo PX & Lee TJ (2007) Viral nanomotors for packaging of dsDNA and dsRNA. *Mol. Microbiol.*64: 886-903.

39. Casjens SR (2011) The DNA-packaging nanomotor of tailed bacteriophages. *Nat Rev. Microbiol.*9: 647-657.

40. Jing P, Haque F, Vonderheide A, Montemagno C, & Guo P (2010) Robust Properties of Membrane-Embedded Connector Channel of Bacterial Virus Phi29 DNA Packaging Motor. *Mol. Biosyst.*6: 1844-1852.

41. Jing P, Haque F, Shu D, Montemagno C, & Guo P (2010) One-Way Traffic of a Viral Motor Channel for Double-Stranded DNA Translocation. *Nano Lett.*10: 3620-3627.

42. Wendell D, Jing P, Geng J, Subramaniam V, Lee TJ, Montemagno C, & Guo P (2009) Translocation of double-stranded DNA through membrane-adapted phi29 motor protein nanopores. *Nat. Nanotechnol.*4: 765-772.

43. Haque, F. & Guo, P. (2011) in *Nanopores, Sensing and Fundamental Biological Interactions,* eds. Iqbal, S. M. & Bashir, R. (Springer, pp. 77-106.

44. Fang H, Jing P, Haque F, & Guo P (2012) Role of channel Lysines and "Push Through a One-way Valve" Mechanism of Viral DNA packaging Motor. *Biophysical Journal*102: 127-135.

45. Geng J, Fang H, Haque F, Zhang L, & Guo P (2011) Three reversible and controllable discrete steps of channel gating of a viral DNA packaging motor. *Biomaterials*32: 8234-8242.

46. Shu D & Guo P (2003) Only one pRNA hexamer but multiple copies of the DNA-packaging protein gp16 are needed for the motor to package bacterial virus phi29 genomic DNA. *Virology*309(1): 108-113.

47. Lee CS & Guo P (1995) Sequential interactions of structural proteins in phage phi29 procapsid assembly. *J. Virol.*69: 5024-5032.

48. Moore SD & Prevelige PE, Jr. (2001) Structural transformations accompanying the assembly of bacteriophage P22 portal protein rings in vitro. *J. Biol. Chem.*276: 6779-6788.

49. Fu C & Prevelige P (2009) In vitro incorporation of the phage Phi29 connector complex. *Virology*394: 149-153.

50. Tuma R, Tsuruta H, French KH, & Prevelige PE (2008) Detection of intermediates and kinetic control during assembly of bacteriophage P22 procapsid. *J Mol Biol*381: 1395-1406.

51. Fu CY, Morais MC, Battisti AJ, Rossmann MG, & Prevelige PE, Jr. (2007) Molecular dissection of o29 scaffolding protein function in an in vitro assembly system. *J Mol Biol.*366: 1161-1173.

52. Rodriguez-Casado A, Moore SD, Prevelige PE, & Thomas GJ (2001) Structure of bacteriophage P22 portal protein in relation to assembly: Investigation by Raman spectroscopy. *Biochemistry*40: 13583-13591.

53. Fane BA & Prevelige PE (2003) Mechanism of scaffolding-assisted viral assembly. *Virus Structure*64: 259-+.

54. Tang JT, Lander GC, Olia A, Li R, Casjens S, Prevelige P, Cingolani G, Baker TS, & Johnson JE (2011) Peering Down the Barrel of a Bacteriophage Portal: The Genome Packaging and Release Valve in P22. *Structure*19: 496-502.

55. Olia AS, Prevelige PE, Johnson JE, & Cingolani G (2011) Three-dimensional structure of a viral genome-delivery portal vertex. *Nat Struct Mol Biol*18: 597-603.

56. Shu D, Shu Y, Haque F, Abdelmawla S, & Guo P (2011) Thermodynamically stable RNA three-way junctions for constructing multifuntional nanoparticles for delivery of therapeutics. *Nature Nanotechnology*6: 658-667.

57. Haque F, Shu D, Shu Y, Shlyakhtenko L, Rychahou P, Evers M, & Guo P (2012) Ultrastable Synergistic Tetravalent RNA Nanoparticles For Targeting To Cancers. *Nano Today*7: 245-257.

58. Shu Y, Haque F, Shu D, Li W, Zhu Z, Kotb M, Lyubchenko Y, & Guo P (2013) Fabrication of 14 Different RNA Nanoparticles for Specific Tumor Targeting without Accumulation in Normal Organs. *RNA*in press.

59. Guo P, Bailey S, Bodley JW, & Anderson D (1987) Characterization of the small RNA of the bacteriophage phi29 DNA packaging machine. *Nucleic Acids Res.*15: 7081-7090.

60. Lee TJ & Guo P (2006) Interaction of gp16 with pRNA and DNA for genome packaging by the motor of bacterial virus phi29. *J. Mol Biol.*356: 589-599.

61. Shu D, Huang L, & Guo P (2003) A simple mathematical formula for stoichiometry quantitation of viral and nanobiological assemblage using slopes of log/log plot curves. *J. Virol Meth.*115(1): 19-30.

62. Trottier M & Guo P (1997) Approaches to determine stoichiometry of viral assembly components. *J. Virol.*71: 487-494.

63. Zhang H, Endrizzi JA, Shu Y, Haque F, Guo P, & Chi YI (2013) Crystal Structure of 3WJ Core Revealing Divalent Ion-promoted Thermostability and Assembly of the Phi29 Hexameric Motor pRNA. *RNA* Submitted.

64. Reid RJD, Bodley JW, & Anderson D (1994) Characterization of the prohead-pRNA interaction of bacteriophage phi29. *J Biol Chem*269: 5157-5162.

65. Garver K & Guo P (1997) Boundary of pRNA functional domains and minimum pRNA sequence requirement for specific connector binding and DNA packaging of phage phi29. *RNA.*3: 1068-1079.

66. Zhang CL, Lee C-S, & Guo P (1994) The proximate 5' and 3' ends of the 120-base viral RNA (pRNA) are crucial for the packaging of bacteriophage f29 DNA. *Virology*201: 77-85.

67. Reid RJD, Bodley JW, & Anderson D (1994) Identification of bacteriophage phi29 prohead RNA (pRNA) domains necessary for *in vitro* DNA-gp3 packaging. *J. Biol. Chem.*269: 9084-9089.

68. Reid RJD, Zhang F, Benson S, & Anderson D (1994) Probing the structure of bacteriophage phi29 prohead RNA with specific mutations. *J Biol Chem*269: 18656-18661.

69. Shu D & Guo P (2003) A Viral RNA that binds ATP and contains an motif similar to an ATP-binding aptamer from SELEX. *J. Biol. Chem.*278(9): 7119-7125.

70. Lee TJ, Zhang H, Liang D, & Guo P (2008) Strand and nucleotide-dependent ATPase activity of gp16 of bacterial virus phi29 DNA packaging motor. *Virology*380: 69-74.

71. Grimes S & Anderson D (1990) RNA Dependence of the Bateriophage phi29 DNA Packaging ATPase. *J. Mol. Biol.*215: 559-566.

72. Ibarra B, Valpuesta JM, & Carrascosa JL (2001) Purification and functional characterization of p16, the ATPase of the bacteriophage phi29 packaging machinary. *Nucleic Acids Res.*29: 4264-4273.

73. Zhang CL, Tellinghuisen T, & Guo P (1997) Use of circular permutation to assess six bulges and four loops of DNA-Packaging pRNA of bacteriophage phi29. *RNA*3: 315-322.

74. Zhao W, Morais MC, Anderson DL, Jardine PJ, & Grimes S (2008) Role of the CCA bulge of prohead RNA of bacteriophage o29 in DNA packaging. *J. Mol. Biol.*383: 520-528.

75. de Haas F, Paatero AO, Mindich L, Bamford DH, & Fuller SD (1999) A symmetry mismatch at the site of RNA packaging in the polymerase complex of dsRNA bacteriophage phi6. *J Mol Biol*294: 357-372.

76. Maurizi MR & Li CC (2001) AAA proteins: in search of a common molecular basis. International Meeting on Cellular Functions of AAA Proteins. *EMBO Rep.*2: 980-985.

77. Morais MC, Koti JS, Bowman VD, Reyes-Aldrete E, Anderson D, & Rossman MG (2008) Defining molecular and domain boundaries in the bacteriophage phi29 DNA packaging motor. *Structure*16: 1267-1274.

78. Schwartz C, Fang H, Huang L, & Guo P (2012) Sequential action of ATPase, ATP, ADP, Pi and dsDNA in procapsid-free system to enlighten mechanism in viral dsDNA packaging. *Nucleic Acids Res.*40: 2577-2586.

79. Hohn T (1976) Packaging of genomes in bacteriophages: a comparison of ssRNA bacteriophages and dsDNA bacteriophages. *Philos Trans R Soc London Ser B*276: 143-150.

80. Earnshaw WC & Casjens SR (1980) DNA packaging by the double-stranded DNA bacteriophages. *Cell*21: 319-331.

81. Fuller DN, Raymer DM, Rickgauer JP, Robertson RM, Catalano CE, Anderson DL, Grimes S, & Smith DE (2007) Measurements of single DNA molecule packaging

dynamics in bacteriophage lambda reveal high forces, high motor processivity, and capsid transformations. *J Mol Biol*373: 1113-1122.

82. Fuller DN, Raymer DM, Kottadiel VI, Rao VB, & Smith DE (2007) Single phage T4 DNA packaging motors exhibit large force generation, high velocity, and dynamic variability. *Proc. Natl. Acad. Sci. U. S. A*104: 16868-16873.

83. Mueller-Cajar O, Stotz M, Wendler P, Hartl FU, Bracher A, & Hayer-Hartl M (2011) Structure and function of the AAA+ protein CbbX, a red-type Rubisco activase. *Nature*479: 194-199.

84. Feiss M & Rao VB (2012) The bacteriophage DNA packaging machine. *Adv. Exp. Med. Biol*726: 489-509.

85. Ibarra B, Caston J.R., Llorca O., Valle M, Valpuesta J.M., & Carrascosa J.L. (2000) Topology of the components of the DNA packaging machinery in the phage phi29 prohead. *J. Mol. Biol.*298: 807-815.

86. Yu J, Moffitt J, Hetherington CL, Bustamante C, & Oster G (2010) Mechanochemistry of a viral DNA packaging motor. *J. Mol. Biol.*400: 186-203.

87. Aathavan K, Politzer AT, Kaplan A, Moffitt JR, Chemla YR, Grimes S, Jardine PJ, Anderson DL, & Bustamante C (2009) Substrate interactions and promiscuity in a viral DNA packaging motor. *Nature*461: 669-673.

88. Johnson DS, Bai L, Smith BY, Patel SS, & Wang MD (2007) Single-molecule studies reveal dynamics of DNA unwinding by the ring-shaped T7 helicase. *Cell*129: 1299-1309.

89. Rao VB & Black LW (1985) Evidence that a phage T4 DNA packaging enzyme is a processed form of the major capsid gene product. *Cell*42: 967-977.

90. Sun SY, Kondabagil K, Gentz PM, Rossmann MG, & Rao VB (2007) The structure of the ATPase that powers DNA packaging into bacteriophage T4 procapsids. *Mol. Cell.*25: 943-949.

91. Zheng H, Olia AS, Gonen M, Andrews S, Cingolani G, & Gonen T (2008) A Conformational Switch in Bacteriophage P22 Portal Protein Primes Genome Injection. *Mol. Cell.*29: 376-383.

92. Agirrezabala X, Martin-Benito J, Caston JR, Miranda R, Valpuesta JM, & Carrascosa JL (2005) Maturation of phage T7 involves structural modification of both shell and inner core components. *EMBO J.*24: 3820-3829.

93. Butcher SJ, Bamford DH, & Fuller SD (1995) DNA packaging orders the membrane of bacteriophage PRD1. *EMBO J*14: 6078-6086.

94. Dubé P, Tavares P, Lurz R, & van Heel M (1993) The portal protein of bacteriophage SPP1: a DNA pump with 13-fold symmetry. *EMBO J.*12: 1303-1309.

95. Gutierrez C, Freire R, Salas M, & Hermoso JM (1994) Assembly of phage phi29 genome with viral protein p6 into a compact complex. *EMBO*13(1): 269-276.

96. Lebedev AA, Krause MH, Isidro AL, Vagin AA, Orlova EV, Turner J, Dodson EJ, Tavares P, & Antson AA (2007) Structural framework for DNA translocation via the viral portal protein. *EMBO J.*26: 1984-1994.

97. Orlova EV, Gowen B, Droge A, Stiege A, Weise F, Lurz R, van HM, & Tavares P (2003) Structure of a viral DNA gatekeeper at 10 A resolution by cryo-electron microscopy. *EMBO J.*22: 1255-1262.

98. Sousa R & Padilla R (1995) A mutant T7 RNA polymerase as a DNA polymerase. *EMBO J.*14: 4609-4621.

99. Stewart PL, Fuller SD, & Burnett RM (1993) Difference imaging of adenovirus: bridging the resolution gap between X- ray crystallography and electron microscopy. *EMBO J*12: 2589-2599.

100. Xiang Y, Morais MC, Battisti AJ, Grimes S, Jardine PJ, Anderson DL, & Rossmann MG (2006) Structural changes of bacteriophage phi29 upon DNA packaging and release. *EMBO J.*25: 5229-5239.

101. Xiao F, Moll D, Guo S, & Guo P (2005) Binding of pRNA to the N-terminal 14 amino acids of connector protein of bacterial phage phi29. *Nucleic Acids Res*33: 2640-2649.

102. Atz R, Ma S, Gao J, Anderson DL, & Grimes S (2007) Alanine Scanning and Fe-BABE Probing of the Bacteriophage phi29 Prohead RNA-Connector Interaction. *J. Mol. Biol.*369: 239-248.

103. Serwer P (2003) Models of bacteriophage DNA packaging motors. *J Struct. Biol*141: 179-188.

104. Ray K, Sabanayagam CR, Lakowicz JR, & Black LW (2010) DNA crunching by a viral packaging motor: Compression of a procapsid-portal stalled Y-DNA substrate. *Virology*398: 224-232.

105. Ray K, Ma J, Oram M, Lakowicz JR, & Black LW (2010) Single-molecule and FRET fluorescence correlation spectroscopy analyses of phage DNA packaging: colocalization of packaged phage T4 DNA ends within the capsid. *J. Mol. Biol.*395: 1102-1113.

106. Black LW (1989) DNA Packaging in dsDNA bacteriophages. *Ann Rev Microbiol*43: 267-292.

107. Burroughs, A. M., Iyer, L. M., & Aravind, L. (2007) in *Gene and Protein Evlolution. Genome Dyn.*, ed. Volff J-N pp. 48-65.

108. Iyer LM, Makarova KS, Koonin EV, & Aravind L (2004) Comparative genomics of the FtsK-HerA superfamily of pumping ATPases: implications for the origins of

chromosome segregation, cell division and viral capsid packaging. *Nucleic Acids Res.*32: 5260-5279.

109. Koti JS, Morais MC, Rajagopal R, Owen BA, McMurray CT, & Anderson D (2008) DNA packaging motor assembly intermediate of bacteriophage phi29. *J Mol. Biol.*381: 1114-1132.

110. Guo P, Peterson C, & Anderson D (1987) Initiation events in *in vitro* packaging of bacteriophage f29 DNA-gp3. *J Mol Biol*197: 219-228.

111. Lee TJ, Zhang H, Chang CL, Savran C, & Guo P (2009) Engineering of the fluorescent-energy-conversion arm of phi29 DNA packaging motor for single-molecule studies. *Small*5: 2453-2459.

112. Lee CS & Guo P (1994) A highly sensitive system for the assay of in vitro viral assembly of bacteriophage phi29 of Bacillus subtilis. *Virology*202: 1039-1042.

113. Shlyakhtenko LS, Gall AA, Filonov A, Cerovac Z, Lushnikov A, & Lyubchenko YL (2003) Silatrane-based surface chemistry for immobilization of DNA, protein-DNA complexes and other biological materials. *Ultramicroscopy*97: 279-287.

114. Lyubchenko YL & Shlyakhtenko LS (2009) AFM for analysis of structure and dynamics of DNA and protein-DNA complexes. *Methods*47: 206-213.

115. Guo P (2002) Structure and function of phi29 hexameric RNA that drive viral DNA packaging motor: Review. *Prog Nucleic Acid Res Mol Biol*72: 415-472.

116. Green DJ, Wang JC, Xiao F, Cai Y, Balhorn R, Guo P, & Cheng RH (2010) Self-Assembly of Heptameric Nanoparticles Derived from Tag-Functionalized Phi29 Connectors. *ACS Nano*4: 7651-7659.

117. Chen C, Trottier M, & Guo P (1997) New approaches to stoichiometry determination and mechanism investigation on RNA involved in intermediate reactions. *Nucleic Acids Symposium Series*36: 190-193.

118. Sim J, Ozgur S, Lin BY, Yu JH, Broker TR, Chow LT, & Griffith J (2008) Remodeling of the Human Papillomavirus Type 11 Replication Origin into Discrete Nucleoprotein Particles and Looped Structures by the E2 Protein. *J Mol Biol*375: 1165-1177.

119. Skordalakes E & Berger JM (2006) Structural Insights into RNA-Dependent Ring Closure and ATPase Activation by the Rho Termination Factor. *Cell*127: 553-564.

120. Ziegelin G+, Niedenzu T, Lurz R, Saenger W, & Lanka E (2003) Hexameric RSF1010 helicase RepA: the structural and functional importance of single amino acid residues. *Nucleic Acids Res.*31: 5917-5929.

121. Frickey T & Lupas AN (2004) Phylogenetic analysis of AAA proteins. *J Struct Biol*146: 2-10.

122. Iyer LM, Leipe DD, Koonin EV, & Aravind L (2004) Evolutionary history and higher order classification of AAA plus ATPases. *J Struct Biol*146: 11-31.

123. Singleton MR, Dillingham MS, & Wigley DB (2007) Structure and mechanism of helicases and nucleic acid translocases. *Ann. Rev. Biochem.*76: 23-50.

124. Pyle AM (2008) Translocation and unwinding mechanisms of RNA and DNA helicases. *Annual Review of Biophysics*37: 317-336.

125. Wang J (2004) Nucleotide-dependent domain motions within rings of the RecA/AAA(+) superfamily. *J. Struct. Biol. 2004 Dec.*148: 259-267.

126. Rao VB & Feiss M (2008) The Bacteriophage DNA Packaging Motor. *Annu. Rev. Genet.*42: 647-681.

127. Chemla YR, Aathavan K, Michaelis J, Grimes S, Jardine PJ, Anderson DL, & Bustamante C (2005) Mechanism of force generation of a viral DNA packaging motor. *Cell.*122: 683-692.

128. Hwang Y, Catalano CE, & Feiss M (1996) Kinetic and mutational dissection of the two ATPase activities of terminase, the DNA packaging enzyme of bacteriophage lambda. *Biochemistry*35: 2796-2803.

129. Huang LP & Guo P (2003) Use of acetone to attain highly active and soluble DNA packaging protein gp16 of phi29 for ATPase assay. *Virology*312: 449-457.

130. Huang LP & Guo P (2003) Use of PEG to acquire highly soluble DNA-packaging enzyme gp16 of bacterial virus phi29 for stoichiometry quantification. *J Virol Methods*109: 235-244.

131. Hawkes, R. (1986) in *Methods in Enzymology* (Academic Press,Inc., pp. 484-491.

132. Hou X, Yang F, Li L, Song Y, Jiang L, & Zhu D (2010) A Biomimetic Asymmetric Responsive Single Nanochannel. *J. Am. Chem. Soc.*132: 11736-11742.

133. Lisal J, Kainov DE, Bamford DH, Thomas GJ, Jr., & Tuma R (2004) Enzymatic mechanism of RNA translocation in double-stranded RNA bacteriophages. *J. Biol. Chem.*279: 1343-1350.

134. Dixit A, Ray K, Lakowicz JR, & Black LW (2011) Dynamics of the T4 Bacteriophage DNA Packasome Motor ENDONUCLEASE VII RESOLVASE RELEASE OF ARRESTED Y-DNA SUBSTRATES. *J Biol Chem*286: 18878-18889.

135. Turner DH, Sugimoto N, & Freier SM (1988) RNA structure prediction. *Annu. Rev. Biophys. Chem.*17: 167-192.

136. Hess H & Vogel V (2001) Molecular shuttles based on motor proteins: Active transport in synthetic environments. *J Biotechnol.*82: 67-85.

137. Skordalakes E & Berger JM (2006) Structural insights into RNA-dependent ring closure and ATPase activation by the Rho termination factor. *Cell*127: 553-564.

138. Matias PM, Gorynia S, Donner P, & Carrondo MA (2006) Crystal structure of the human AAA+ protein RuvBL1. *J. Biol. Chem.*281: 38918-38929.

139. McGeoch AT, Trakselis MA, Laskey RA, & Bell SD (2005) Organization of the archaeal MCM complex on DNA and implications for the helicase mechanism. *Nat. Struct. Mol. Biol.*12: 756-762.

140. Lisal J & Tuma R (2005) Cooperative mechanism of RNA packaging motor. *J Biol Chem*280: 23157-23164.

141. Mancini EJ, Kainov DE, Grimes JM, Tuma R, Bamford DH, & Stuart DI (2004) Atomic snapshots of an RNA packaging motor reveal conformational changes linking ATP hydrolysis to RNA translocation. *Cell*118: 743-755.

142. Morita M, Tasaka M, & Fujisawa H (1993) DNA packaging ATPase of bacteriophage T3. *Virology*193: 748-752.

143. Sun S, Kondabagil K, Draper B, Alam TI, Bowman VD, Zhang Z, Hegde S, Fokine A, Rossmann MG, & Rao VB (2008) The structure of the phage T4 DNA packaging motor suggests a mechanism dependent on electrostatic forces. *Cell.*135: 1251-1262.

144. Roos WH, Ivanovska IL, Evilevitch A, & Wuite GJL (2007) Viral capsids: Mechanical characteristics, genome packaging and delivery mechanisms. *Cellular and Molecular Life Sciences*64: 1484-1497.

145. Kainov DE, Mancini EJ, Telenius J, Lisai J, Grimes JM, Bamford DH, Stuart DI, & Tuma R (2008) Structural basis of mechanochemical coupling in a hexameric molecular motor. *J Biol Chem*283: 3607-3617.

146. Mastrangelo IA, Hough PV, Wall JS, Dodson M, Dean FB, & Hurwitz J (1989) ATP-dependent assembly of double hexamers of SV40 T antigen at the viral origin of DNA replication. *Nature*338: 658-662.

147. Egelman HH, Yu X, Wild R, Hingorani MM, & Patel SS (1995) Bacteriophage T7 helicase/primase proteins form rings around single- stranded DNA that suggest a general structure for hexameric helicases. *Proc Natl Acad Sci U. S. A*92: 3869-3873.

148. Niedenzu T, Roleke D, Bains G, Scherzinger E, & Saenger W (2001) Crystal structure of the hexameric replicative helicase RepA of plasmid RSF1010. *J. Mol. Biol.*306: 479-487.

149. Willows RD, Hansson A, Birch D, Al-Karadaghi S, & Hansson M (2004) EM single particle analysis of the ATP-dependent BchI complex of magnesium chelatase: an AAA(+) hexamer. *J Struct Biol*146: 227-233.

150. Parsons CA, Stasiak A, Bennett RJ, & West SC (1995) Structure of a multisubunit complex that promotes DNA branch migration. *Nature*374: 375-378.

151. Putnam CD, Clancy SB, Tsuruta H, Gonzalez S, Wetmur JG, & Tainer JA (2001) Structure and mechanism of the RuvB Holliday junction branch migration motor. *J. Mol. Biol.*311: 297-310.

152. Grainge I, Bregu M, Vazquez M, Sivanathan V, Ip SC, & Sherratt DJ (2007) Unlinking chromosome catenanes in vivo by site-specific recombination. *EMBO J.*26: 4228-4238.

153. Grainge I (2008) Sporulation: SpoIIIE is the key to cell differentiation. *Curr. Biol.*18: R871-R872.

154. McNally R, Bowman GD, Goedken ER, O'Donnell M, & Kuriyan J (2010) Analysis of the role of PCNA-DNA contacts during clamp loading. *BMC. Struct. Biol.*10: 3.

155. Guenther B, Onrust R, Sali A, O'Donnell M, & Kuriyan J (1997) Crystal structure of the delta' subunit of the clamp-loader complex of E. coli DNA polymerase III. *Cell*91: 335-345.

156. Serwer P (2010) A Hypothesis for Bacteriophage DNA Packaging Motors. *Viruses*2: 1821-1843.

157. Jimenez J, Santisteban A, Carazo JM, & Carrascosa JL (1986) Computer graphic display method for visualizing three-dimensional biological structures. *Science*232: 1113-1115.

158. Demarre G, Galli E, & Barre FX (2013) The FtsK Family of DNA Pumps. *Adv. Exp. Med. Biol*767: 245-262.

159. Bath J, Wu LJ, Errington J, & Wang JC (2000) Role of Bacillus subtilis SpoIIIE in DNA transport across the mother cell-prespore division septum. *Science*290: 995-997.

160. Massey TH, Mercogliano CP, Yates J, Sherratt DJ, & Lowe J (2006) Double-stranded DNA translocation: structure and mechanism of hexameric FtsK. *Mol. Cell*23: 457-469.

161. Gomis-Ruth FX, Moncalian G, Perez-Luque R, Gonzalez A, Cabezon E, de la CF, & Coll M (2001) The bacterial conjugation protein TrwB resembles ring helicases and F1-ATPase. *Nature*409: 637-641.

162. Amitani I, Baskin RJ, & Kowalczykowski SC (2006) Visualization of Rad54, a chromatin remodeling protein, translocating on single DNA molecules. *Mol. Cell*23: 143-148.

163. Chen YJ, Yu X, & Egelman EH (2002) The hexameric ring structure of the Escherichia coli RuvB branch migration protein. *J. Mol. Biol.*319: 587-591.

164. Maluf NK, Gaussier H, Bogner E, Feiss M, & Catalano CE (2006) Assembly of Bacteriophage Lambda Terminase into a Viral DNA Maturation and Packaging Machine. *Biochemistry.*45: 15259-15268.

165. Chistol G, Liu S, Hetherington CL, Moffitt JR, Grimes S, Jardine PJ, & Bustamante C (2012) High Degree of Coordination and Division of Labor among Subunits in a Homomeric Ring ATPase. *Cell*151: 1017-1028.

166. Xiao F, Demeler B, & Guo P (2010) Assembly Mechanism of the Sixty-Subunit Nanoparticles via Interaction of RNA with the Reengineered Protein Connector of phi29 DNA-Packaging Motor. *ACS Nano.*4: 3293-3301.

167. Morais MC, Tao Y, Olsen NH, Grimes S, Jardine PJ, Anderson D, Baker TS, & Rossmann MG (2001) Cryoelectron-Microscopy Image Reconstruction of Symmetry Mismatches in Bacteriophage phi29. *J Struct Biol*135: 38-46.

168. Kad NM, Wang H, Kennedy GG, Warshaw DM, & Van HB (2010) Collaborative dynamic DNA scanning by nucleotide excision repair proteins investigated by single-molecule imaging of quantum-dot-labeled proteins. *Mol. Cell*37: 702-713.

169. Story RM & Steitz TA (1992) Structure of the rec-A protein-ADP Complex. *Nature*355.

170. Fujisawa H, Shibata H, & Kato H (1991) Analysis of interactions among factors involved in the bacteriophage T3 DNA packaging reaction in a defined *in vitro* system. *Virology*185: 788-794.

171. Shibata H, Fujisawa H, & Minagawa T (1987) Early events in a defined *in vitro* system for packaging of bacteriophage T3 DNA. *Virology*159: 250-258.

172. Morita M, Tasaka M, & Fujisawa H (1995) Analysis of the fine structure of the prohead binding domain of the packaging protein of bacteriophage T3 using a hexapeptide, an analog of a prohead binding site. *Virology*211: 516-524.

173. Mayanagi K, Kiyonari S, Saito M, Shirai T, Ishino Y, & Morikawa K (2009) Mechanism of replication machinery assembly as revealed by the DNA ligase-PCNA-DNA complex architecture. *Proc. Natl. Acad. Sci. U. S. A*106: 4647-4652.

174. Roy A, Bhardwaj A, & Cingolani G (2011) Crystallization of the nonameric small terminase subunit of bacteriophage P22. *Acta Crystallographica Section F-Structural Biology and Crystallization Communications*67: 104-110.

175. Zhao Z, Khisamutdinov E, Schwartz C, & Guo P (2013) Mechanism of One-Way Traffic of Hexameric Phi29 DNA Packaging Motor with Four Electropositive Relaying Layers Facilitating Anti-Parallel Revolution. *ACS Nano* In Press.

176. Grimes S, Ma S, Gao J, Atz R, & Jardine PJ (2011) Role of phi29 connector channel loops in late-stage DNA packaging. *J. Mol. Biol.*410: 50-59.

177. Geng J, Huaming F, shaoying W, & Peixuan G (2013) Channel Size Conversion of Phi29 DNA-Packaging Nanomotor for Discrimination of Single- and Double-Stranded DNA and RNA. *ACS Nano*.

178. Soong RK, Bachand GD, Neves HP, Olkhovets AG, Craighead HG, & Montemagno CD (2000) Powering an inorganic nanodevice with a biomolecular motor. *Science*290: 1555-1558.

179. Khaled A, Guo S, Li F, & Guo P (2005) Controllable Self-Assembly of Nanoparticles for Specific Delivery of Multiple Therapeutic Molecules to Cancer Cells Using RNA Nanotechnology. *Nano Letters*5: 1797-1808.

180. Guo S, Tschammer N, Mohammed S, & Guo P (2005) Specific delivery of therapeutic RNAs to cancer cells via the dimerization mechanism of phi29 motor pRNA. *Hum Gene Ther.*16: 1097-1109.

181. Liu H, Guo S, Roll R, Li J, Diao Z, Shao N, Riley MR, Cole AM, Robinson JP, Snead NM *et al.* (2007) Phi29 pRNA Vector for Efficient Escort of Hammerhead Ribozyme Targeting Survivin in Multiple Cancer Cells. *Cancer Biol. Ther.*6: 697-704.

182. Zhou J, Shu Y, Guo P, Smith D, & Rossi J (2011) Dual functional RNA nanoparticles containing phi29 motor pRNA and anti-gp120 aptamer for cell-type specific delivery and HIV-1 Inhibition. *Methods*54: 284-294.

183. Guo P, Coban O, Snead NM, Trebley J, Hoeprich S, Guo S, & Shu Y (2010) Engineering RNA for Targeted siRNA Delivery and Medical Application. *Advanced Drug Delivery Reviews*62: 650-666.

184. Guo P (2010) The emerging field of RNA nanotechnology. *Nat Nanotechnol.*5: 833-842.

185. Shu Y, Cinier M, Shu D, & Guo P (2011) Assembly of multifunctional phi29 pRNA nanoparticles for specific delivery of siRNA and other therapeutics to targeted cells. *Methods***54**: 204-214.

186. Zhang CL, Garver K, & Guo P (1995) Inhibition of phage phi29 assembly by antisense oligonucleotides targeting viral pRNA essential for DNA packaging. *Virology*211: 568-576.

187. Trottier M, Zhang CL, & Guo P (1996) Complete inhibition of virion assembly *in vivo* with mutant pRNA essential for phage phi29 DNA packaging. *J. Virol.*70: 55-61.

188. Bogner E (2002) Human cytomegalovirus terminase as a target for antiviral chemotherapy. *Rev. Med. Virol.*12: 115-127.

189. Visalli RJ & van ZM (2003) DNA encapsidation as a target for anti-herpesvirus drug therapy. *Antiviral Res*59: 73-87.

Vita

Chad Tyler Schwartz

Born

Fort Thomas, KY 41075

Educational Institutions

University of Kentucky	2004-2008	Bachelors of Science	Agricultural Biotechnology
University of Cincinnati	2008-2011	Ph. D. Candidate	Biomedical Engineering
University of Kentucky	2012-2013	Ph. D. Candidate	Pharmaceutical Sciences

Professional Publications

(1) T.J. Lee, C. Schwartz and P. Guo. "**Construction of Bacteriophage Phi29 DNA Packaging Motor and its Applications in Nanotechnology and Therapy"**. *Annals of Biomedical Engineering*. 37(10): 2064-2081 (Oct. 2009).

(2) C. Schwartz, H. Fang, L. Huang, and P. Guo. "**Sequential action of ATPase, ATP, ADP, Pi and dsDNA in procapsid-free system to enlighten mechanism in viral dsDNA packaging".** *Nucleic Acids Research.* 40(6): 2577-86 (Mar. 2012).

(3) H. Zhang, C. Schwartz, G. De Donatis, and P. Guo. "**AAA+ Hexameric Viral DNA Packaging Motor Using "Push Through One-Way Valve" Mechanism".** *Advances in Viral Research*. 83: 415-65. (2012).

(4) C. Schwartz, H. Zhang, and P. Guo. **"Push Through One-Way Valve Mechanism of Viral Hexameric Nanomotor in DNA Packaging".** *Encyclopedia of Biophysics*. In Press.

(5) Z. Zhao, E. Khisamutdinov, C. Schwartz, and P. Guo. "**Mechanism of One-Way Traffic of Hexameric Phi29 DNA Packaging Motor with Four Electropositive Relaying Layers Facilitating Anti-Parallel Revolution**". *ACS Nano*. In Press.

(6) C. Schwartz, H. Zhang, H. Fang, G. De Donatis, and P. Guo. **"Revolution rather than rotation of AAA+ hexameric phi29 nanomotor for viral dsDNA packaging without coiling".** *Virology*. In Press

(7) C. Schwartz, G. De Donatis, H. Fang, and P. Guo. **"Mechanism of mighty force generation of the hexameric phi29 DNA-packaging motor".** *Virology*. In Press.

Scholastic and Professional Honors

KHEAA KEES Scholarship	2004 – 2008
Commonwealth Scholarship	2004 – 2008
University Graduate Scholarship	2008 – Present